The Effects of Extracellular Matrix Mechanics and Composition on the Behaviors of Nucleus Pulposus Cells from the Intervertebral Disc

by

Christopher Lee Gilchrist

Department of Biomedical Engineering
Duke University

Date:_____

Approved:

_____
Lori A. Setton, Supervisor

_____
Jun Chen

_____
Farshid Guilak

_____
George A. Truskey

_____
Stefan Zauscher

Dissertation submitted in partial fulfillment of
the requirements for the degree of Doctor
of Philosophy in the Department of
Biomedical Engineering in the Graduate School
of Duke University

2009

ABSTRACT

The Effects of Extracellular Matrix Mechanics and Composition on the Behaviors of Nucleus Pulposus Cells from the Intervertebral Disc

by

Christopher Lee Gilchrist

Department of Biomedical Engineering
Duke University

Date:_____
Approved:

_____
Lori A. Setton, Supervisor

_____
Jun Chen

_____
Farshid Guilak

_____
George A. Truskey

_____
Stefan Zauscher

An abstract of a dissertation submitted in partial fulfillment of the requirements for the degree of Doctor of Philosophy in the Department of Biomedical Engineering in the Graduate School of Duke University

2009

Abstract

Intervertebral disc (IVD) disorders are a major contributor to disability and health costs. Disc disorders and resulting pain may be preceded by changes which first occur in the nucleus pulposus (NP) region of the IVD, where significant alterations in tissue cellularity, composition, and structure begin early in human life and continue with increasing age and degeneration. These changes coincide with the loss of a distinct cell population, notochordally-derived immature NP cells, which may play a key role in the generation and maintenance of this tissue. These cells reside in a gelatinous, highly-hydrated extracellular matrix (ECM) environment and exhibit *in situ* cell-matrix and cell-cell interactions which are quite distinct from cells in other regions of the disc or in other cartilagenous, including expression of laminin cell-matrix receptors and cell-associated laminin proteins. The ECM environment is known to be a key regulator of cellular behaviors, with ECM ligands and elasticity modulating cell adhesion, organization, differentiation, and phenotype. The primary motivating hypothesis of this thesis is that the unique ECM environment of the NP plays a key role in modulating immature NP cell behaviors, and that laminin ligands, in combination with ECM elasticity, modulate immature NP cell behaviors including adhesion, organization, and phenotype.

To investigate this hypothesis, flow cytometric analyses were performed to examine IVD cell integrin receptor expression over time in culture, including assessment of key laminin-binding integrin subunits. The roles of specific integrin receptors modulating NP cell adhesion to ECM proteins were identified in studies utilizing function-blocking antibodies. NP cell adhesion, spreading, and relative cell adhesion strength was assessed on various ECM constituents, including specific isoforms of laminin. Additionally, studies were performed to examine the roles of ECM ligand and substrate stiffness in modulating NP cellular organization, utilizing polyacrylamide gel substrates with tunable mechanical properties and functionalized with different ECM ligands. Finally, the role of ECM environment was examined on one key measure of NP cell function, proteoglycan production, over time in culture.

NP cells isolated from immature NP tissues were found to express high levels of the laminin-binding integrin subunit α6 *ex situ* and maintain this expression over time in culture. Function blocking studies revealed this receptor to be a key regulator of NP cell adhesion to laminin, in contrast to cells from the adjacent AF region, which did not express this receptor nor adhere to laminin. Cell adhesion studies demonstrated that NP cells preferentially interact with two laminin isoforms, LM-511 and LM-332, in comparison to other ECM proteins, with enhanced cell attachment, spreading, and adhesion strength on surfaces coated with these ligands. These findings correspond with laminin isoform and receptor expression patterns identified in immature NP

tissues. Additionally, NP cell-cell interactions were found to be modulated by both ECM ligand and substrate stiffness, with soft, laminin-functionalized substrates promoting self-assembly of NP cells into cell clusters with morphologies similar to those identified in immature NP tissues. Finally, culture of immature NP cells on soft, laminin-rich substrates was found to promote a key measure of NP cell function, proteoglycan synthesis.

The studies presented here demonstrate that immature NP cells interact uniquely with laminin extracellular matrix proteins, and that laminin ligands and matrix elasticity are two key regulators of NP cell organization and phenotype in the IVD. These findings suggest that alterations in one or both of these factors during IVD aging or degeneration may contribute to the differentiation or loss of this unique cell population. Additionally, these results indicate that soft, laminin-functionalized biomaterials may be appropriate for *in vitro* culture and expansion of immature NP cells, as well as for use in NP tissue engineering strategies.

Contents

List of Tables

List of Figures

1. Introduction

The human intervertebral disc (IVD) is a dynamic tissue which undergoes significant changes in matrix structure, composition, and cell population during growth, aging, and with disc degeneration. The most dramatic changes in the IVD occur within the disc's centrally located nucleus pulposus (NP) region, a gelatinous, highly-hydrated tissue which acts to resist and redistribute spinal compressive loads. The human NP transitions from a fluid-like gel to more cartilage-like tissue within the first decades of life, and with aging or degeneration exhibits further decrease in proteoglycan and water content [25,70]. The initiating factors leading to early changes in the NP, as well as whether they are detrimental or beneficial to disc function, are not fully understood. However, it has been noted that soon after undergoing this transition (within the second decade of human life) the first signs of disc degeneration can be observed [19].

One documented change in the human NP which appears to coincide with or precede the tissue's compositional and structural changes is the loss of a unique cell population, the notochordally-derived immature NP cells. These cells, which are remnants from the embryonic notochord [37,156], are morphologically and phenotypically distinct from other cells within the disc, appearing as large, highly-vacuolated cells with strong cell-cell interactions (e.g. gap junctions, desmosomes) arranged in cell clusters [86,165]. Although the phenotype and function of these immature NP cells are not fully understood, they have been shown to be metabolically

active and produce a proteoglycan-rich matrix [31,53], and thus are thought to participate directly in the generation and maintenance of the highly-hydrated NP. Additionally, these cells may also have stimulatory effects on other cells in the disc, releasing soluble factors which promote proteoglycan production [5,21,53]. This immature NP cell population disappears from the human disc within the first decade of life, with a only a sparse population of chondrocyte-like cells remaining in the adult NP [19,162]. In a number of animal species, however, immature NP cells persist into or throughout adult life [87].

Although this immature NP cell population does not remain in the adult human, significant interest in these cells exists due to their possible role in generating and maintaining a proteoglycan-rich, functional NP tissue. Further knowledge of this cell's phenotype may be useful in developing cell replacement therapies or tissue engineering strategies for the NP, as well as for identifying specific soluble factors produced by these cells which stimulate the disc's existing cell population. However, relatively little is understood about the phenotype and function of this cell population, including basic information such as appropriate methods for *in vitro* culture. Immature NP cells isolated from various animal species are not highly adhesive and appear to lose their phenotype (as identified by loss of unique morphological features) rapidly in culture. Thus, the environmental factors and conditions necessary to maintain, expand, or promote this

unique cell phenotype for further study or use in therapeutic applications are as yet unknown.

The extracellular matrix (ECM) environment is known to be a key regulator of cell behavior in numerous tissues, with factors such as ECM ligand and mechanical stiffness playing important roles in directing cell adhesion, phenotype, organization and tissue patterning [3,46,47,186]. Previous work suggests that a unique feature of immature NP cells is an ECM environment rich in cell-adhesive protein laminin, as well as high *in situ* expression of various laminin receptors, in contrast to cells from the adjacent AF (see Section 1.5). Additionally, cells of the immature NP reside in a soft, gelatinous matrix with very low mechanical stiffness. Both the ECM composition and stiffness of the human NP have been documented to change significantly with age and degeneration [25,91], and these alterations may be key factors in the disappearance or differentiation of this cell population. However, it is currently unclear how the ECM environment affects cell behaviors in the NP.

The primary hypothesis of this dissertation is that the unique ECM environment found in the immature NP, including laminin ligands and a 'soft' matrix stiffness, modulates the adhesion, cell-cell interactions, and phenotype of immature NP cells. In the studies presented here, we examine the response of immature NP cells to specific ECM environmental cues, including individual ECM ligands and culture substrates with varying, well-controlled mechanical properties. Studies were conducted with cells

isolated from NP tissues of immature pigs, which retain immature ('notochordal-like') NP cells well into their adult lives. Outcome measures assessed include NP cell adhesion and spreading, cell-matrix receptor expression, and identification of functional cell-matrix receptors in studies using function-blocking antibodies. Additionally, studies were performed to examine the roles of ECM ligand and substrate stiffness in modulating NP cellular organization and matrix production over time in culture.

This dissertation will demonstrate that immature NP cells interact uniquely with the extracellular matrix protein laminin, and that laminin ligands and matrix elasticity are two key regulators of NP cell organization and phenotype in the IVD. First, the studies presented here show that NP cells isolated from immature NP tissues express high levels of the laminin-binding integrin subunit α6 *ex situ* and maintain this expression over time in culture. This receptor is demonstrated to be a key regulator of NP cell adhesion to laminin, in contrast to cells from the adjacent AF region, which do not express high levels of this receptor nor adhere to laminin. Second, NP cells are found to rapidly and preferentially interact with two laminin isoforms, LM-511 and LM-332, in comparison to other ECM proteins, with enhanced cell attachment, spreading, and adhesion strength on surfaces coated with these ligands. These findings correspond with laminin isoform and receptor expression patterns identified in immature NP tissues. Third, NP cell-cell interactions are found to be modulated by both ECM ligand and substrate stiffness, with soft, laminin-functionalized substrates promoting self-

assembly of NP cells into cell clusters with morphologies similar to those identified in immature NP tissues. Finally, culture of immature NP cells on soft, laminin-rich substrates was found to promote a key measure of NP cell function, proteoglycan synthesis. Together, these findings indicate ECM ligand and stiffness are key regulators of immature NP cell behaviors, and that alterations in one or both of these factors during IVD aging or degeneration may contribute to the differentiation or loss of this unique cell population. Additionally, these results suggest that soft, laminin-functionalized biomaterials may be appropriate for *in vitro* culture and expansion of immature NP cells, as well as for use in NP tissue engineering strategies.

1.1 Intervertebral Disc Structure and Function

The intervertebral disc (IVD) is a heterogeneous, fibrocartilagenous tissue which provides load support, energy dissipation, and flexibility in the spine. The IVD is situated between adjacent vertebral bodies and acts as the main joint of the spinal column, occupying approximately 1/3 of it's total height [18,168]. Each disc consists of two primary components: the outer anulus fibrosus (AF), and the centrally located nucleus pulposus (NP), as shown in Figure 1. The IVD is separated from the vertebral bodies on top and bottom by a thin horizontal layer of hyaline cartilage known as the cartilaginous endplate (CE), which provides a pathway for nutrient transfer

longitudinally from the vascularized vertebral bodies to the adjacent avascular discs [18,168].

The AF consists of concentric rings, or lamellae, of aligned collagen fibers, with 15-25 lamella in a mature human IVD [121]. Fibers within a given lamella are oriented at approximately 60°-70° from the vertical plane, with concentric rings alternating in fiber direction (~120° to each other). Lamella are thicker anteriorly, and thinner posteriorly, inserting into the adjacent vertebral bodies above and below. The periphery of the AF is innervated and contains some radially penetrating vasculature which aids nutrient supply to the avascular center of the disc. Mechanically, the AF resists compressive and torsional spinal loads, restricts motion between adjacent vertebrae, and constrains the more fluid-like NP. Compositionally, the ECM of the AF contains a high percentage of collagen (70% of dry weight), primarily type I collagen fibers in the outer anulus, with the percentage of type II collagen increasing radially towards the inner AF (with a corresponding decrease of type I) [56]. Aggrecan is the major proteoglycan of the disc [96], maintaining tissue hydration and resisting compressive loading via the osmotic pressure from its' negatively charged chondroitin and keratin sulphate chains. Other compositionally minor (though potentially critical functionally) ECM components include collagen types III, VI, IX, and XI [152] , small proteoglycans (e.g. biglycan, decorin) [126], as well as elastin fibers [182] and the cell adhesive glycoprotein fibronectin [138]. The cells of the outer AF are fibrochondrocytic, elongated, and found

aligned parallel to collagen fibers, with cells becoming more rounded towards the inner AF [11,24,30].

The NP is a highly hydrated, viscoelastic gel [39,92,93] which acts mechanically to resist compressive loads and redistribute them radially to the surrounding AF. The structure, biochemical composition, and cell population of the human NP varies substantially with age and degeneration grade (degenerative changes described in Section 1.2). In the young, healthy human, the NP is comprised primarily of water (70-90% of wet wt.), proteoglycans (65% of dry wt.), and randomly oriented type II collagen (15-20% dry wt.) [56,70,162]. A high concentration of proteoglycans gives the tissue a high negative fixed-charge density and associated swelling pressure, binding water and giving the tissue fluid-like behaviors. Proteoglycans found in the NP contain primarily chondroitin and keratin sulphate side chains and are typically freely dispersed, with only ~30% found linked to hylaronan in aggregates [95]. The remaining components of the NP include elastin, small proteoglycans, and minor collagens (types III, VI, IX) [126,152,182]. Additionally, cell-associated laminin isoforms have been identified in immature NP tissues, as discussed in Section 1.5. The cell population of the human NP is also dynamic. Initially populated by cells derived from the embryonic notochord (see Section 1.3), these morphologically-distinct immature cells disappear within the first decade of human life and are replaced by a sparse population of small, rounded chondrocyte-like cells [165]. The cellular environment within the avascular NP is harsh,

with a limited nutrient supply including hypoxic conditions and low glucose levels [167]. These conditions are thought to worsen with age due to endplate structural changes, with decreased NP cell metabolism and viability with age or degeneration.

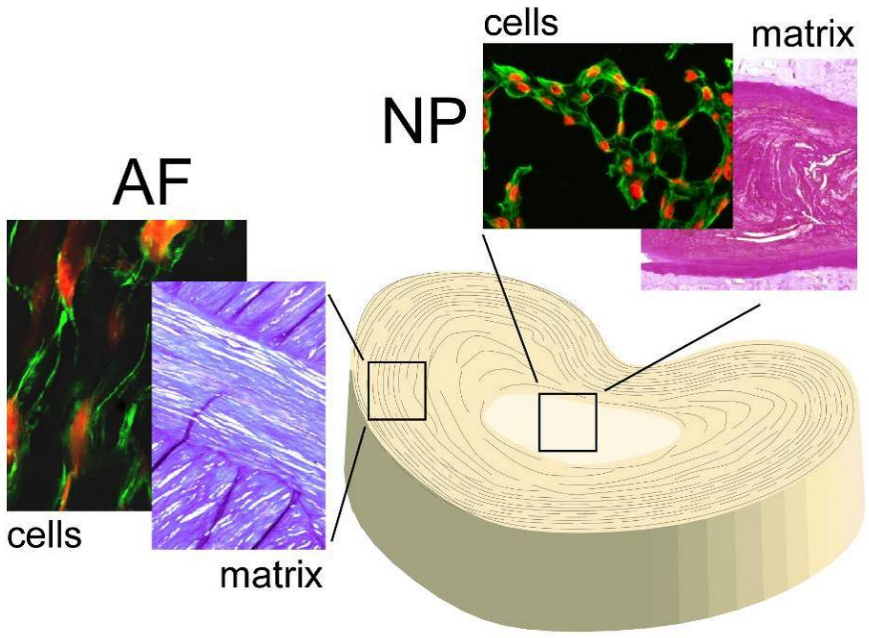

Figure 1: Matrix structure and cellular organization in the intervertebral disc. Cytoskeletal staining for AF (actin) and NP (vimentin) cells in immature porcine IVD tissues.

1.2 Intervertebral Disc Degeneration and Aging

Intervertebral disc (IVD) disorders are a major contributor to disability and health costs. Back pain is the most common musculoskeletal condition in the United States, affecting ~5-30% of the population annually [23,148,181] and having a lifetime prevalence of at least 60% [181]. Direct costs for spine related conditions in the U.S.

were estimated to be $194 billion per year for the years 2002-2004 [1], with surgical procedures to treat back pain numbering over 500,000 per year [101]. Intervertebral disc degeneration is complex and remains incompletely understood, but is closely associated with aging, inherited genetic factors [13,157,172], including defects in extracellular matrix genes (e.g. type IX, XI, II collagen [7,22,124,136]), as well as environmental factors such as physical activity and mechanical loading [4,171]. Anatomic features of disc disorders include IVD herniations, extrusions and tears, endplate changes, as well as loss of tissue hydration and disc height [19,25,151]. These features may result in nerve compression, spinal canal impingement, inflammation, and altered loading configurations which contribute to symptomatic back pain [89].

Disc disorders and resulting pain may be preceded by changes which first occur in the nucleus pulposus (NP) region of the IVD, where significant alterations in tissue cellularity, composition, and structure begin early in life and continue with increasing age and degeneration [19,25,183]. Cell density decreases significantly in the NP soon after birth as the disc grows and cells deposit large amounts of proteoglycan-rich matrix [18,142]. As the disc matures, changes in endplate structure, along with the disc's increasing size and avascular nature (the IVD is the largest avascular tissue in the human body), limit nutrient oxygen and glucose transport to NP cells responsible for tissue homeostasis [71,169], with increasing levels of cell death identified in the NP with aging (~50% of cells in young adults, ~80% in elderly adults) [25]. This decrease in cell

viability and metabolic activity impedes tissue maintenance and repair in the NP, resulting in a metabolic imbalance and tissue breakdown [71,154]. Correspondingly, proteoglycan and water content in the NP both decrease significantly with increasing age [25,70], impairing the tissue's primary function of resisting and redistributing compressive loads. As a result, higher compressive loads may be transferred to the AF, compromising its structure and function (e.g. overload leading to clefts, buckling, or rupture).

Significant interest exists in biological approaches to treat IVD disorders [17,98,154], with therapies to repair or replace the NP of particular interest as a means to restore normal disc function or impede degeneration. These may include cell replacement or tissue engineering strategies to replenish the population of healthy cells and hydrated matrix in the NP [99,135,139], as well as growth factor supplementation to stimulate matrix production by existing cells [122,123]. However, a number of questions remain regarding these strategies and their feasibility. For cell replacement therapies, these include: (1) What is the appropriate matrix composition for tissue repair, since the NP's matrix structure transitions from fluid-like gel to cartilage-like tissue during human life? (2) What is the appropriate NP cell phenotype and cell source to create this tissue, and are immature (notochordal-like) NP cells an appropriate cell type for producing this matrix? (3) What are the appropriate environmental cues (e.g.

biomaterial composition, cell-adhesive ligands, material stiffness, growth factors or other nutrients) to promote or maintain an NP-like phenotype?

1.3 IVD Development and the Role of the Notochordal Cell

1.3.1 Notochordal Cells of the Immature NP

The IVD contains cells of both mesenchymal (AF) and notochordal (NP) origins. During development, the notochord, a rod-like line of cells which forms the axial skeleton during embryogenesis, disappears in the regions of the vertebral bodies and expands (or is squeezed) to form the nucleus pulposus (NP) in the center of the IVD [37,41,67,156], as shown in Figure 2. Notochordal cells proliferate within the newly formed NP and synthesize a highly-hydrated extracellular matrix, including large amounts of negatively-charged proteoglycans, as well as collagenous and non-collagenous proteins [141,179].

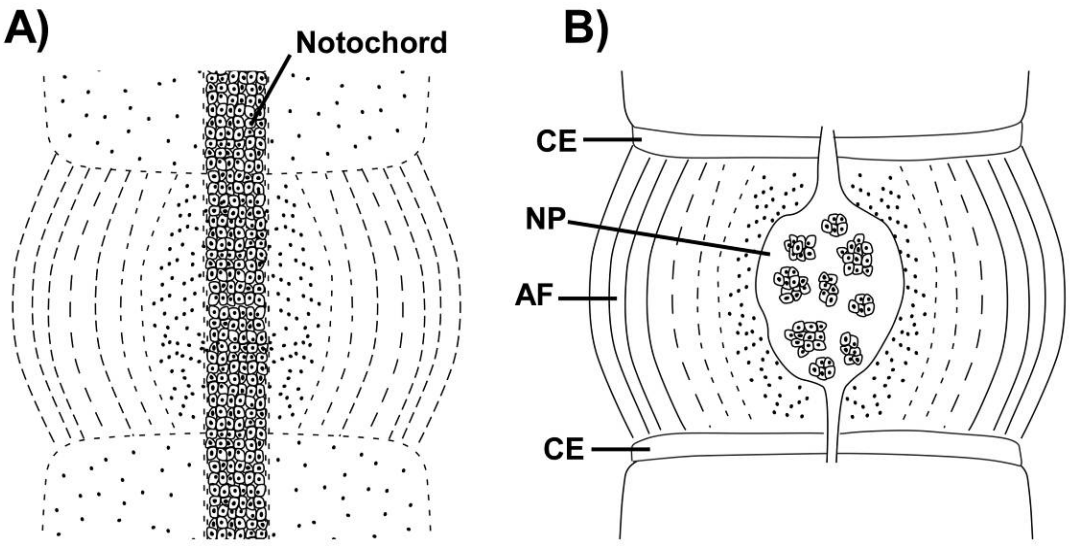

Figure 2: Intervertebral disc development. (A) A mesenchymal disc forms around the central notochord in the embryo, with peripheral cells aligning to form the future AF lamellae. (B) The notochord expands to form the nucleus pulposus (NP), with cartilage end plates (CE) forming above and below the disc.

Notochordal NP cells exhibit several phenotypic and morphological features that reflect their unique embryologic origin and distinguish them from other cells of the disc. They are large in diameter [75,165], highly vacuolated, and organized in clusters [86,165] with strong cell-cell interactions characterized by desmosomal cell-cell adhesions [80,111], gap junctions [86,165] and expression of cadherins, as shown in Figure 3B [69,80]. They are rich in cytoskeletal proteins, with high expression of both cytokeratin (Figure 3A, isoforms 8, 18, 19) and vimentin intermediate filaments [69,75,111,160]. These two cytoskeletal proteins are often used to distinguish cells of epithelial

(cytokeratins) and mesenchymal (vimentin) phenotypes [100,125], and co-expression of these proteins may indicate that NP notochordal cells possess characteristics of cells from both origins, or transition from an epithelial to a mesenchymal phenotype during development and aging [69]. Additionally, these cells express laminin receptors and cell-associated laminin extracellular matrix proteins, as detailed in Section 1.5. A summary of documented notochordal-like cell features is listed below in Table 1.

Table 1: Summary of Notochordal-like Cell Features

Category	Features	References
Morphological	large cell size intracellular vacuoles	[75,165]
Cell-Cell and Cell-Matrix Adhesions	desmosomes gap junctions cadherins α6, β4 integrins CD239 cell-associated laminins	[33,34,65,69,80,86,111,131,165]
Cytoskeleton	cytokeratins 8, 18, 19 vimentin	[69,75,111]

1.3.2 Notochordal Cell Fate and Possible Function in the IVD

In humans, notochordal-like NP cells begin to disappear (as identified morphologically) soon after birth and are rarely observed in the NP after age 7 [162]. A sparse population of smaller chondrocyte-like cells appears in the NP at this time [165]; however, the origin of these remaining NP cells remains poorly understood. It has been postulated that these remaining cells may migrate to the NP from the adjacent inner AF or cartilage endplates [103,104], or alternatively, may be notochordal cells which have undergone terminal differentiation. Changes in the human disc composition and structure occur around this same time, with the most dramatic changes occurring in the NP region [25]. Cell numbers, proteoglycan levels, and water content all decrease in the human NP [8,19,143,151] within the first decade of life, with tissue stiffness increasing

with age [91]. These changes result in a loss of NP hydration and swelling pressure, which in turn may eventually contribute to altered IVD mechanics and anatomical features (loss of disc height, facet osteophyte formation) characteristic of disc degeneration. Thus, it has been hypothesized that notochordal cells play a key role in maintaining metabolic balance in the disc, and that loss of this cell population may be an initiating event in a progression towards human IVD degeneration [137].

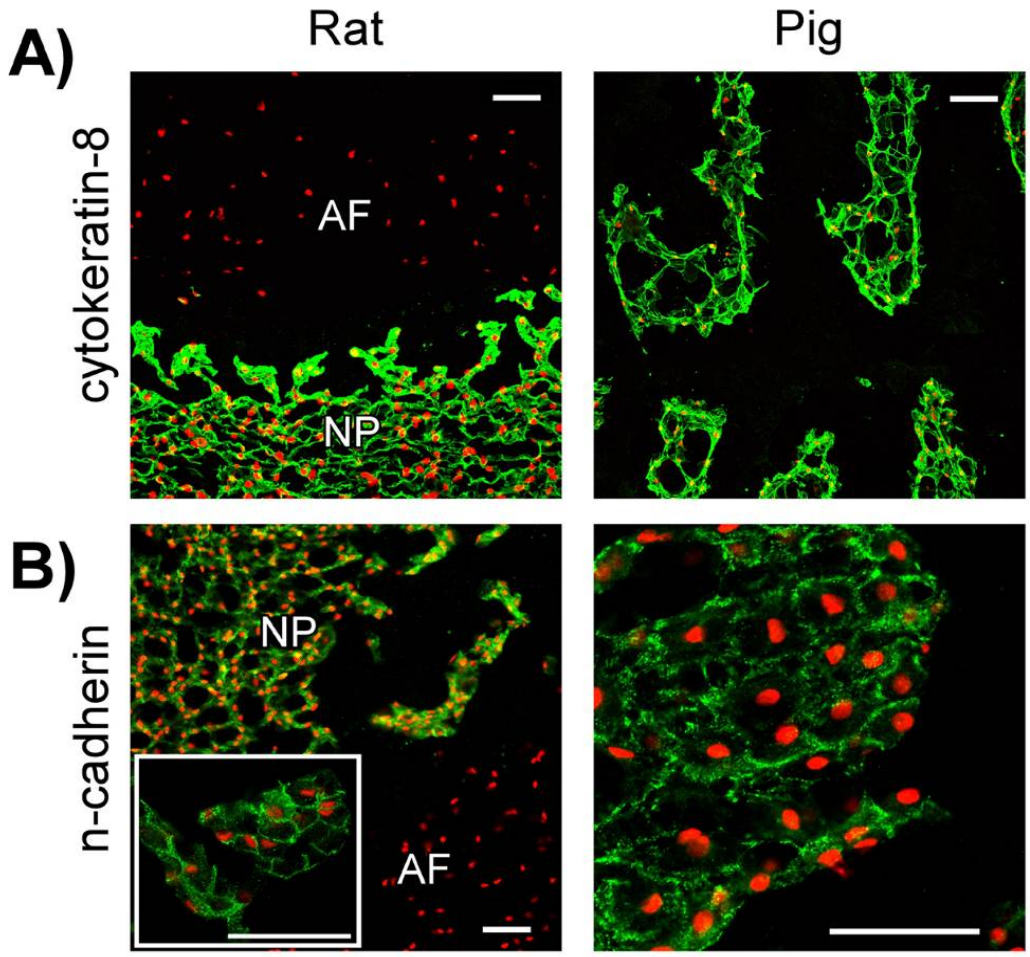

Figure 3: Expression of (A) cytokeratin-8 and (B) n-cadherin in rat and porcine NP tissues. N-cadherin staining (see high magnification inset for rat) identifies cell-cell boundaries within NP cell clusters. Scale bars = 50μm.

In other species, however, the fate of notochordal cells in the NP varies, with species such as rat, rabbit, pig, and some breeds of dog maintaining immature (notochordal-like) cells much later into (or throughout) life [26,32,87]. These animal models provide an opportunity to study immature NP cells *ex vivo* in order to gain

further knowledge of their biology and function. In vitro studies indicate immature NP cells may play a critical role in maintaining IVD metabolism, both by producing proteoglycan-rich ECM and acting as stimulators of other disc cell types. Immature NP cells have been shown to be biosynthetically active [14,31,54], including the finding that large (immature) NP cells had proteoglycan production rates 50% higher than that of smaller (chondrocyte-like) NP cells from the same animal [31]. Furthermore, several studies examining the co-culture of immature NP cells with other cell types from the disc (chondrocyte-like NP cells, AF cells) indicate immature NP cells release soluble factors which stimulate proteoglycan production, alter gene expression, and increase proliferation in other disc cells [5,21,54]. A key soluble factor produced by immature NP cells may be connective tissue growth factor (CTGF), which has been identified via mass spectrophotometric analysis of conditioned media and shown to stimulate proteoglycan production in a similar manner to NP conditioned media [53]. In addition to these *in vitro* findings, several studies have examined the effects of allografting immature NP cells or tissue into an animal model of disc degeneration, with findings that this procedure delayed degeneration [135,139]. These results suggest immature NP cells may be effective for use in NP replacement tissue engineering strategies.

Further study of the phenotype and function of immature NP cells has been limited in part due to lack of knowledge of appropriate culture conditions necessary to maintain or expand this population of cells *in vitro*. Monolayer culture of immature NP

cells has proven challenging, as these cells are not adhesive to standard culture surfaces (tissue culture plastic, gelatin-coated plastic), with just a small fraction of isolated cells attaching to surfaces after days of culture [54,174]. Once adherent, these cells quickly lose many of their unique morphological characteristics (loss of vacuoles, spread fibroblastic morphology, decreased cell size [174], unpublished observations) and potentially their phenotype. Alternatively, hydrogel systems (agarose, alginate) have been utilized in some studies [35,36], with reports of significant apoptosis [88,119] and little analysis of phenotypic maintenance or cell proliferation. Thus, appropriate cell culture environments for immature NP cells are as yet unknown, but are critical for further investigations of the phenotype, function, expansion of this cell population.

1.4 Role of Matrix Ligands (Laminins) in Modulating Cell Behaviors

It is well-established that cell-matrix interactions play important roles in controlling cell behaviors, with particular ECM ligand-receptor (e.g. integrins [90]) interactions eliciting specific cellular responses, including directing cell phenotype, survival, and organization. Previous work (see Section 1.6) indicates a unique feature of the immature NP is an ECM environment rich in the extracellular matrix protein laminin, with NP cells expressing many laminin receptors, in stark contrast to adjacent AF tissues. Laminins are cross-shaped heterotrimeric glycoproteins consisting of α,β, and γ polypeptide chains (Figure 4) which form 15 known laminin isoforms [10,40,128]

(specific laminin isoforms are identified using the chain numerals: for example, the isoform containing α5, β1, and γ1 chains is identified as LM-511). Laminin isoform expression varies widely across tissue types and with developmental stage, including acting as a critical cell-adhesive ligand within basement membrane tissues [184]. Cellular interactions with laminins are mediated via several integrin receptors, including α6β1, α6β4, α7β1, α1β1 and α3β1 [102,127,134]. Non-integrin proteins, including Lutheran (CD239), α-dystroglycan and CD151, also contribute to cell interactions with laminins and may potentiate the strength of cell adhesion in conjunction with integrins [94,102,110,134].

Cell adhesion to laminins has been shown to direct a number of important biological processes. Laminins play key roles throughout development, where they are involved in tissue morphogenesis and organization [128,186], with temporal and spatial expression of specific laminin isoforms playing critical roles in tissue formation [113,132]. Laminins and laminin receptors (α6β1 and α6β4 integrins, in particular) have also been shown to be involved in the invasion, progression, and survival of cancers [38,127], including promoting cell survival in response to environmental stress conditions such as nutrient deprivation and hypoxia [38,72]. Additionally, several laminin isoforms (LM-111, LM-511) have been shown to drive cadherin-mediated cell-cell interactions [105,176] in embryonic and epithelial cells. In 3-dimensional models of breast cancers, laminin (LM-111) has been shown to be critical for *in vitro* formation of

functional, polarized cell clusters (acini) similar to those found *in situ* in mammary tissues [73,177]. Finally, laminins have also been shown to be critical regulators of cell phenotype, with specific laminin isoforms possibly inhibiting or driving cell differentiation. Embryonic stem cells cultured on laminin isoform LM-511 were found to self-renew and maintain pluripotency markers (over 169 days of culture), in contrast to culture on other ligands (e.g. gelatin, poly-lysine, LM-111, LM-332) [48]. In contrast, mesenchymal stem cells cultured on LM-332 have been shown to differentiate towards an osteoblastic phenotype [106,107]. Thus, laminins may play important roles in directing cellular phenotype and organization, with individual isoforms eliciting unique responses.

Additionally, cell-laminin interactions are known to play important functions in cell adhesion and cell-matrix mechanical interactions. Binding of the integrin receptor $\alpha 6\beta 4$ to laminins (e.g. LM-332) may lead to the formation of hemidesmosomes, which are stable cell-matrix adhesions linking the ECM to the intermediate filament cytoskeleton [20,114,133]. These adhesions are responsible for maintaining tissue mechanical integrity in tissues such as epithelia [60], with genetic defects in hemidesmosomal components (including $\alpha 6\beta 4$ and LM-332) resulting in reduced mechanical strength and blistering of epithelia [20]. Additionally, the intermediate filament cytoskeleton may have direct links to the cell nucleus [62,83], potentially creating a pathway for mechanotransduction from ECM to the nucleus [120]. The

expression of α6 and β4 integrins, as well as LM-332, in immature NP tissues (see Section 1.6) suggests that laminins may play important roles in NP adhesion and cell-matrix mechanical interactions.

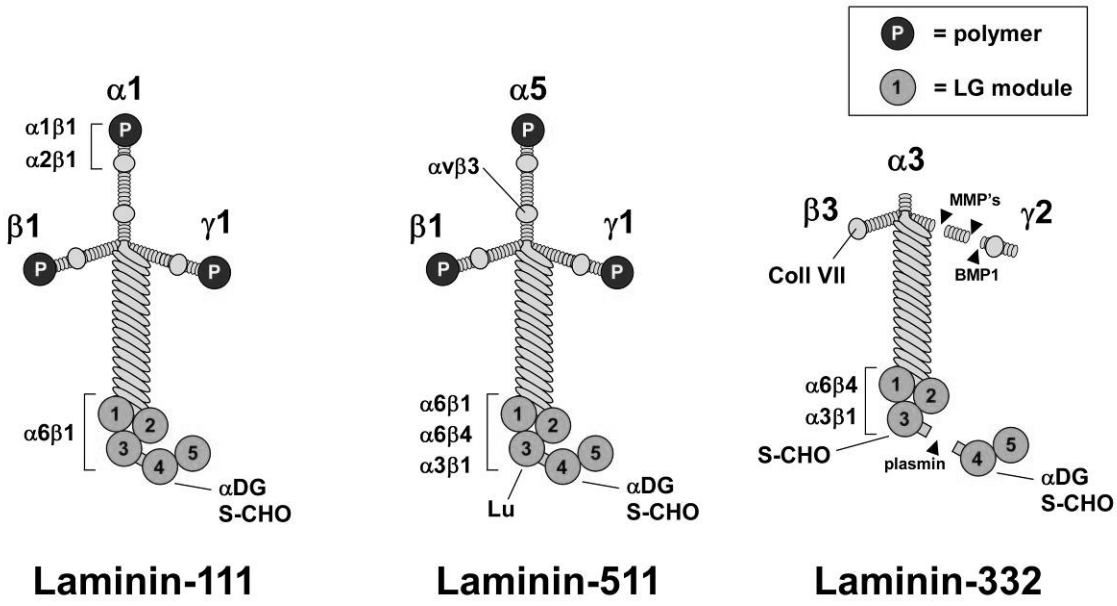

Figure 4: Structure and receptor binding domains of laminin isoforms LM-111, LM-511, and LM-332. αDG: alpha dystroglycan receptor; S-CHO: cell surface sulfated carbohydrates; Lu: Lutheran receptor (CD239). Laminin receptor binding and cleavage information from [102,128,134].

1.5 Laminin and Laminin Receptor Expression in the Immature NP

In the IVD, laminin expression was initially documented in the developing rat [81], where in early developmental stages the laminin γ1 chain is present in the notochord, localized on cell surfaces and within the notochordal sheath. In later developmental stages and the neonate laminin γ1 was found to be strongly expressed in

the nucleus pulposus, with weak pericellular staining within the inner, but not outer, anulus region [81]. This corresponds with findings in our laboratory for strong γ1 expression in the NP, but not AF, of immature porcine, rat, and young (2 year old) human IVD tissues, as shown in Figure 5. However, the γ1 chain is part of multiple laminin isoforms (10 of 15), and thus does not identify the specific laminin isoforms present. More recently, the laminin α5 chain (LM-511, LM-521 isoforms) has been shown to be highly expressed in the NP extracellular matrix in immature porcine and rat, as well as juvenile human NP tissues (Figure 5, left panel) [33]. Additionally, the LM-332 isoform has also been identified exclusively in NP region of immature rat and porcine IVD tissues, as shown in Figure 6A. Together, these findings indicate that laminin is uniquely and highly expressed in the NP region of the immature IVD, with the isoforms LM-511 (or -521) and LM-332 present and appearing to be cell-associated.

In conjunction with these findings, a number of laminin-specific cell-matrix receptors have also been shown to be uniquely expressed in the NP of immature IVD tissues. Immunohistochemical staining of porcine, rat, and human tissues has identified the presence of laminin-binding integrin receptors (α3, α6, β4, as well as non-integrin receptors Lutheran blood group glycoprotein (Lu or CD239) and tetraspanin (CD151) [33,131]. Porcine NP tissues demonstrated strong staining for α6 and β4 integrins (Figure 7), Lu (Figure 7), and CD151 (not shown), whereas the porcine AF did not. Similar expression patterns were identified in human and rat tissues, although in older

human NP tissues expression of Lu was lost [33]. Dramatic regional differences in laminin receptor expression can be visualized in immature rat tissues (β4 integrin), shown in Figure 6B, where the small tissue size permitted preservation of the NP-AF interface. Together these data indicate receptors capable of interacting with laminins LM-511/-521 (α6β1, α6β4 integrins, Lu, and CD151), LM-111 (α6β1), and LM-332 (α6β4) are highly expressed in the immature NP, but not AF, tissues of pig, rat, and young human.

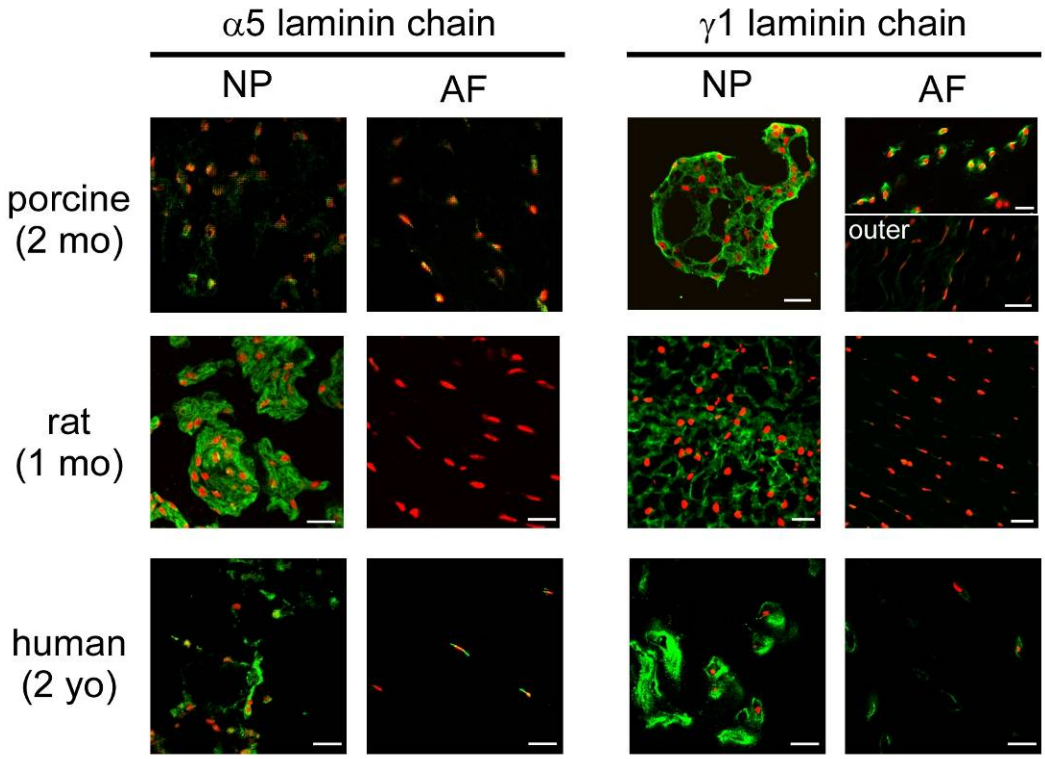

Figure 5: Expression of laminin chains in IVD tissues identified via immunohistochemistry. Differential expression of laminin α5 and γ1 chains between NP and AF regions of immature porcine, rat, and human IVD tissues. (green: laminin, red: cell nuclei). Scale bars = 50 μm.

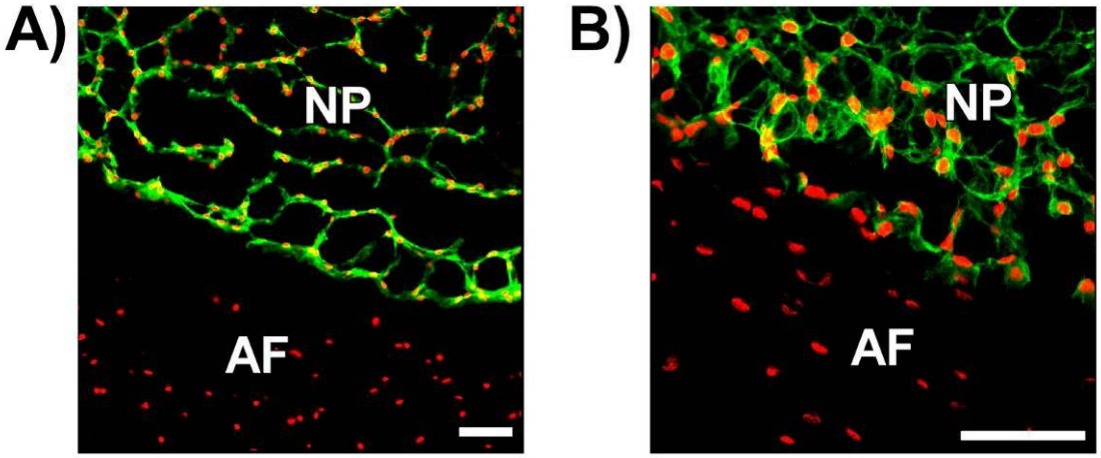

Figure 6: Rat IVD tissues (1 mo. old) with immunostaining for (A) laminin isoform LM-332 and (B) β4 integrin, with expression of both confined to NP tissue (green: (A) laminin or (B) integrin, red: cell nuclei). Scale bars = 50μm.

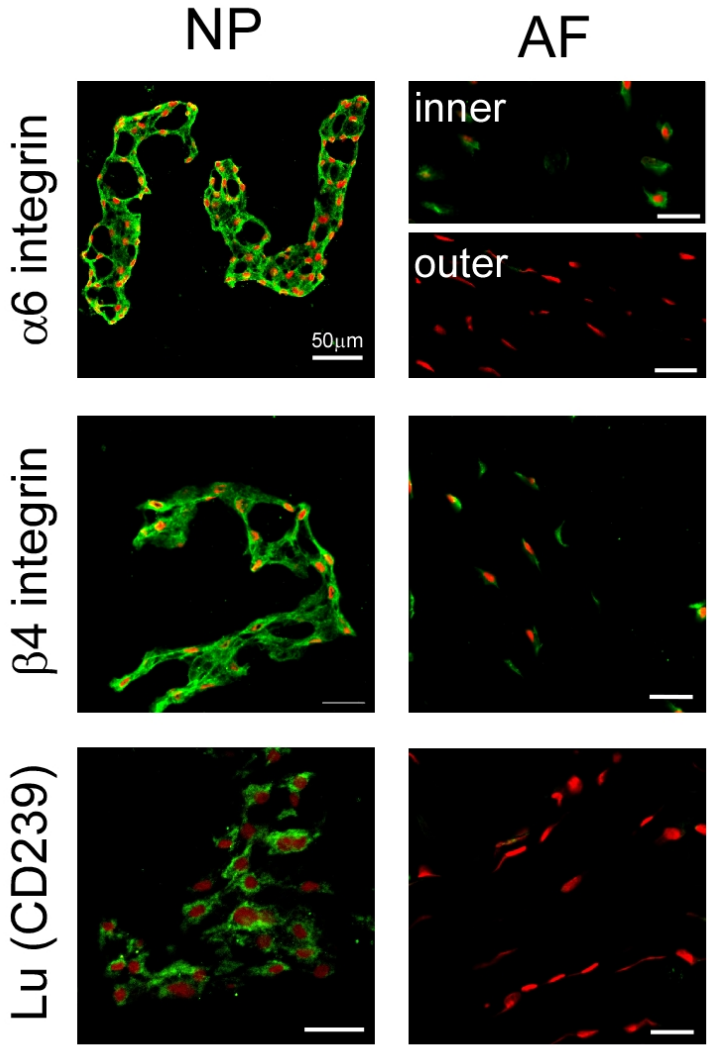

Figure 7: Laminin receptor expression in immature porcine IVD tissues (green: receptor, red: cell nuclei). Scale bars = 50μm.

1.6 Role of Matrix Elasticity in Modulating Cell Behaviors

In addition to ECM ligand, another important extracellular signal guiding cell behaviors is the mechanical stiffness of the matrix environment. Integrin ligand

occupancy alone has been shown to generate minimal downstream cell signaling responses as compared to tethered ligands, which result in integrin clustering and cytoskeletal force generation [61,64,129,130]. Original observations of fibroblasts seeded on unrestrained (floating) collagen gels showed cell responses distinct from those on restrained gels, with cells in unrestrained gels lacking pronounced actin stress fibers [79] and down-regulating focal adhesion protein levels [175]. Epithelial cells form functional, polarized cell clusters when seeded in soft (<1000 Pa) gels containing laminin-rich basement membrane extract [153,161,176,177], but this organization and function is disrupted in gels with higher stiffnesses [140]. However, isolating the specific effects of matrix elasticity has proven challenging using natural ECM gels, since mechanical properties are not easily tuned without changing gel composition (e.g. increasing collagen concentration), and enzymatic breakdown may lead to changes in mechanical properties of the gel over time in culture. Hydrogels are another soft material culture system which can preserve rounded cell morphologies by encapsulating cells, and have been functionalized with ligand-mimicking peptides or ECM proteins [155,159]; however, providing fully functional ligands and presenting ligands at sufficiently high densities remains a challenge.

1.6.1 Studies of Matrix Elasticity with Polyacrylamide Gel Substrates

Thin gels of polyacrylamide [144] have facilitated studies of matrix elasticity by permitting the user to tune the stiffness of a 2-dimensional soft gel by altering the concentration of bis-acrylamide crosslinker, while maintaining a constant gel chemical composition. Gels can be tuned over a range of physiologically relevant elasticities (0.1 – 35 kPa) and exhibit linearly elastic properties [49,144]. ECM proteins are covalently-coupled to the surface of the gel (via photo-activatable crosslinker) to present a cell adhesive ligand. Studies utilizing this system have identified important roles for substrate stiffness in modulating cell adhesion, spreading, motility, and organization [49,78,144,145]. On more flexible substrates, cells (e.g. fibroblasts, epithelial cells) become less spread, more motile, have unstable and irregular cell-matrix adhesions, and exhibit decreased adhesion strength as compared to cells on stiff substrates [78,144]. Substrate stiffness may modulate cell-cell interactions, with the observation that cells compact into multi-cell 3D aggregates on soft but not stiff substrates, and migrate out of tissue explants onto stiff, but not soft, substrates [78]. These findings suggest that cells may seek to maximize mechanical input from their surroundings, with cell-cell adhesions potentially competing directly with cell-matrix adhesions.

Substrate elasticity also plays a critical role in directing or maintaining cell phenotype. Studies suggest differentiated cells may have an "optimal" or preferred tissue stiffness that matches the stiffness of the native tissue or the cells themselves.

Myoblasts exhibit optimal differentiation into myotubes on substrates with stiffnesses that matched those of the native tissue and cells, but not on softer or stiffer substrates [51]. Cardiomyocytes derived from embryos maintain spontaneous beating patterns on substrates with stiffnesses similar to, or softer than, native cardiac tissues, but not on stiffer substrates [50]. Substrate elasticity has also been shown to be an important factor directing stem cell differentiation [47,52,55], with human mesenchymal stem cells cultured on tissue-appropriate stiffnesses (i.e. bone: stiff substrate) differentiating towards that stiffness's lineage (demonstrated for neuronal, myoblastic, and osteoblastic lineages), even in the absence of chemical inductive factors [52]. Thus, substrate stiffness may play a key roles in directing or maintaining cellular phenotypes.

2. Nucleus Pulposus Cell Adhesion and Functional Interactions with Extracellular Matrix Proteins

Partially adapted from : Gilchrist CL, Chen J, Richardson WJ, Loeser RF, and Setton LA, "Functional Integrin Subunits Regulating Cell–Matrix Interactions in the Intervertebral Disc", *Journal of Orthopaedic Research*, 25(6):829-40, 2007.

2.1 Introduction

Cell-matrix interactions play important roles in controlling a wide range of cell behaviors, with particular ECM ligand-receptor (e.g. integrins [90]) interactions eliciting specific cellular responses. Immunohistochemical staining of immature IVD tissues suggests NP cells reside in a unique ECM environment, with expression of cell-associated laminin and expression of laminin receptors, in stark contrast to cells of the adjacent AF [33,65,131]. Whether these observed tissue-level expression patterns translate into functional differences between IVD cell types or preferential adhesion of NP cells to particular ECM constituents (including specific laminin isoforms) is not yet known. Knowledge of preferred ECM ligands for NP cells is potentially useful for a variety of reasons, including : (1) to facilitate *in vitro* NP cell culture studies, as these cells exhibit limited adhesion to standard culture surfaces (e.g. tissue culture treated plastic, gelatin-coated plastic), (2) examine the abilities of these ligands to affect NP cell phenotype *ex-situ*, with the potential to develop NP cell-adhesive biomaterials which promote or maintain an NP cell phenotype via outside-in signaling, (3) to investigate whether differential receptor expression patterns observed in IVD tissues might be

useful for selection or sorting of NP cells from a mixed IVD cell population (which likely exists in maturing NP tissues).

Based on evidence of laminin and laminin-receptor expression *in situ* that appears to be unique to the nucleus pulposus region, it was hypothesized that cells from the NP would preferentially interact with laminin ligands as compared to several other ECM ligands found in the IVD, and in contrast to cells from the adjacent AF region (**Hypothesis 2.A**). Additionally, it was hypothesized that these NP cell-laminin interactions are mediated by specific laminin-binding integrin receptors (**Hypothesis 2.B**). Finally, it was hypothesized that preferentially interact with two laminin isoforms, LM-511 and LM-332, as compared to other ECM proteins (including other laminin isoforms; **Hypothesis 2.C**). To investigate these hypotheses, quantitative assays of cell attachment, cell spreading, and mechanical attachment strength were used to compare NP cell interactions with different ECM ligands, with function-inhibiting antibodies utilized to determine the roles of specific integrin receptors in mediating these interactions.

2.2 Methods and Materials

2.2.1 Cell Isolation and Culture

Lumbar spines were obtained from pigs immediately following sacrifice (L1–L5, 3-6 months old). Cells were isolated from the NP and AF regions of IVD's via overnight

enzymatic digestion. NP tissue was digested overnight at 37°C in wash medium (Dulbecco's Modified Eagle's Medium (Gibco, Invitrogen, Carlsbad, CA) containing 5% FBS (Hyclone, Thermo Fisher Scientific, Pittsburgh, PA), 1.65 mL of 300X Gentamycin (Gibco, Invitrogen), 5mL of 100X Kanamycin (Sigma, St. Louis, MO), and 2 mL of 250X Amphotericyn B (Gibco, Invitrogen)) with 0.08% collagenase type 2 (Worthington Biochemicals, Lakewood, NJ) and 0.04% pronase (Roche Applied Science, Mannheim, Germany). The remaining cell suspension was spun at 400g to collect the cell pellet, and washed with wash medium, with this washing procedure repeated twice. In some cases where NP cells remained in cell clusters (aggregates) following washing, cells were resuspended briefly (3-5 minutes) in non-enzymatic cell dissociation buffer (Mediatech, Manassas, VA) and passed through a 70 μm cell strainer (BD Falcon, Bedford, MA). AF cells were isolated using a similar procedure, except a sequential pronase-collagenase digestion was performed, with minced AF tissue placed in wash medium with 0.2% pronase for 1h at 37°C, washed twice with wash medium, then incubated overnight in 0.1% collagenase type 2. Following washing, isolated NP and AF cells were resuspended in culture media (Ham's F-12 media (Gibco, Invitrogen) supplemented with 10% FBS (unless otherwise noted), 10mM HEPES (Gibco), 100 U/mL penicillin (Gibco) and 100 mg/mL streptomycin (Gibco) and counted using a standard hemocytometer. Isolated cells were either used immediately for some experiments, or

cultured in subconfluent monolayers (50,000 cells/cm^2) on 0.1% gelatin-coated (Sigma, St. Louis, MO) T75 tissue culture flasks for 2–6 days in culture media.

2.2.2 Flow Cytometry

AF and NP cells were analyzed via flow cytometry to quantify expression levels of integrin receptor subunits. Integrin subunits selected for analysis were previously identified in porcine IVD tissues [131] as being highly expressed (α1, α5, β1) or regionally varying (α6). Freshly isolated (Day 0) and monolayer cultured (Day 3 and 7) cells (n=3 separate cell isolations from AF and NP tissues; each isolation pooled from 2 spines) were resuspended in serum-free F12 media (Ham's F12 media with 10mM HEPES, 100 U/mL penicillin (Gibco), and 100 mg/mL streptomycin (Gibco)) and allowed to recover in suspension for 2h at 37°C. Cells were then incubated for 30 min at 4°C with one of the following integrin antibodies (10 μg/mL) specific for the extracellular domain of a particular integrin subunit: α1 (MAB1973Z, Chemicon, Temecula, CA), α5 (555651, BD Pharmingen, San Diego, CA), α6 (555734, BD Pharmingen), β1 (4B4, Beckman Coulter, Fullerton, CA), or appropriate IgG isotype negative controls (mouse IgG1, CBL600; rat IgG2a, CBL605, Chemicon). All flow cytometry integrin antibodies were confirmed (by manufacturer or using porcine IVD cells) to cross-react with pig. Cells were washed twice with PBS and incubated with appropriate secondary antibody (10 μg/mL Alexa 488, Molecular Probes, Eugene, OR) for 30 min at 4°C. Cells were analyzed on a FACScan flow cytometer (Becton Dickinson) to measure the (geometric)

mean fluorescence intensity (MFI) and percentage of cells with positive surface proteins (%). IgG control values were recorded and subtracted from experimental values of fluorescence. Differences were analyzed via two-way ANOVA (tissue region, culture time) at a significance level of $p=0.05$.

2.2.3 Integrin Blocking

96-well culture plates (Corning Costar) were coated with one of the following matrix proteins (Sigma) diluted in PBS: bovine type I collagen (40 μg/mL), chicken type II collagen (40 μg/mL), human plasma fibronectin (1 μg/mL), by overnight incubation at 4°C; or mouse laminin-111 (mouse EHS laminin, 20 μg/mL, Chemicon) incubated 2h at 37°C. Coated wells were then blocked with 3.75% BSA (Gibco, Gaithersburg, MD) for 3h at 37°C. Wells without matrix protein (BSA blocked only) were used as a substrate negative control to identify non-specific cell attachment.

Cells in monolayer culture (n=3 separate isolation pools each for NP and AF cells) were detached from the culture surface using 0.025% trypsin/EDTA (Cambrex, East Rutherford, NJ) and immediately washed in soybean trypsin inhibitor (Sigma, 1mg/mL) to prevent enzymatic cell damage without introducing serum, which contains exogenous matrix proteins (e.g. fibronectin present in serum). Cells were resuspended in serum-free F12 media containing one of the following integrin function-blocking antibodies specific for a particular integrin subunit or dimer (from Chemicon, 10 μg/mL, unless otherwise noted): α1 (clone FB12), α2β1 (BHA2.1), α3 (P1B5), α5 (P1D6), α6

(NKI-GoH3, 40 μg/mL), αv (AV1), αvβ3 (LM609), αvβ5 (P1F6), β1 (4B4, Beckman Coulter). Cross-reactivity with pig was confirmed by the manufacturer or via flow cytometry and an ability to functionally inhibit attachment; confirmation was obtained for all antibodies except those against the α5 subunit, for which no cross-reacting function-blocking antibody could be identified. Control cells were resuspended without blocking antibody or with non-blocking mouse IgG antibody. Additionally, small peptides containing the RGD sequence (1mM GRGDSP, Anaspec, San Jose, CA) or control RGE sequence (GRGESP, Anaspec) were used to investigate whether cell attachment was dependent on this common integrin-binding peptide sequence contained in matrix proteins such as fibronectin.

Cells were pre-incubated in suspension with antibodies or peptides for 30 min, seeded on matrix-coated culture plates, and incubated at 37°C for 1h to allow for attachment (20,000 cells per well, 4 replicates (wells) per blocking condition). Wells were rinsed twice with serum-free media to remove unattached cells. Remaining cells were fixed with 4% formaldehyde, cell nuclei were labeled (Hoechst 33342, Sigma), and cells in the central region of each well were imaged via fluorescence microscopy (Zeiss Axiovert S100 equipped with Nikon CoolPix 990 digital camera). Total number of cells per image were counted and normalized to unblocked controls for each substrate. Differences in cell attachment between unblocked control and integrin-inhibited cells were compared for each substrate via ANOVA ($p<0.05$).

To further elucidate findings on laminin-111 substrates, porcine NP cell attachment to laminin was evaluated by microscopy to quantify the distribution of attached cell diameters. DIC images of attached cells in each well (1 image field/well, 10X) were recorded and cell diameters were measured using ImageJ software (NIH, Bethesda, MD). Attached NP cells were spherical and had not spread out on substrates at time of fixation.

2.2.4 Collagen Gel Contraction

An established collagen gel contraction assay [76] was performed to assess IVD cells' ability to mechanically interact with fibrillar type I collagen, and the role of particular integrin subunits in mediating this mechanical interaction. 96-well plates were coated with 3.75% BSA at 4ºC overnight and washed twice with PBS. Porcine AF cells were trypsinized from plates as described above and resuspended in culture media with or without integrin function-blocking antibodies (α1, β1) and incubated at 37ºC for 30 min. The cell suspension was combined with collagen solution (Cultrex bovine type I collagen solution, Trevigen, Gaithersburg, MD; HEPES, and NaOH) to yield a final concentration of 300,000 cells/mL, 1.5 mg/mL collagen, and 10 μg/mL of blocking antibody or IgG control. One hundred microliters of cell/collagen solution was dispensed per well (3-4 wells per condition) and the plate was immediately incubated for 45 min at 37ºC to allow for collagen gelation. After collagen gels had formed, 100 μL per well of culture media was injected to release gels from the plate, resulting in free-

floating gels. The plate was then incubated at 37°C and gel diameters were measured via inverted microscope at 0 and 18hr. Differences in gel diameter between integrin function-blocking conditions and unblocked control cells were detected via ANOVA ($p<0.05$).

2.2.4 Adhesion of Freshly Isolated NP Cells to Laminin Isoforms

96-well culture plates (Corning Costar) were coated (overnight at 4°C) with one of the following matrix proteins diluted in PBS: chicken type II collagen (40 μg/mL, Sigma), human plasma fibronectin (40 μg/mL, Gibco), mouse laminin-111 (40 μg/mL, Sigma), laminin-511 (human placental laminin, Sigma, 20μg/mL; this commercial preparation has been determined to consist primarily of laminin-511 [180]); coating densities were saturating densities which maximized NP cell adhesion. In addition to these purified proteins, a surface rich in laminin-332 (which was unavailable in a purified form) was created by incubating culture wells with conditioned medium collected from rat carcinoma cell line 804G (as described below). All coated wells were blocked with 3.75% BSA (Gibco) for 3h at 37°C, and wells without matrix protein (BSA blocked only) were used to identify non-specific cell attachment.

The rat carcinoma cell line 804G (a gift from Dr. George Plopper) [147] was used to generate conditioned media containing LM-332. To generate conditioned media, 804G cells were first grown in T175 flasks in culture media (DMEM supplemented with 10% FBS, 10mM HEPES, and 2mM L-glutamine) until reaching semi-confluence (~80-

90%). Culture media was then replaced with 30 mL serum-free media (same as formulation above, without serum) and cells cultured for an additional 3 days. Conditioned medium was collected, clarified (centrifuged at 15000g for 5min), and the supernatant stored at -20C until use. Wells were coated with undiluted conditioned media overnight (4°C), washed with PBS, and blocked with BSA as described above. The presence of laminin-332 on well surfaces was confirmed using a mouse anti-laminin-332 antibody (clone FM3 [146], gift from G. Plopper), detected using a goat anti-mouse Alexa 488 fluorescent secondary antibody and quantified via fluorescence microscopy.

Immediately following isolation from NP tissue, cells in serum-free F12 media were seeded (20,000 cells/well) and allowed to attach for either 30 min or 4h (37°C, 5% CO_2). Wells were gently rinsed twice with serum-free media to remove unattached cells. Remaining cells were fixed with 4% formaldehyde, cell nuclei were labeled (Hoechst 33342, Sigma), and cells were imaged via fluorescence microscopy (1 image/well, 10X objective, Zeiss Axiovert S100 equipped with Nikon CoolPix 990 digital camera). Differences in attachment numbers between substrates were detected via ANOVA ($p<0.05$) for each attachment time.

2.2.5 NP Cell Spreading and Morphology

To examine the effect of ECM ligand on NP cell morphology and spreading dynamics, primary NP cells were seeded onto ECM substrates and cell spread areas (2D

projection) were measured over time. NP cells (enzymatically isolated as described above, cultured for 2-6 days on gelatin-coated flasks in F12 culture medium with 5% FBS) were detached from the culture surface (0.025% trypsin/EDTA), resuspended in serum free media, and seeded (5,000 cells per well) onto ECM protein-coated clear 96–well plates. ECM ligands and coating concentrations were the same as those used in Section 2.2.4. Cells were allowed to attach for 1, 2, 3.25, and 4 hours at 37°C, then fixed in 4% formaldehyde (diluted in prewarmed Dulbecco's PBS with Ca^{++}, Mg^{++}.) for 15 min at room temperature. To fluorescently label the actin cytoskeleton (used to define cell boundary) and cell nuclei (used to identify individual cells), cells were first permeabilized with 0.2% Triton X-100 in PBS, then incubated with Alexa Fluor 488 phalloidin (1:250 in PBS) and propidium iodide (200 μg/mL) for 45 min. Images of cells were obtained using an inverted laser scanning confocal microscope (Zeiss LSM 510, Plan-Neofluar 20X objective, pinhole fully open, confocal slice thickness = 215 μm), with projected areas and perimeters of individual cells (cells not in contact with adjacent cells) measured from acquired images using Nikon image analysis software (Nikon NIS-Elements BR, Melville, NY). As a measure of cell morphology, a dimensionless cell shape factor SF was computed for each cell, defined as $SF = 4\pi A/p^2$, where A = cell area and p = cell perimeter. A total of three (n=3) independent spreading experiments were performed, with a minimum of 100 cells analyzed for each condition (substrate, time point). A two-way ANOVA (substrate, time) was performed to analyze cell spreading

and shape factor experiments, using Tukey's post hoc test to detect differences between substrates ($p<0.05$ significant).

2.2.6 NP Cell Attachment Strength

A centrifugal cell adhesion assay [118,150] was performed to assess the relative attachment strength on varying ECM substrates. NP cells cultured in monolayer (as described above, 2-7 days culture) were incubated with calcein-AM diluted in 2 mM PBS-dextrose for 20 min in 37°C. Fluorescently-labeled cells were detached with 0.025% trypsin/EDTA and immediately washed with soybean trypsin inhibitor (1mg/mL, Sigma). Cells were resuspended in PBS-dextrose , seeded at 10,000 cells per well onto ECM-coated 96–well plates (Corning Costar, black opaque), with 6 replicate wells per condition. Cells were incubated for 90 min at room temperature to allow for cell attachment. After one gentle wash with PBS-dextrose, a pre-spin reading was performed with a fluorescence plate reader (Tecan Genios, Mannendorf, Switzerland) to quantify cell numbers in each well prior to application of a defined centrifugal detachment force. Plates were then covered with sealing tape, inverted, and spun in a benchtop centrifuge at either 200g or 600g. Wells were refilled with PBS, washed once gently to remove detached cells, and a post-spin fluorescence reading was obtained.

Pre-spin and post-spin values for each well were normalized by subtracting out the background signal from negative controls of BSA blocked wells (no seeded cells). The fraction of adherent cells, f, was then computed for each well as:

$$f = \frac{\boldsymbol{RFU}_{post}}{\boldsymbol{RFU}_{pre}},$$

where RFU is relative fluorescence units as measured by the plate reader. Three independent experiments (n=3 separate cell isolations, 6 replicate wells/condition) were performed. Differences between substrates were detected via repeated measures ANOVA with Tukey's post-hoc analysis, with $p<0.05$ considered significant.

2.3 Results

2.3.1 IVD Cell Integrin Expression

Immediately upon isolation from immature porcine IVD tissues (Day 0), all integrin subunits examined were expressed at detectable levels (% of cells positive and MFI greater than zero) for both AF and NP cells (Figure 8), with the exception of the α6 subunit, which was not detectable in AF cells (MFI, % positive not different from zero). Day 0 expression of all integrin subunits was low, possibly reflecting a need for cells to "recover" (i.e. re-express damaged receptors) following the cell isolation procedure. Integrin expression (MFI, % positive) increased significantly (ANOVA, main effect of culture time, $p<0.05$) after 3 and 7 days in monolayer culture across all integrins examined and both cell types (Figure 8). For the α1, α5, and β1 subunits, MFI levels increased 2-8 fold and the percentage of positive cells increased to between 70-95% after 3 days of culture for cells from both regions. Differences between cell type (IVD region)

were detected for two integrin subunits, regardless of culture time (ANOVA, cell type by integrin subunit interaction). For the α5 subunit, cells from the AF region were found to exhibit significantly higher MFI levels than NP cells (Figure 8A, $p<0.01$), although no differences were detected for the percentage of cells that were positive for this subunit (Figure 8B). For the α6 subunit, a prominent difference in integrin expression between cell type was detected, with NP cells expressing significantly higher MFI levels and percent cells positive (Figure 8A and B, both $p<0.01$) as compared to AF cells. Upon isolation (Day 0), 29% of NP cells had detectable levels of α6, while just 3% of AF cells were positive. After 3 and 7 days in culture, α6 expression for NP cells was comparable to or higher than other alpha subunits (89-97% of cells positive, MFI=155-170) while expression in AF cells remained low (% positive = 45-57%, MFI = 35-43). These results indicate that regional differences in α6 integrin expression identified *in situ* [131] are maintained upon cell isolation, and over 7 days of monolayer culture.

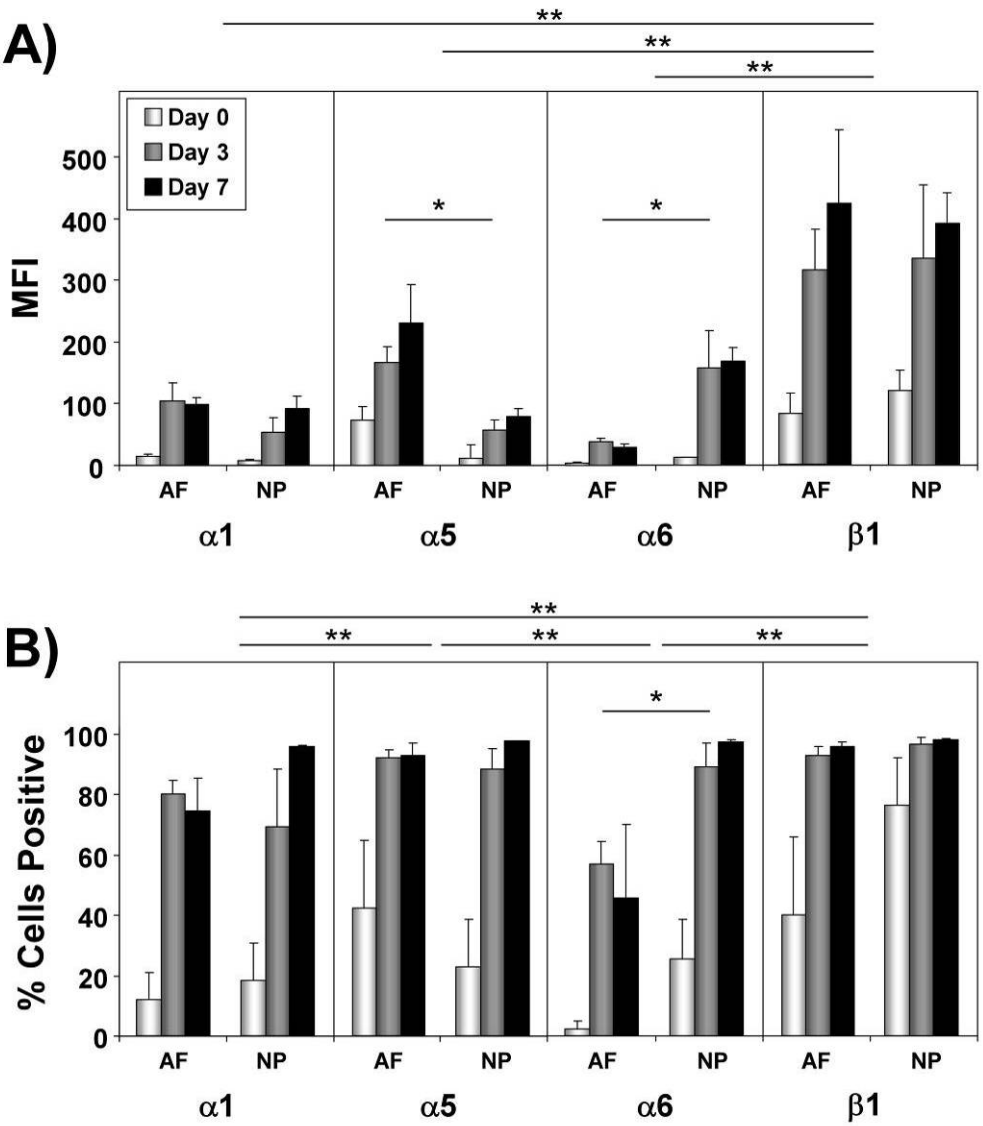

Figure 8: Integrin expression for IVD cells isolated from AF and NP tissue regions and analyzed via flow cytometry. Cells were analyzed for mean fluorescence intensity (MFI, A) and percent cells positive (B) immediately following isolation (Day 0) and after monolayer culture for 3 and 7 days. Data shown (mean±SEM) represents results from 3 separate cell isolations (n=3). Significant main effects between tissue regions (*, $p<0.01$) and integrin subunit (, $p<0.05$) are shown. Additionally, a significant effect of culture time was detected ($p<0.05$) for all integrins for both MFI and % positive.**

2.3.2 Functional Integrins Regulating IVD Cell Adhesion

2.3.2.1 Integrins Regulating IVD Cell Adhesion to Collagen and Fibronectin

Cells from both regions of the porcine IVD were found to attach readily to types I and II collagen substrates, as well as fibronectin substrates. Attachment to surfaces without protein (wells blocked with BSA) was negligible (always <10% of control), indicating cell attachment was due to cellular interactions with the matrix protein coated on the well surface.

On type I collagen substrates, blocking the α1 integrin subunit partially inhibited cell attachment (49% inhibition for AF, 64% NP), whereas blocking the β1 subunit resulted in almost complete inhibition of attachment (AF: 97%, NP: 82%), as shown in Figure 9A. These results suggest that the α1β1 integrin partially mediates attachment of IVD cells to type I collagen, but other β1-containing integrins are also involved. However, blocking another known collagen-binding heterodimer, α2β1, did not inhibit attachment of AF cells and showed slight effects (19% inhibition) for NP cells. Incubation in the presence of RGD peptide or blocking the αvβ3 heterodimer showed no inhibitory effect of binding to type I collagen, indicating a secondary interaction via cell-secreted fibronectin was not involved in attachment. For IVD cells seeded on type II collagen substrates, cell attachment was found to be mediated entirely by the α1 (AF: 97%, NP: 96%) and β1 (AF: 97%, NP: 83%) integrin subunits, as shown in Figure 9B, while other blocking conditions showed no inhibitory effects.

On fibronectin substrates (Figure 9C), function-blocking antibodies to the known fibronectin-binding subunit αv and heterodimers αvβ3 and αvβ5 showed no inhibitory effect for either cell type. Blocking with the β1 antibody or with RGD peptide completely inhibited porcine AF and NP cell attachment to fibronectin, while blocking the α1 subunit showed no effects. We were unable to identify a function-blocking antibody for the α5 subunit that cross-reacted with porcine cells. This corroborates the findings of another study where another anti-human α5 function-blocking antibody (clone SAM-1) was found to be ineffective in blocking porcine monocyte attachment to human fibronectin [163]. Since the α5β1 heterodimer is a common fibronectin receptor in numerous cell types and the primary fibronectin receptor involving the β1 subunit and blocking antibodies to the αv, αvβ3 and αvβ5 integrins were unable to inhibit attachment, it is likely that the α5β1 integrin heterodimer is the critical receptor in IVD cell attachment to fibronectin. When porcine AF cells were allowed to spread on fibronectin substrates (overnight in low-serum media) and labeled with α5 polyclonal and β1 antibodies, staining was intense and localized to focal contacts (data not shown). Together these results strongly suggest that α5β1 is a functional receptor involved in attachment and spreading on fibronectin for IVD cells.

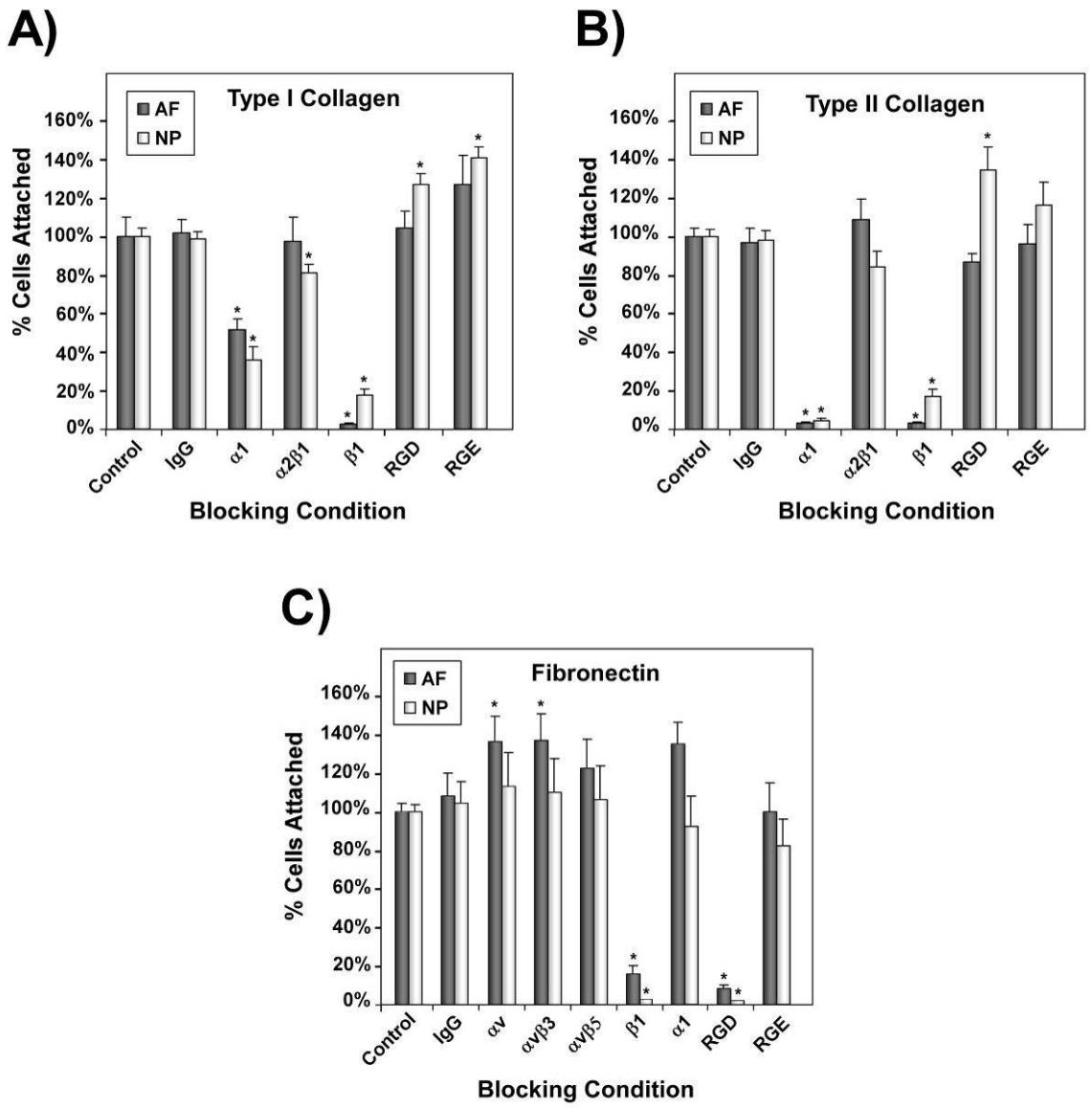

Figure 9: Effects of integrin function-blocking antibodies on IVD cell attachment to substrates coated with (A) type I collagen, (B) type II collagen, (C) fibronectin. Attachment numbers (mean ± SEM) were normalized to uninhibited control cells for each cell type. n=3 cell isolations for each substrate, 4 replicates per condition for each experiment. *ANOVA, $p<0.05$ from control and IgG.

2.3.2.2 Integrins Regulating IVD Cell Interactions with Fibrillar Collagen

AF cells seeded in type I fibrillar collagen gels were found to actively contract the free-floating gels, with reductions of over 30% in gel area for control gels after 18h (no antibody: 33% contraction; non-blocking IgG antibody: 31% contraction), as shown in Figure 10. Pre-incubating cells with function-blocking antibodies for α1 and β1 integrin subunits inhibited gel contraction almost completely (α1: 7% contraction; β1: 4%), indicating α1β1 is critical for forming mechanically functional integrin interactions with fibrillar type I collagen in AF cells.

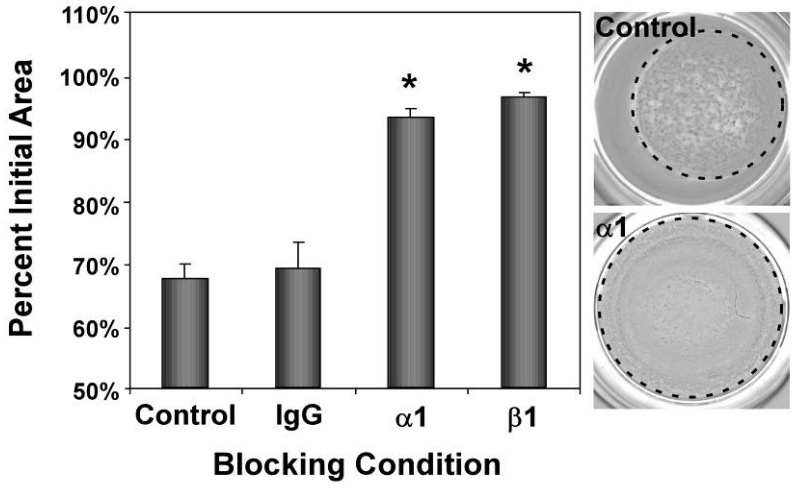

Figure 10: AF cell-mediated collagen gel contraction (mean ± SEM) and inhibition by integrin function-blocking antibodies. Cells suspended in collagen gels and allowed 18 hrs to contract. n=3 separate cell isolations, 3-4 replicates per condition. *ANOVA, significant difference from control and IgG, $p<0.0001$.

2.3.2.3 IVD Cell Attachment to Laminin-111

NP cells were found to attach readily and in high numbers on laminin-111 (LM-111) coated substrates. In contrast, AF cell attachment to LM-111 was very minimal (< 15% of NP control values, compared to 10% attachment on BSA-coated surfaces). NP cell attachment to laminin was partially inhibited by blocking the α6 (64% inhibition) and β1 (46%) integrin subunits as shown in Figure 11, with a significant difference detected between these two integrin function-blocking conditions. Because of very low attachment numbers for control AF cells, differences in AF cell attachment due to integrin blocking were not evaluated.

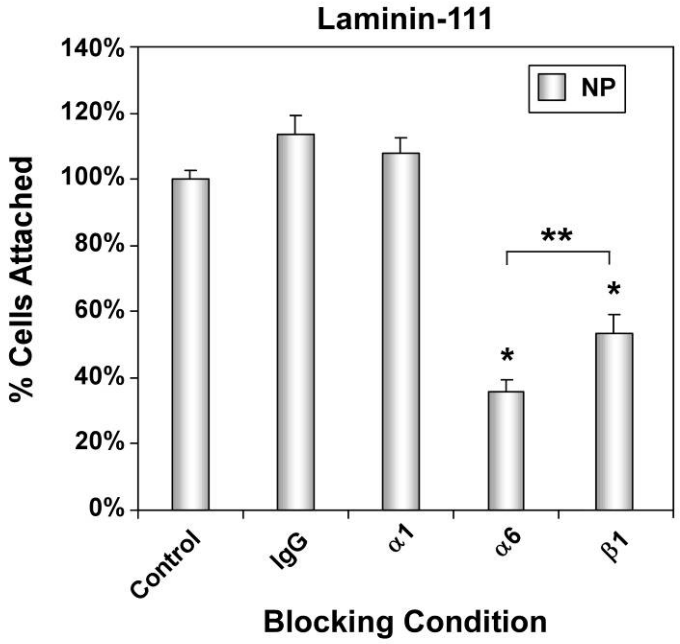

Figure 11: Effects of integrin function-blocking antibodies on NP cell attachment to laminin-111 substrates. Attachment numbers (mean ± SEM) were normalized to uninhibited control cells for each cell type. AF cell attachment not shown or analyzed due to low cell attachment numbers (<15% of NP control). n=3 cell isolations for each substrate, 4 replicates per condition for each experiment. * p<0.05 from control and IgG; **p<0.05 between conditions.

While performing laminin attachment experiments, it was observed that the size distribution of NP cells attaching to laminin substrates appeared to vary depending on blocking condition. Since the NP region of the immature IVD has been reported to contain a phenotypically mixed cell population that may include both large, vacuolated "notochordal-like" cells as well as smaller chondrocyte-like cells [165], we decided to quantify the size distribution of attached cells for different blocking conditions. Cell diameters for NP cells attached to laminin were found to range in diameter from 10-50

μm, with peak cell numbers between 10-20 μm and a second peak occurring between 25-30 μm (Figure 12). Blocking the α6 subunit prevented attachment of larger cells to laminin, with the majority of attached NP cells being smaller than 20 μm. Blocking the β1 subunit did not completely eliminate larger NP cells from attaching to laminin.

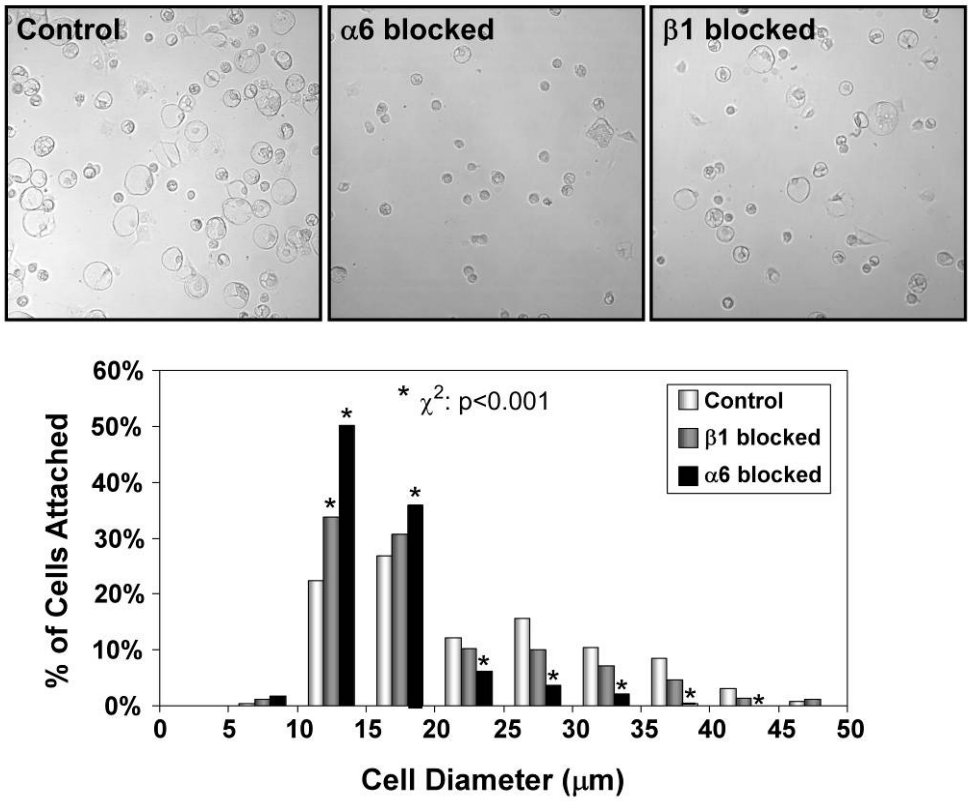

Figure 12: Distribution of cell size for NP cells attached to laminin-111-coated substrates for unblocked control cells and cells pre-incubated with function-blocking antibodies to either integrin α6 or β1. Asterisks denote cell diameter groupings where blocking condition deviates significantly (p<0.001) from control.

2.3.3 Adhesion of Freshly Isolated NP Cells to Laminin Isoforms

In the studies presented above, NP cells readily attached to the LM-111 isoform, as compared with cells from the adjacent AF region. The LM-111 isoform was selected in these studies due to its' commercial availability (as an extract from mouse EHS tumor) and the presence of the γ1 laminin subunit *in situ.* However, recent studies in our laboratory indicate that NP cells express laminin cell surface receptors (CD239, β4 integrin [33,131]) known to have high affinities for two other laminin isoforms, LM-511 and LM-332, and immunostaining of NP tissues indicates these isoforms may be cell-associated *in situ*. In order to assess NP cells' relative attachment affinity for different laminin isoforms, we quantified the numbers of freshly isolated NP cells adhering to several different laminin isoforms and laminin-containing substrates: LM-111, LM-511, LM-332-containing conditioned media (LM-332CM, produced by the 804G rat carcinoma cell line), and LM-111-rich basement membrane extract (BME) gel. Additionally, type II collagen and fibronectin substrates were tested for comparison with laminins. All substrates were coated at saturating densities which maximized adhesion for each ECM ligand (40 μg/mL for fibronectin, collagen II, LM-111, 20 μg/mL for LM-511).

Following both 30 min and 4h of incubation (Figure 13), approximately twice as many NP cells were found to attach to LM-511 and LM-332CM substrates as compared to type II collagen substrates. In contrast, LM-111 substrates supported attachment at approximately half the levels of collagen at 30minutes and increased to levels similar to

collagen at 4h. However, cell attachment to LM-111-rich BME gels was not different from collagen at 30 minutes, and increased to levels similar to LM-332CM and LM-511 (1.9X and 2.2X collagen level) after 4 hours incubation. Interestingly, freshly isolated NP cells did not adhere to fibronectin substrates at either time point (doubling the fibronectin coating concentration had no effect on attachment numbers, nor did using fibronectin from another source (R&D Systems; data not shown) .

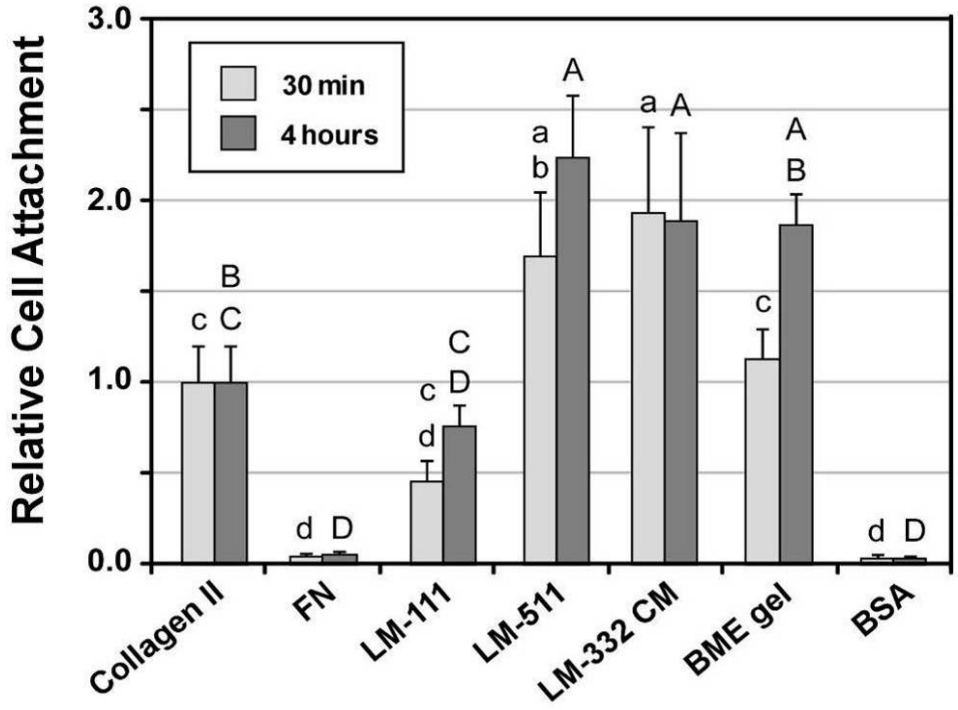

Figure 13: Relative attachment of freshly isolated NP cells to ECM substrates. Cells were allowed to attach for either 30m or 4h, with cell numbers normalized to cell numbers attaching to collagen substrates at each time point. n=4 independent experiments, 4 replicates/condition, mean±SEM. Conditions labeled with the same letter were not statistically different; lower case = 30m, upper case = 4h; comparisons between time points were not analyzed.

2.3.4 NP Cell Spreading on Specific ECM Ligands

NP cells (cultured 2-6 days in monolayer prior to experiments) were found to spread rapidly on LM-511 and LM-332CM substrates, with spread areas after 1h approximately two- to three-fold higher than cells on collagen, fibronectin, and LM-111 substrates (Figure 14). Over a 4 hour time course, cells on LM-511 and LM-332CM spread at similar rates and appeared to approach a maximum spread area of approximately 2000μm^2, whereas cells on LM-111, FN, and type II collagen spread significantly less, with slowly increasing spreading over the time period. A two-way analysis of variance detected significant effects of substrate ($p<0.0001$) and time ($p<0.01$), with no interaction ($p=0.93$). Spreading on LM-511 and LM-332CM substrates was significantly greater than on other substrates, with less spreading found on (in decreasing order) LM-111, FN, and type II collagen substrates. The results for LM-511 and LM-332CM correspond with attachment findings of Section 2.3.2, suggesting these two laminin isoforms are highly adhesive ligands for NP cells and promote rapid cell spreading following attachment. Analysis of cell shape factor during spreading (Figure 15) indicated NP cells on LM-511 and LM-332, as well as on LM-111, had significantly lower shape factors (greater deviation from spherical shape, $p<0.001$) than cells on collagen or fibronectin. Shape factor differences between substrates were apparent at 1h and were maintained over the 4h spreading experiment. Whereas NP cells on LM-111 substrates had intermediate spread areas in comparison to other substrates (greater than

collagen/fibronectin but less than other laminin isoforms, Figure 14), they exhibited shape factors comparable to (or less than at 4h, Figure 15) the other laminin isoforms. Examination of NP cell morphology on LM-111 substrates revealed that cells typically exhibited a more elongated, spindle-shaped morphology in comparison to other substrates, which corresponds with the findings of an intermediate cell area with low shape factor.

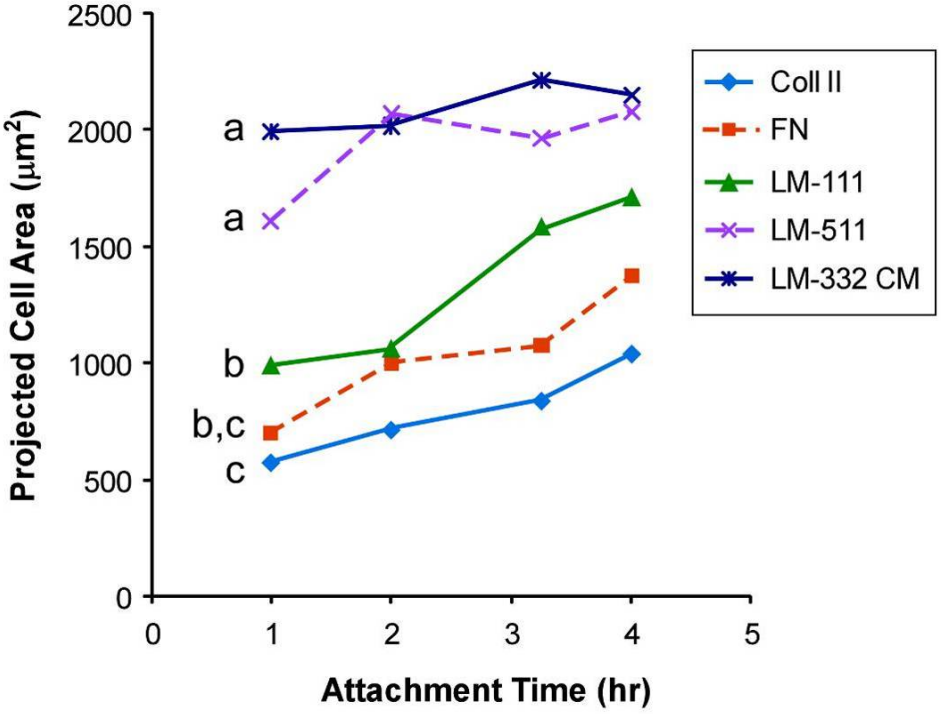

Figure 14: NP cell spreading dynamics on ECM substrates. Data points represent mean of n=3 independent experiments, > 100 cells/condition. Error bars omitted for clarity. Significant effects of substrate and time were detected (two-way ANOVA, $p<0.01$); substrates not labeled with same letter were statistically different.

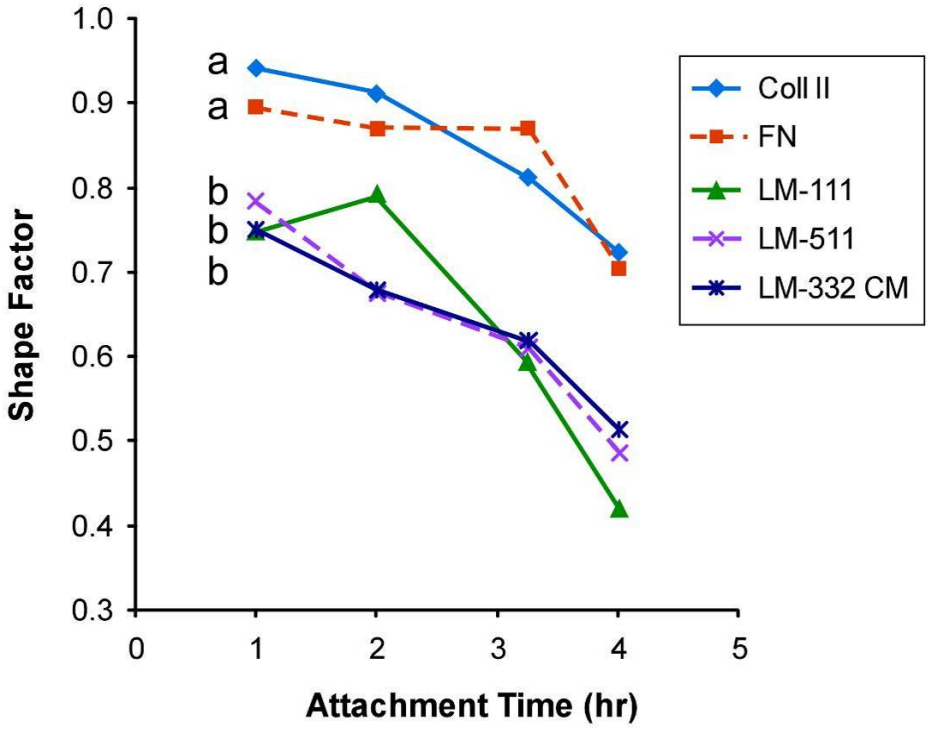

Figure 15: NP cell shape factor during attachment and spreading on ECM substrates. Data points represent mean of n=3 independent experiments, > 100 cells/condition. Error bars omitted for clarity. Significant effects of substrate and time (two-way ANOVA, $p<0.001$); substrates labeled with different letters were statistically different.

2.3.5 NP Cell Attachment Strength

Finally, the attachment strength of NP cells was investigated by examining the ability of adherent NP cells to withstand a defined centrifugal detachment force. Control wells containing known amounts of cells confirmed that cell fluorescence signal was linearly related to cell number (data not shown), with $R^2 > 0.99$. Following the application of a 200g force, NP cells were found to remain adherent in significantly

greater numbers on LM-511 and LM-332CM surfaces, with an adherent cell fraction approximately twice that of cells on collagen and fibronectin substrates as shown in Figure 16. The fraction of cells remaining on LM-111 surfaces was greater than on collagen surfaces, but less than on LM-511. A similar pattern was observed following application of a 600g force (Figure 16), with LM-511 having a significantly higher fraction than other substrates and collagen having the lowest adherent cell fraction. These results correspond closely with cell spreading results of Section 2.3.4, where LM-511 and LM-332CM surfaces promoted significantly greater cell spreading rates as compared to collagen and fibronectin, and LM-111 spreading generally less than other laminins but greater than collagen and fibronectin. These findings indicate NP cells can form rapid, mechanically functional interactions with laminin isoforms LM-511 and LM-332, as compared to collagen and fibronectin ligands.

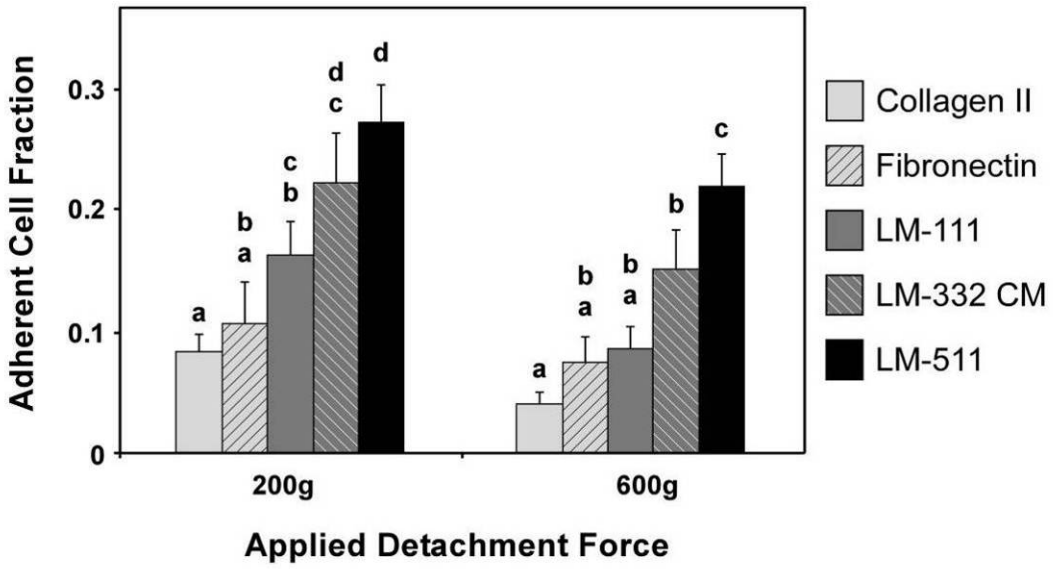

Figure 16: NP cell attachment following centrifugal loading. For a given detachment force (200g, 600g), conditions not connected by same letter were statistically different (ANOVA, $p<0.05$).

2.4 Discussion

2.4.1 Integrin Expression

Several observations were noted in examining overall integrin expression patterns of isolated IVD cells. Upon isolation (Day 0), integrin expression for all subunits was very low, including low expression of the typically ubiquitous (in other cell types) β1 subunit (<50% of cells were found to be positive for any subunit, other than β1 on NP cells). However, by Day 3 both MFI levels and the percentage of positive cells had increased dramatically for most subunits of both cell types, with expression remaining relatively constant between Days 3 and 7. This pattern suggests that damage

to cell surface receptors may have occurred during enzymatic digestion, but cells rapidly re-expressed receptors within the first few days of culture.

A difference in integrin expression between IVD cell types was detected for two integrin subunits: the laminin receptor α6 (which pairs with the β1 or β4 subunit to bind various laminin isoforms), and the fibronectin receptor α5 (which pairs with β1). For the α6 subunit, NP cells showed significantly higher expression (both MFI and % positive) in comparison to AF cells; for example, at Day 3 NP cells exhibited 4-fold higher α6 MFI levels as compared to AF cells, with 90% of NP cells positive for α6 compared to just 58% of AF cells. Over one week of culture, AF cells expressed little α6 integrin, with only 47% exhibiting detectable levels at Day 7. These results provide confirmation of previous immunohistochemical staining studies [33,131], where a dramatic differential expression of α6 was observed between IVD regions in various species (pig, rat, 2 year old human). Additionally, this difference in integrin expression between cell populations was maintained in culture over 1 week, suggesting that α6 expression may be a valid phenotypic marker that distinguishes these cells from other cell types in the disc.

For the α5 subunit, NP cells showed low levels of expression upon isolation and over the 7 day culture period, with MFI levels that were just 16% of AF cell levels at Day 0 and 34% at Day 7. Interestingly, the expression pattern for α5 observed here was corroborated in evidence from functional studies performed later in this chapter, with

NP cells showing very low affinity for fibronectin substrates (no attachment following isolation (Section 2.4.3), and low fraction of adherent cells following centrifugal force application (Section 2.4.6)).

2.4.2 Functional Integrins Regulating IVD Cell Adhesion

IVD cell attachment to LM-111 highlighted differential laminin-binding abilities of NP and AF cells, with low numbers of AF cells attaching to LM-111-coated substrates (<15% of NP cells). This differential adhesion is likely due to the presence of the α6 integrin subunit on NP cells, as blocking of α6 with a function-inhibiting antibody resulted in 64% inhibition of NP cell attachment to LM-111; blocking the β1 subunit of NP cells also produced similar inhibitory effects on LM-111 (46%). Together this data corresponds with previous studies identifying the α6β1 heterodimer as a primary receptor for the globular cell adhesion domain of the LM-111 isoform [134]. Interestingly, blocking the α6 integrin appeared to shift the size distribution of the attached NP cell population to smaller, more chondrocyte-like cells, suggesting that a population of larger, notochordal-like NP cells mediates interactions with laminin solely via the α6 subunit.

Integrins involved in IVD cell attachment to collagen substrates appeared to be similar for cells from both AF and NP regions of the IVD, with a potential role for additional as-yet unidentified receptors. For cells from both regions, attachment to type II collagen was found to be mediated primarily by the α1β1 receptor. We detected no

significant attachment inhibition on Type II collagen with a blocking antibody to α2β1, corresponding with previous immunostaining of porcine IVD tissues [131] where significant levels of α2 were not detected *in situ*. In contrast to type II collagen, IVD cell attachment to type I collagen was only partially (~50%) inhibited when blocking the α1 integrin subunit, although blocking β1 entirely inhibited attachment. In addition, blocking α2β1 only slightly (19%) reduced adhesion of NP cells and had no detectable affect on AF cells. These findings point towards roles for other collagen-binding integrins in mediating the IVD cell attachment to type I collagen. Other known collagen-binding integrins are the less studied α10β1 [28] and α11β1 [170] integrins, which have been localized to cartilaginous tissues including findings for the α10 subunit in the inner AF of the mouse [29] and α11 subunit in the outer AF of human and mouse embryos [164]. One possible explanation for only partial inhibition on Type I collagen is that both AF and NP tissues contain subpopulations (e.g. chondrocyte-like inner AF cells) that utilize α10 or α11 subunits. Tools to assay α10 and α11 protein expression and functional interactions with collagens remain limited and were not available for this study.

In contrast to cell attachment experiments, findings from collagen gel contraction experiments provided evidence of a dominant functional role for the α1 and β1 integrin subunits in mediating AF cell mechanical interactions with fibrillar type I collagen. Treatment with blocking antibodies to either subunit inhibited AF cell-mediated gel

contraction almost completely, with similar findings for blocking α1 and β1 subunits (7% and 4% contraction, respectively, compared to 31% in controls), suggesting that even though other β1-containing integrins may be involved in attachment to monomeric type I collagen, α1β1 functions to promote fibrillar collagen gel contraction. The α1β1 integrin has previously been shown to have a higher affinity for monomeric and beaded-filament collagens (e.g. Type VI collagen) than for Type I fibrils [97,166], but also to participate in type I collagen fiber contraction for some mesenchymal cell types [68,149]. Thus, our own findings, and those of prior studies, suggest that the role of the α1β1 integrin and individual collagen-binding integrins may be cell-type or context specific.

Cell assays on fibronectin substrates suggest that the α5β1 integrin mediates IVD cell attachment for both NP and AF cells. These results are similar to those for articular chondrocytes, where blocking α5β1 also prevents cell attachment to fibronectin [117]. In chondrocytes, the α5β1 integrin also binds proteolytic fragments of fibronectin, which have been shown to initiate a distinct signaling cascade with downstream effects that may lead to matrix degradation or remodeling [59,85]. Several studies present evidence that a similar pathway may exist in disc [6,9], and thus the α5β1 integrin may be a key receptor for cell-mediated responses to matrix degradation in the IVD.

2.4.3 Adhesion of Freshly Isolated NP Cells to Laminin Isoforms

Experiments examining the attachment of freshly isolated NP cells revealed several notable differences between different ECM substrates, including different isoforms of laminin. LM-511 and LM-332CM substrates were found to support rapid adhesion of freshly isolated NP cells, with approximately twice the number of attached cells as compared to type II collagen surfaces, with even greater differences compared to LM-111 (4X greater) and FN (which supported no adhesion). It is notable that these two laminin isoforms (LM-511 and -332) are known to be bound by an almost identical set of integrin receptors: α6β4, α6β1, and α3β1 integrins [128,134]. This corresponds with knowledge of receptor expression by NP cells, where high integrin α6 (tissue immunostaining [131], flow cytometry (see Section 2.3.1), and β4 (tissue [131]) expression has been documented (expression of the α3 integrin in IVD tissue has not yet been investigated). Additionally, immunostaining of immature NP tissues has identified cell-associated localization of these laminins *in situ*, with LM-511 (α5 laminin subunit) [33] and LM-332 (unpublished data, shown in Figure 6) staining intensely and exclusively in the NP region

In contrast, the LM-111 isoform was found to support comparatively low levels of NP cell attachment (approximately 25% of LM-511 and LM-332CM values); however, LM-111-rich basement membrane extract gel (BME) supported high levels of cell attachment, with cell numbers at 4h similar to the other laminin isoforms investigated.

BME is a self-polymerizing gel containing primarily LM-111 (>50%), collagen IV (~30%), and entactin (<10%). Differences in attachment levels between these two LM-111-containing substrates could be due to several factors: (1) a higher concentration of ECM ligand on gel substrates, as the BME used here contains 14 mg/mL of protein (with approximately 7 mg/mL LM-111), which could present ECM ligand in orders-of-magnitude greater concentrations than protein adsorbed to plastic surfaces; (2) proper ligand conformation or presentation, since under gelation conditions (37°C, in presence of divalent cations) the short arms of LM-111 self-polymerize into networks, which may provide the proper orientation and/or spacing (to facilitate integrin clustering) of the protein's integrin-binding LG domains [186]; (3) the presence of other ECM and non-ECM constituents, such as collagen IV and entactin , as well as low levels of growth factors.

Finally, fibronectin surfaces were found to support no attachment for freshly isolated NP cells after 30m and 4h. This finding was somewhat different than for cells that have been cultured for several days, which adhere and spread on FN at moderate levels (Section 2.3.4), but does correspond with integrin expression levels for freshly isolated NP cells (Section 2.3.1), where few NP cells showed detectable levels of α5 (< 50% positive at Day 7) and expression was much lower than for AF cells.

A number of epithelial cell types (e.g. airway epithelial cells [82]) also do not express the α5 subunit in normal tissues, which fits together with other data suggesting

NP cells share similar cell-ECM receptors with epithelial cell types (α6, β4 integrins, non-integrin laminin receptor CD239) [33]. Additionally, various epithelial cell types exhibit an upregulation of α5 in injury models, and upon exposure to fibronectin in culture [82]; this may explain why NP cells did express some α5 following 7 days of culture (99% of NP cells positive for α5 at Day 7, although MFI levels remained at just 34% of AF MFI levels), and did attach and spread on FN substrates following 2-6 days culture in media supplemented with FBS (which includes significant amounts of FN) while completely failing to attach immediately following isolation from the tissue.

2.4.4 NP Cell Spreading on ECM Substrates

Cell spreading experiments highlighted NP cells' differential interactions with specific ECM ligands, with laminin ligands (two isoforms in particular) exhibiting higher levels of spreading as compared to fibronectin and collagen substrates. On LM-511 and LM-332CM substrates, NP cells were found to rapidly spread (area approximately twice that of other substrates at 1h) and maintain a significantly higher spread area over the 4h time course. LM-111 substrates showed an intermediate level of spreading, with FN and collagen showing progressively lower spread areas. One potentially confounding factor in this experiment may be the presence of a mixed cell population in isolated NP cells, which could account for some of the difference in spread area (at early time points) if larger NP cells preferentially attached to laminin substrates.

Comparing actin images of spread cells at the 1h time point, cells attaching to collagen substrates appeared to be primarily small, rounded cells, while LM-511 and LM-332CM substrates appeared to contain a mix of cell sizes. However, NP cells on laminins already had shape factors much less than 1 (shape factor of 0.75±.12 on LM-332CM compared to 0.94±0.02 on collagen; a perfectly round cell has a shape factor of 1.0), suggesting cells had immediately begun to interact with and spread on laminins but not other substrates.

2.4.5 NP Cell Attachment Strength

The results of centrifugal cell attachment strength studies again highlighted differential adhesion characteristics of NP cells on varying ECM substrates. Following application of a 200g centrifugal force, LM-332CM and LM-511 substrates had significantly higher adherent cell fractions than fibronectin and collagen substrates, with LM-111 substrates exhibiting intermediate adherent fractions. These results closely correlated with cell spread area findings for these same substrates (Section 2.3.5), with the substrates exhibiting the highest (LM-332CM, LM-511) and lowest (collagen II) spread areas also yielding the highest and lowest adherent fractions, respectively. This result implies that NP adhesion strength was dependent primarily on the area of cell in contact with the surface. At a higher detachment force (600g), the relative adhesive order of substrates remained the same, although LM-511 showed a significantly higher

fraction as compared to LM-332CM at this higher force. It should be noted that this assay differs from other attachment assays performed in this chapter (which involved gentle washing to remove unattached cells), in that unattached cells were removed by gentle washing and the remaining attached cells were subjected to force application. Thus the adherent cell fraction represents percentage of attached cells that withstood the detachment force, providing a comparative measure of adhesion strength.

2.5 Conclusions

The results presented in this chapter highlight the unique interactions of immature NP cells with laminin extracellular matrix proteins, and also identify functional integrins regulating IVD cell-matrix interactions. NP cells isolated from immature tissues showed preferential attachment, spreading, and adhesion strength on laminin substrates in comparison with type II collagen and fibronectin, two other ECM constituents found in the disc. These findings confirm that laminin protein and receptor expression identified in immature NP tissues translate into functional behaviors of isolated NP cells. Major conclusions from the studies presented in this chapter include:

1. **NP cells were found to have strong interactions with two laminin isoforms, LM-511 and LM-332CM, in comparison with several other ECM ligands (type II collagen, fibronectin, as well as another laminin isoform, LM-111), confirming Hypothesis 2.C**. This included two-fold higher levels of attachment

following cell isolation, rapid and greater cell spreading, and strong mechanical interactions. These two laminin isoforms are known to have similar receptor set, many of which have been detected in NP tissues and isolated cells (α6β4, α6β1, and α3β1 integrins). Additionally, these two laminin isoforms have been shown to be cell-associated in immature NP tissues, in contrast to LM-111, which has not been identified at the tissue level.

2. Attachment to laminin (LM-111) identified differential adhesion between cells from different IVD regions, with **NP cells attaching to LM-111 at dramatically higher levels as compared to cells from the adjacent AF, confirming Hypothesis 2.A**. This result may be attributed to the laminin-binding α6 integrin, which was shown to be differentially expressed in isolated cells between these two cell types (with differences maintained over time in culture). **Additionally, inhibition of the α6 integrin subunit resulted in significantly reduced NP cell adhesion to LM-111 substrates, confirming Hypothesis 2.B**. These findings suggest LM-111 substrates may be useful as a tool for differential selection of immature NP cells from a mixed disc cell population.
3. Results on collagen substrates identified the α1β1 integrin as a key receptor for both NP and AF cells collagen interactions. However, there may be a role for other collagen-binding integrins (α10, α11 subunits) in adhesion to type I collagen, as blocking the α1 subunit inhibited only ~50% of cells from attaching

to this substrate (in contrast to ~95% inhibition by blocking α1 on type II collagen). AF cell mechanical interactions with fibrillar collagens were found to be blocked almost completely by inhibiting either the α1 or β1 subunit. This finding may suggest a role for α1β1 as a mechanotransducer in AF tissues, where cells are embedded within lamellae containing numerous type I collagen fibers.

4. NP cells showed low levels of attachment on fibronectin substrates, with no adhesion immediately following cell isolation, and low levels of attachment and spreading following short times in culture. This finding corresponded with low levels of α5 integrin expressed by NP cells as compared to cells from the adjacent AF region.

3. Roles of ECM Ligand and Substrate Stiffness in Modulating NP Cell-Cell Interactions

3.1 Introduction

Immature NP cells reside in a soft, gelatinous extracellular matrix environment. Previous studies indicate that the NP cell environment is rich in laminins that cells interact with integrin and non-integrin laminin receptors [33,65,131]. Morphologically, these immature NP cells are arranged in cell clusters with strong cell-cell interactions (including gap junctions, desmosomes [80,86,111,165]), and possess large intracellular vacuoles [86,87,165]. In the human IVD, however, this cell population disappears during maturation (as identified morphologically, with loss of cell clusters and vacuolated cells) and cell density decreases significantly, with only a sparse population of chondrocyte-like cells remaining in the adult NP [19,165]. These changes appear to precede or coincide with structural changes in the disc, including loss of disc height and decreased proteoglycan and water content [19,25,143,151], and thus may be an initiating event in disc degenerative changes [137]. However, the mechanisms or factors leading to the disappearance of this immature NP cell population are not well understood.

Cell-cell interactions and cell morphology have been shown to be critical in cell phenotypic maintenance and survival in response to stress in various cell types [58,74,176]. Environmental cues provided by the extracellular matrix are known to be important factors modulating cell-cell interactions, with ECM stiffness and ligand being critical regulators of cell organization and function [43,55,78,113,140]. However, the

appropriate environmental cues necessary to maintain or promote an immature NP cell phenotype are not well understood. In this chapter, several hypotheses were investigated relating to the roles of ECM ligand and stiffness in modulating NP cell-cell interactions.

Self-polymerizing basement membrane gel (i.e. Matrigel) substrates have been shown to promote cell-cell interactions for several cell types, including various epithelial cell types [112,153,177]. As immature NP cells appear to have cell-matrix and cell-cell interactions similar to those of epithelial cells, including interactions with laminin ligands and expression of laminin receptors (see Chapters 1 and 2), it was hypothesized (**Hypothesis 3.A) that culture of NP cells on soft, laminin-rich basement membrane extract (BME) substrates would promote NP cell-cell interactions and morphologies similar to those observed in immature NP tissues**. Additionally, we investigated whether the observed NP cell responses on BME gels were modulated by ECM ligand, substrate stiffness, or both, by culturing NP cells on polyacrylamide gel substrates with tunable mechanical properties and functionalized with specific ECM ligands. It was hypothesized (**Hypothesis 3.B)** that **both laminin ligands and substrate stiffness play critical roles in the maintenance of NP cell organization and phenotype *in vitro***.

Finally, several studies suggest that various cell types physically probe their surroundings, sensing the mechanical stiffness of their environment through cell-matrix and (potentially) cell-cell adhesions, and preferentially interacting with (e.g. migrating

towards) stiffer environments [78,115]. Here, the mechanical properties of isolated NP cells were measured and compared to those of substrates on which strong NP cell-cell interactions (i.e. cell "clustering" behaviors) were observed. We hypothesized (**Hypothesis 3.C)** that **NP cells would exhibit strong cell-cell (clustering) behaviors on substrates with elastic moduli less than their own stiffness, but not on substrates stiffer than NP cells.**

3.2 Methods

3.2.1 IVD Cell Isolation and Culture

NP cells were isolated enzymatically (as described in Section 2.2.1) from porcine tissues (4-6 mos., n=3). Freshly isolated cells were rinsed twice (DMEM wash media), centrifuged (400g, 10 min), and resuspended in cell dissociation buffer (3mL, Cell Stripper, Mediatech) to break up any remaining cell clusters. Cells were then centrifuged and resuspended in culture media (as described in Section 2.2.1; F12 media with 5% FBS and antibiotics), passed through a 70μm cell strainer, and seeded immediately onto gel substrates (see below) at a density of 18000 cells/cm^2. Cells were cultured for 7 days in hypoxic conditions (5% O_2, 5% CO_2, 37°C), with culture media exchanged every 3 days.

NP and anulus fibrosus (AF) cells used for cell mechanical testing were isolated via enzymatic digestion as described in Section 2.2.1, resuspended in culture media, seeded on 0.1% gelatin-coated tissue culture plastic petri dishes.

3.2.2 Basement Membrane Extract Gel Substrates

Thin two-dimensional gel substrates of basement membrane extract (BME) were created by dispensing 90 μL of ice-cold, unpolymerized BME solution (Trevigen, Inc; growth factor-reduced, 13.8 mg/mL) into 12mm diameter wells (schematic shown in Figure 17; custom PDMS rings pressed onto 22 mm square glass coverslip bottoms) and allowed to gel for 30 minutes at 37°C in a humidified incubator. Resulting 2D gels were approximately 500 μm in thickness. BME is a solubilized basement membrane preparation extracted from the Engelbreth-Holm-Swarm (EHS) mouse sarcoma tumor, which contains high concentrations of several ECM proteins: laminin-111 (~60%), type IV collagen (~30%), entactin (~8%), and heparin sulfate [109]. This extract gel also goes by the trade name Matrigel™, which is produced by another manufacturer (Becton Dickinson). Following gelation, substrates were washed once with culture media, and freshly isolated cells were seeded and allowed to attach.

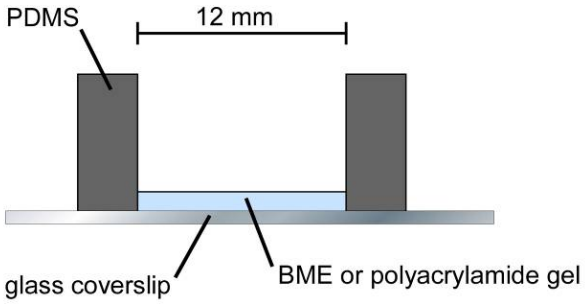

Figure 17: Cross-section of PDMS wells used for culturing NP cells on 2D gel substrates (BME or polyacrylamide gels).

3.2.3 Polyacrylamide Gel Substrates

Two-dimensional polyacrylamide (PA) gel culture substrates with varying mechanical properties were created by polymerizing acrylamide with varying amounts of bis-acrylamide crosslinker. An acrylamide solution (5 or 8% final concentration, mixed from a 40% stock solution, Bio-Rad) was mixed with bis-acrylamide (0.02-0.15%, from 2% stock solution, Bio-Rad) to create gels of different stiffnesses. Solutions were degassed (20min under vacuum in degassing sonicator bath (Branson B1510), and polymerization initiated by adding 10% ammonium persulfate (1:200, Bio-Rad) and n,n,n'n'-(tetra)ethylenediamine (TEMED, 1:2000, Bio-Rad). Thin gels were formed by pipetting a 12μl drop of polymerizing acrylamide solution onto aminosilanated glass coverslips (22mm square coverslip treated with 3-aminopropyltrimethoxysilane, Sigma), and immediately covering drop with a hydrophobic coverslip (12mm-diameter glass treated with Rain-X, Rain-X Inc.). Gels were allowed to polymerize for 30 minutes at room temperature, then submersed in buffer (HEPES, pH 8.0) for 3 minutes, and top

coverslips were removed with a fine forceps. Gels were stored (up to 1 week) in HEPES buffer at 4°C until use. Gel thickness was determined by mixing fluorescent microspheres (2μm-diameter Fluospheres, Molecular Probes; nile red fluorophore, Ex/Em: 535/575 nm) in gel solution prior to polymerization, with thickness measured via confocal microscopy (Zeiss LSM 510, 63X water immersion objective, NA = 1.2).

3.2.4 ECM Functionalization of Polyacrylamide Gel Substrates

Polyacrylamide gels were functionalized to permit NP cell adhesion by covalently linking specific ECM ligands to gel surfaces. Ligands were coupled by first reacting gels with a UV-activated heterobifunctional crosslinker (Sulfo-SANPAH, Pierce; 0.5mg/mL in HEPES, pH 8.5) under UV light (365nm, 8 min exposure). The crosslinker solution was removed and the procedure was repeated a second time. Gels were next washed twice with cold HEPES buffer (pH 8.5) to remove unreacted crosslinker, then incubated with ECM ligand (overnight at 4°C on shaker plate): either unpolymerized BME (growth factor-reduced, Trevigen Inc.; 200μg/mL in cold 50mM HEPES w/5mM EDTA, pH 8.5 to prevent BME self-polymerization), or collagen type II (Sigma; 200μg/mL in 50 mM HEPES, pH 8.5). Unreacted crosslinker was quenched (1% ethanolamine, 30min) and gels were washed extensively with PBS (pH 7.4) prior to cell seeding.

Polyacrylamide gels functionalized with covalently-linked BME ligands were found to support limited and inconsistent levels of cell attachment and spreading. However, since laminin-111 has been shown to self-polymerize in solution via interaction of short-arm chains under certain physiologic conditions (temperature ≥ 35°C, in presence of divalent cations, and above a critical concentration of approximately 100μg/mL) [185], we investigated whether incubation with additional BME ligand under self-polymerizing conditions would increase ligand density and cell adhesion on BME-polyacrylamide gels. Following covalent crosslinking of BME ligand, polyacrylamide gels were rinsed twice with ice-cold DPBS to remove any uncoupled ligand, then incubated with dilute BME solution (100 μg/mL in DPBS with Ca^{2+} and Mg^{2+}) for 1h at 37°C on a plate shaker. Gels were rinsed twice with prewarmed DPBS (37°C), and cells were immediately seeded on substrates and transferred to incubator. This procedure was also performed with pure laminin (LM-111, Sigma) for comparison.

To investigate whether an additional BME/laminin incubation under self-polymerizing conditions had an effect on ligand density on the gel surface, the relative amount of laminin linked to polyacrylamide substrate surfaces with or without a secondary protein incubation was investigated via immunofluorescence. Following covalent coupling of BME or secondary BME incubation to polyacrylamide gels (two different gel stiffnesses analyzed: E = 200 Pa and 2200 Pa), gels were rinsed twice with prewarmed DPBS, then incubated with a primary anti-laminin antibody (rabbit anti-

mouse EHS laminin (LM-111) antibody, Sigma L9393, diluted 1:50 in DPBS) for 30 minutes at 37°C. Gels were next washed twice, incubated with fluorescent secondary antibody (Alexa 488 goat anti-rabbit, 1:200 in DPBS, 20 minutes, 37°C), again washed twice, then the gel surface was imaged immediately on a confocal microscope (10X 0.3NA objective, image field size = 921 μm x 921 μm). Fluorescence intensity was quantified as the mean intensity over a given image field, with 5-8 image fields per gel on a total of n=3 gels per condition analyzed. Differences in intensity between gels with or without secondary protein incubation were detected via ANOVA with Tukey's HSD.

Additionally, we examined whether secondary BME/laminin incubation would result in increased NP cell attachment and spreading on polyacrylamide gels. Primary porcine NP cells (cultured 2-7 days in monolayer, 5% FBS media) were seeded (90,000 cells/cm^2) on BME polyacrylamide substrates with or without secondary laminin incubation and allowed to attach for 24h (5% FBS culture media). Substrates were washed twice with culture media and cells were fixed with 4% formaldehyde. Cells were permeabilized with 0.2% Triton X-100 in PBS, incubated with Alexa Fluor 488 phalloidin (actin label, 1:250 in PBS) and propidium iodide (cell nuclei, 200 μg/mL) for 45 min. Images of cells were obtained via confocal microscopy (Zeiss LSM 510, 10X 0.3NA objective), with cell numbers determined by counting cell nuclei (differences in attached cell numbers between substrate conditions detected via ANOVA with Tukey's HSD) and cell spreading assessed from actin staining.

3.2.5 Mechanical Characterization of Gel Substrates

Micro-scale mechanical properties of polyacrylamide gels were measured via atomic force microscopy (AFM) indentation. Cantilevers (nominal stiffness = 60pN/nm, actual stiffness determined via thermal calibration; Novascan Technologies Inc.) with 5μm-diameter borosilicate spherical-tipped probes used to indent gel substrates, with a constant indentation rate of 15μm/sec. The resulting force-indentation curves fit to the Hertz contact model [84] for spherical indentation of a flat surface (Eqn. 1),

$$F = \frac{4ER^{1/2}}{3(1-\nu^2)}\delta^{3/2} \qquad [1]$$

where F is the normal indentation force, E is the Young's modulus, R is the probe radius, ν is the Poisson's ratio, and δ is the indentation. The gel was considered to be a semi-infinite elastic solid (no thin-layer correction applied), as the indentation depth was small (< 2 μm) compared to gel thickness (> 100 μm). A Poisson's ratio of 0.45 was assumed based on macroscopic tension tests performed by others [49]. Probe-surface contact was identified using Contact Point Extrapolation (CPE) [77], a method that uses the indentation portion of the approach curve to back-calculate where the initial probe-surface contact occurs, with the Young's modulus E determined from the slope of $F^{2/3}$ versus δ. A total of n=3 gels were tested per formulation, with 25 indentations (5x5 grid

of points spaced 10μm apart) made at 3 different locations on each gel (total of 75 indentations/gel).

3.2.6 Analysis of NP Cell Organization and Morphology

Following a culture period, cells on gel substrates were washed once with DPBS (Dulbecco's PBS with Ca^{2+} and Mg^{2+}, Gibco) and fixed with 4% formaldehyde (Electron Microscopy Sciences; diluted in DPBS) for 10 minutes at room temperature. Cells were then permeabilized (0.1% Triton X-100, Sigma; 5 min), washed with DPBS, and labeled for actin (Alexa 488 phalloidin, Invitrogen; 1:200 in DPBS for 30 min) and cell nuclei (propidium iodide, Sigma; 0.1 mg/mL in DPBS for 30 min).

Cells were imaged via confocal microscopy (Zeiss LSM 510) to evaluate cell organization (numbers of cells arranged in multi-cell clusters) and dimensions of cell clusters. The percentage of cells present in discrete clusters (defined as groups of >4 cells in contact with each other, separate from other cells) was quantified by counting cell nuclei using image analysis software (Nikon NIS-Elements BR). Since clusters were found to be 3-dimensional (often >5 cell layers high) and individual cell nuclei within clusters could not easily be distinguished, an image analysis method was developed to estimate cell numbers within clusters. The method estimates cell numbers by summing fluorescent nuclear intensities from a 3D confocal image stack of a cluster and normalizing to nuclear signal of individual cells within the same image. Confocal

image stacks of clusters and individual cells were first acquired (20X, 0.5NA objective; each confocal slice = 460μm x 460μm x 6.7μm), with the slice thickness (6.7μm) chosen to approximate the diameter of a cell nucleus (as determined from measuring individual NP cell nuclei within several representative images). Next, single cell nuclear signal was determined by selecting individual (non-clustered) cell nuclei within an image and summing the fluorescent signal from all image slices, yielding an average fluorescent signal per individual cell. For each cell cluster, a volume containing the cluster was outlined and fluorescent signal intensity within the volume summed to give fluorescent signal per cluster. Following background intensity corrections (average fluorescence intensity per area in cell-free areas of each image was subtracted from single cell and cluster intensity values), cluster signal was divided by single cell signal to yield an estimate of cell number per cluster. Background correction and single cell signal estimates were measured for each image to overcome any inter-image variability. The method was verified for several cell clusters via manual counting, with differences always less than 15%. Clustering analysis was performed on multiple image fields and gels for each experiment. For analysis of cell clustering, the percentage of cell present in clusters was calculated for each image field of a given ligand-stiffness substrate condition (n=4-7 image fields per condition across multiple gels, cells from 2-3 separate cell isolations, 20-70 clusters per condition, >3000 cells per condition counted), with

differences in clustering percentage detected using two-way ANOVA (ECM ligand, substrate stiffness) and Tukey's HSD.

Cell cluster dimensions including height (perpendicular to gel surface), area (maximum area project onto gel surface), and maximum dimension (in-plane with gel surface) were measured from confocal image stacks of fluorescent actin label (20X 0.5NA objective, 6.7μm confocal slice thickness) using image analysis software (Zeiss LSM). Cluster dimensions were analyzed for each substrate-ligand condition across multiple gels (n=25 clusters per condition, from 2-3 separate cell isolations), with differences detected via ANOVA and Tukey's HSD.

3.2.8 Mechanical Characterization of IVD Cells

The elastic moduli of IVD cells was also measured via AFM indentation to compare cell mechanical properties with those of gel culture substrates. Freshly isolated cells from NP and AF IVD regions were seeded (10,000 cells/cm^2, 5% FBS culture media) on 0.1% gelatin-coated plastic petri dishes (35mm diameter, tissue culture treated, Becton Dickinson) and allowed to attach for 2hr (37°C, 5% CO_2) prior to testing; at this time point attached cells remained rounded and had not begun to spread. Cells were indented with a 5μm spherical-tipped AFM cantilever using the gel testing protocol and data analysis methods described above, except that a Poisson's ratio of 0.49999 was assumed for cells [42]. NP cells were large enough in size to be indented at 3 different

locations per cell, while AF cells were indented at one location per cell. A total of n=30 NP cells and n=29 AF cells were tested, with differences in elastic modulus and cell height (measured using the difference between indentation contact point on the cell and that of the adjacent substrate) between NP and AF cells analyzed via Student's t-test. The correlation between cell height and elastic modulus was examined using a linear least-squares regression analysis, with $p<0.05$ considered significant.

3.3 Results

3.3.1 Mechanical Characterization of Polyacrylamide Gel Substrates

Polyacrylamide gel formulations were found to produce uniform 2D surfaces with highly controllable material properties. Gels formed between glass coverslips produced 12mm-diameter substrates with a mean thickness of 122 ± 9 μm (n=8 gels). AFM indentation curves were found to correlate closely with the Hertz model for a spherical indenter (Figure 18A, representative curve), with a minimum R^2 value of 0.98. Surface height measurements calculated from AFM indentation probe-surface contact indicated gel surfaces were smooth (i.e. uniform in height), with height standard deviations of less than 1 μm for a typical 50 μm x 50 μm square area (Figure 18B, 25 indentations spaced 10 μm apart).

Polyacrylamide gel formulations tested contained acrylamide at final concentrations of either 5% or 8%, with bis-acrylamide crosslinker concentrations

varying from 0.03%-0.25%. These formulations yielded gels with elastic moduli ranging from 100 ± 18 Pa to 15200 ± 197 Pa, as shown in Figure 18C. As expected, gel elastic moduli were found to increase with increasing amounts of crosslinker up to 0.25% (Figure 19); however, increasing crosslinker concentrations above 0.25% decreased elastic moduli (e.g. 0.4%, Figure 19) for both 5% and 8% acrylamide gels. Gels with bis-acrylamide concentrations below 0.03% resulted in viscous gels which would flow when removing the top coverslip (producing ridges or waves in the gel surface), and which stuck to AFM indenter tip during testing.

Measured gel moduli were found to be lower for a given formulation than those reported by others using similar AFM testing methods, with the modulus values (listed in Figure 18C) approximately 50% of those reported by Engler and co-workers [49]. The gels presented in Figure 18 were created using stock solutions of acrylamide and bis-acrylamide mixed from dry powders (Source A); to examine whether the material source might affect gel moduli, another set of gels was prepared from an alternate material source (Source B: Biorad 40% acrylamide and 2% bis-acrylamide liquids, premixed from manufacturer) and tested. As shown in Figure 19, Source B gels were found to be much stiffer, with moduli approximately 4 times greater than Source A and 2 times greater than literature values. These results suggest that acrylamide material source can impact mechanical properties significantly, and that gel stiffness cannot be assumed based solely on gel formulation. All proceeding cell studies were performed with material

from Source A stock solutions, whose lower properties provided more precise control for stiffnesses in sub-1000 Pa range, which proved to be a range of interest for NP cell studies.

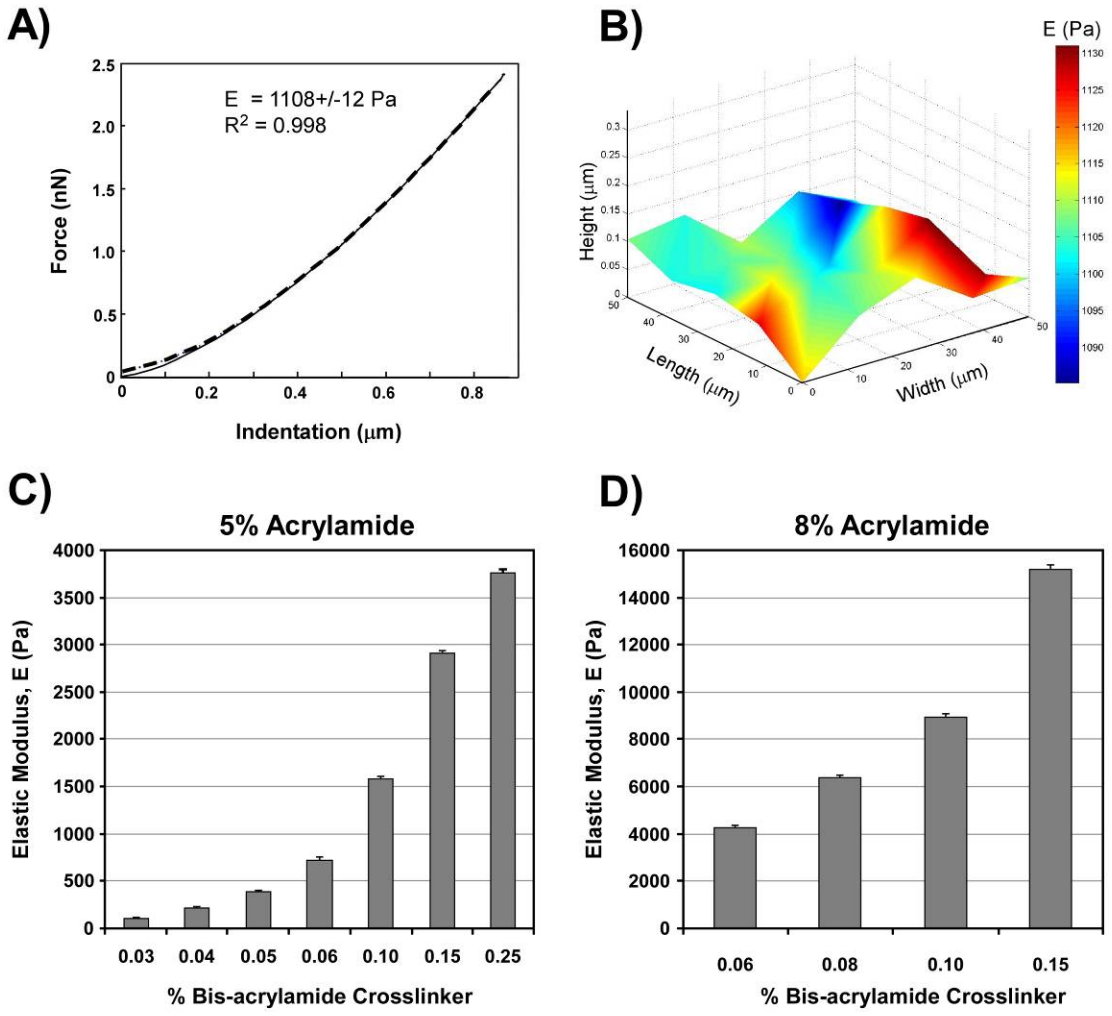

Figure 18: Mechanical properties of polyacrylamide gel substrates. (A) A representative gel AFM force-indentation curve: dotted line = average data curve-fit for 25 indentations over 50μm square area, solid line = Hertz spherical indentation model; (B) Magnified height and stiffness map for same gel area (gel height SD = 40nm); (C) and (D) mean elastic moduli (±SD) for 5% and 8% acrylamide gels (respectively) with varying amounts of bis-acrylamide crosslinker.

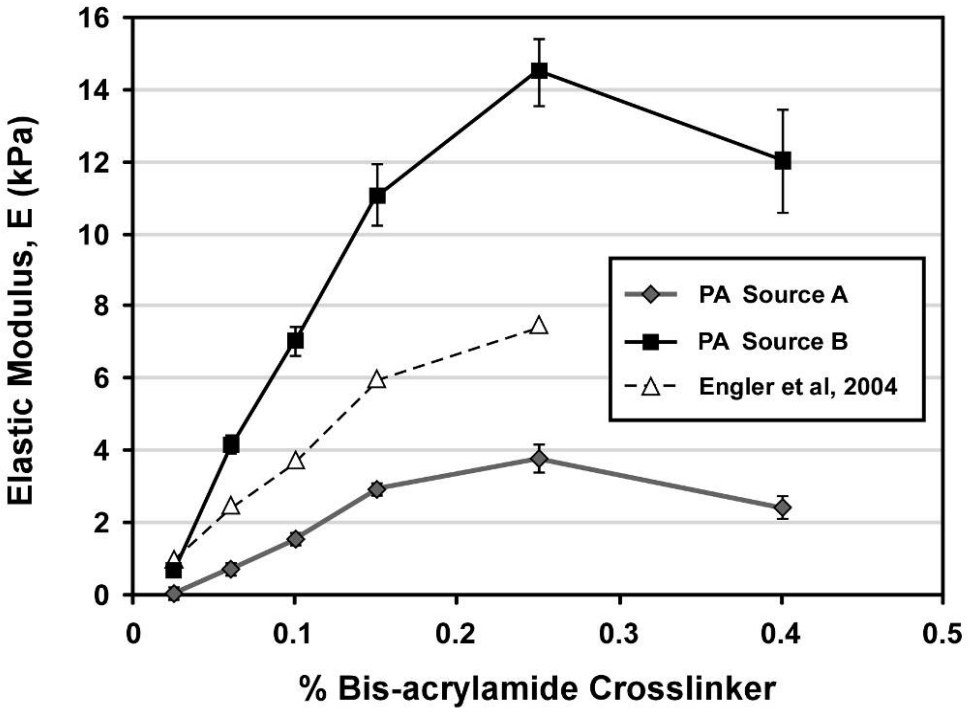

Figure 19: Comparison of polyacrylamide gel mechanical properties (5% acrylamide gels, mean elastic moduli ±SD) from different acrylamide sources, and with literature values [49].

3.3.2 ECM Functionalization of Polyacrylamide Gel Substrates

Polyacrylamide substrates functionalized with type II collagen were found to readily support NP cell attachment, with almost all seeded cells attaching to substrates of all stiffnesses after several hours. However, laminin functionalization of polyacrylamide gels proved to be more challenging, as cell attachment to gels functionalized with covalently linked BME ligand or LM-111 was very minimal, particularly for soft (100-220 Pa) gels (Figure 20B). Immunofluorescent staining for

laminin (LM-111) on BME- and laminin-111-functionalized gels indicated a significant amount of protein present on gel surfaces (Figure 20A, >95X higher than negative controls), with stiffer gels (2100 Pa) showing 3.4X higher fluorescence than soft gels (220 Pa). It was noted that the laminin fluorescent intensities for soft gels were comparable to those of protein adsorbed to the adjacent glass coverslips (data not shown), where cells were found to readily attach and spread. These findings together suggested that covalently-bound laminin was present on the gel surface, but not functional or accessible for cell adhesion.

Since the short arms of LM-111 are known to self-polymerize under specific physiologic conditions, we investigated whether a second incubation of laminin ligand (BME or LM-111) would increase protein levels and cell adhesion on gels of 2 different stiffnesses (220 Pa, 2100 Pa). Following a second incubation, laminin fluorescence was found to increase, particularly for soft (220 Pa) gels where there was approximately a 3-fold increase. No significant signal (no difference from negative control) was detected on gels which did not have laminin initially covalently-linked to the gel surface (Figure 20A, secondary incubation only).

Correspondingly, secondary incubation resulted in a large increase in cell attachment for both BME and LM-111 functionalized soft gels (Figure 20B), with more than a 4-fold increase in cell numbers for both ligands. NP cells allowed to attach for 24h showed spreading behaviors which were dependent upon substrate stiffness (Figure

20C), indicating that additional non-covalently bound laminin did not obviously interfere with cells ability to sense underlying substrate stiffness. NP cells on soft substrates remained spherical, whereas on the stiffer substrate (2100 Pa) NP cells appeared fully spread, with numerous actin stress fibers (Figure 20C). Finally, secondary incubation with BME or laminin did not substantially alter substrate elastic moduli compared to unfunctionalized substrates, as measured by AFM indentation (Figure 20D). BME-functionalized gels showed no decrease in measured E, while LM-111-functionalized gels showed a very slight (<5%, but statistically significant) reduction in modulus.

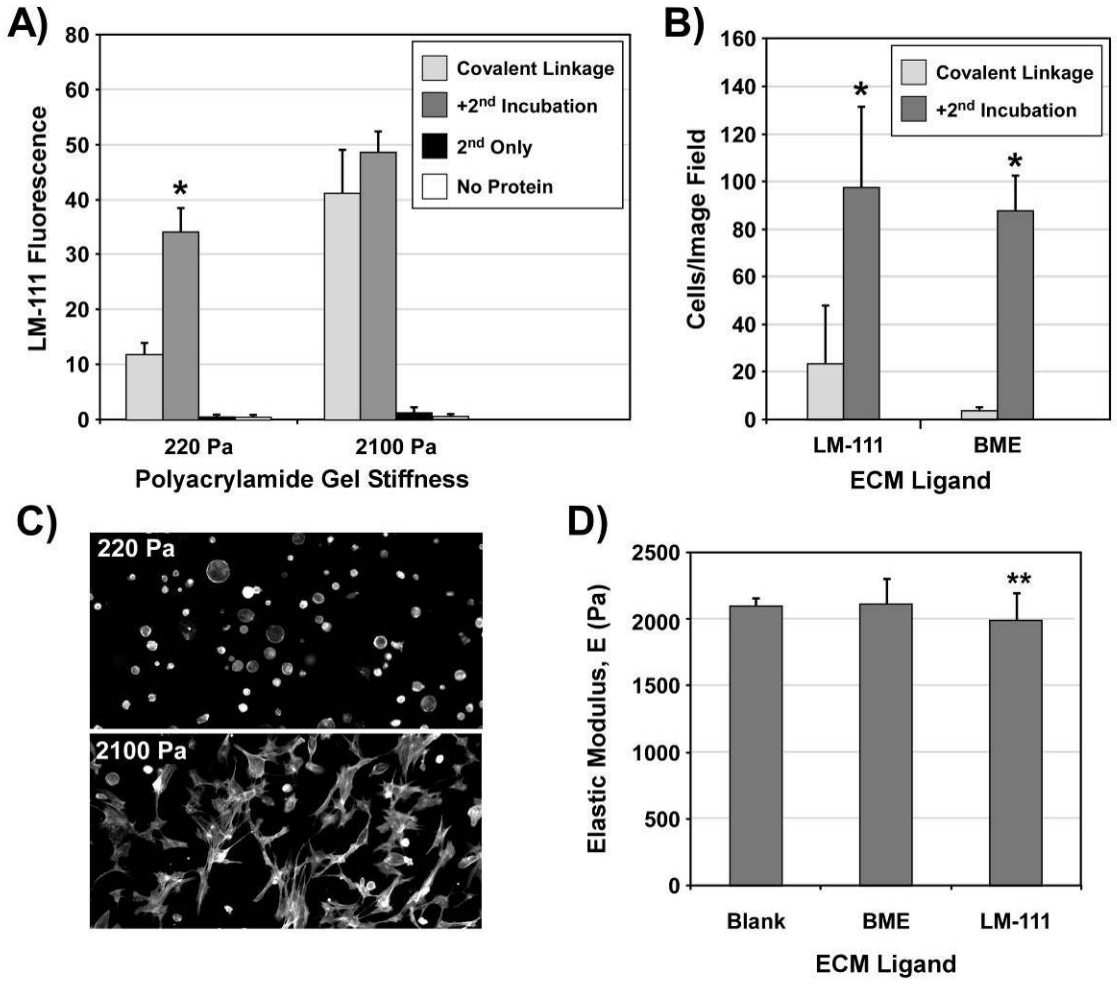

Figure 20: BME and laminin functionalization of polyacrylamide gel substrates. (A) Amount of laminin present on polyacrylamide gel surface, detected via immunofluorescence using anti-LM111 antibody. Second incubation of laminin under self-polymerizing conditions results in greater signal on soft (220 Pa) gels, *p<0.001. (B) Second incubation results in greater cell attachment to soft acrylamide gels functionalized with either BME or LM-111, p<0.001). (C) NP cells show substrate-dependent spreading behaviors on polyacrylamide substrates functionalized with second incubation of BME. (D) Comparison between elastic moduli of blank (non-functionalized) polyacrylamide gels and those functionalized with secondary incubation of BME or LM-111. (significantly different from blank, p<0.01).**

3.3.3 NP Cell-Cell Interactions on Basement Membrane Extract (BME) Gel Substrates

NP cells seeded onto self-polymerizing 2D BME gel substrates were found to attach as individual cells (Figure 21A, left), with 95% of attached cells present as single cells after 5 hours of culture. All cells remained spherical (Figure 21A), with no indication of cell spreading on gel surfaces. Over 7 days of culture, NP cells were found to reorganize to form large cell clusters (Figure 21A right, Figure 21B), with almost all cells (98%) present in multi-cell clusters (defined as a discrete group of 4 or more contacting cells). Cell clusters were typically spaced uniformly over the surface of the gel, as shown in Figure 22. It was noted that in cases where larger clusters (greater cell number) were found (Figure 22, solid arrows), these clusters were surrounded by correspondingly large areas devoid of cells (Figure 22, open arrow), suggesting cells migrate from regions immediately adjacent to clusters.

Clusters were large in size (Table 1), with an average of more than 100 cells per cluster and a maximum dimension of 185±81 μm. Additionally, cell clusters were found to be 3-dimensional (mean height = 99±27 μm), often greater than 5 cell layers high (Figure 23B). Confocal image sections of clusters stained for actin and cell nuclei (Figure 23A) revealed an interconnected network of cells, with large void areas consistent with intracellular vacuoles (Figure 23A, arrows). This morphology and cellular organization is reminiscent of *in situ* NP cell morphology observed in immature porcine and rat tissues (e.g. from Chapter 1).

In contrast to BME gel substrates, NP cells seeded on tissue culture plastic coated with unpolymerized BME formed a uniform monolayer (Figure 21C), with cells exhibiting an elongated, flattened morphology with dense stress fibers. There were no apparent signs of cell clustering, with cell nuclei uniformly distributed (Figure 21C, right) over a given image field. These results suggest that, in addition to BME ligand, there are other extracellular matrix factors critical to driving NP cell-cell interactions *in vitro*. Using the polyacrylamide gel system, we next examined whether ECM ligand, stiffness, or both were important in modulating NP cell-cell interactions observed on BME gel substrates.

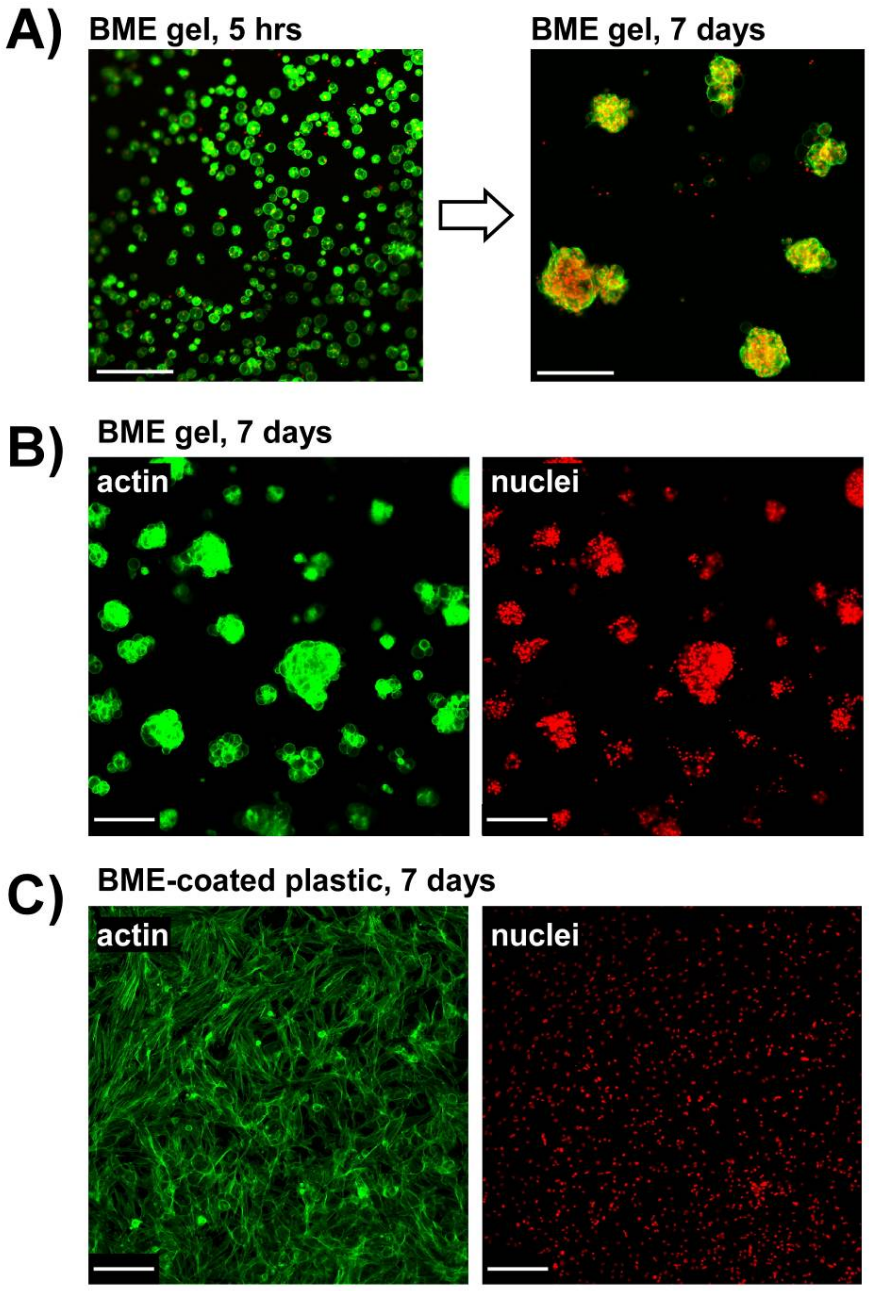

Figure 21: NP cell organization on BME substrates. (A) NP cells seeded on 2D BME gel substrates attach as individual cells (left) and self-assemble into cell clusters (right) following 7 days culture (green: actin, red: cell nuclei). (B) NP cell clusters (7d culture) showing actin cytoskeleton (left) and cell nuclei (right). (C) NP cells (7d culture) on unpolymerized BME-coated tissue culture plastic (left=actin; right=nuclei). Scale bars = 200μm.

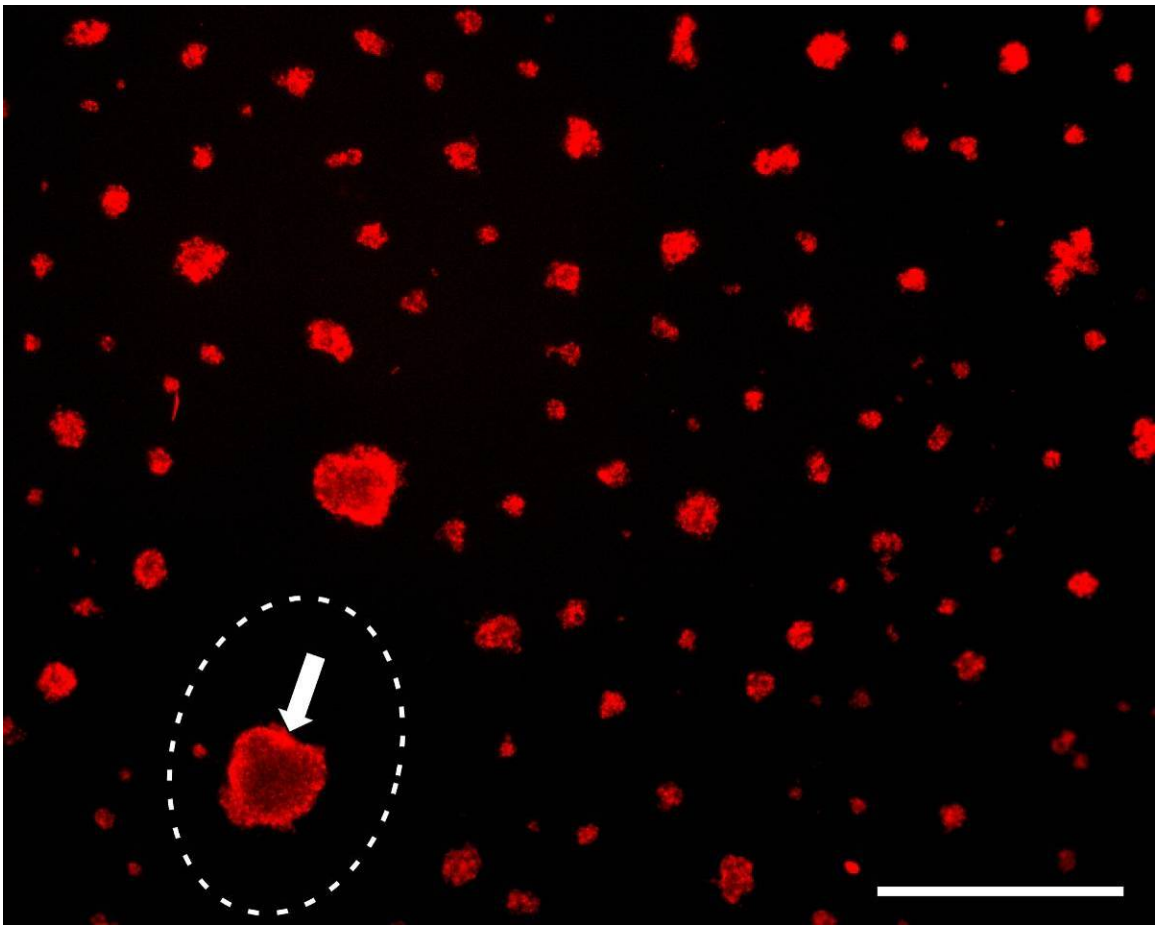

Figure 22: NP cell clustering on BME gel surface following 7 days culture. Low magnification (2.5X) view of fluorescently-labeled cell nuclei illustrates uniformity of cluster size and spacing. Larger cell clusters (solid arrow) were typically surrounded by large areas devoid of cells (dashed line). Scale bar = 1000μm.

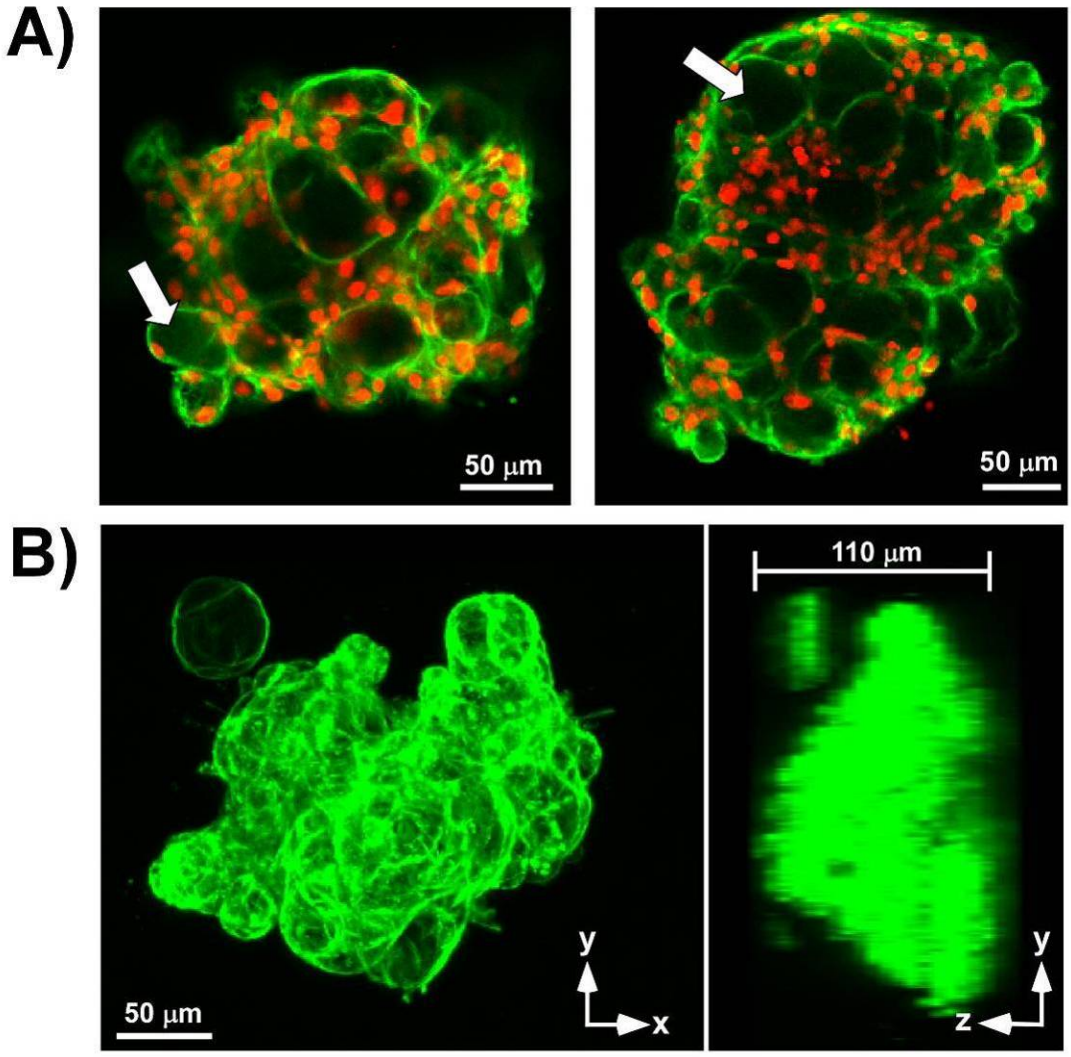

Figure 23: Confocal sections and 3D projections of NP cell clusters following 7 days culture on BME gel substrates. (A) Confocal sections (7μm thick image slice) of two different NP cell clusters show cell nuclei (red) and actin cytoskeleton (green), with voids (white arrows) consistent with intracellular vacuoles. (B) Confocal image stack projections (left: in plane with gel surface; right: perpendicular to gel surface) of actin cytoskeleton illustrating 3D nature of cell clusters.

Table 2: NP cell cluster sizes on BME and BME-functionalized acrylamide gel substrates. Mean ± SD for ≥25 clusters per condition (n= 2-3 separate cell isolations, multiple wells per experiment analyzed). For each measurement (columns), substrates not labeled with the same letter were statistically different, p<0.005.

Substrate	Cell Number	Height (μm)	Max. Dimension (μm)
BME gel	115 ± 100 ^{A}	99 ± 27 ^{A}	185 ± 81 ^{A}
PA-BME (100 Pa)	41 ± 80 ^{B}	53± 16 ^{B}	143 ± 106 ^{A,B}
PA-BME (230 Pa)	32 ± 40 ^{B}	45 ± 22 ^{B}	108 ± 43 ^{B}

3.3.4 Role of ECM Ligand and Substrate Stiffness in Modulating NP Cell-Cell Interactions

To evaluate the specific roles of ECM ligand and substrate stiffness in the observed NP cell-cell interactions, we examined cell clustering behavior on 2-dimensional polyacrylamide gels, which could be tuned to precise stiffnesses and functionalized with specific ECM ligands. The stiffness of self-polymerizing BME gels was measured via AFM indentation, with a mean elastic modulus of E_{BME} = 235±5 Pa. Four formulations of polyacrylamide substrates were then selected which were similar to, or different from, E_{BME} (stiffnesses ranging from 100 Pa to 15200 Pa, Figure 24). Acrylamide gels were functionalized with either unpolymerized BME or type II collagen, and freshly isolated NP cells were then seeded directly onto substrates and cultured for 7 days. On BME-functionalized gels with stiffnesses similar to or less than

E_{BME} (100, 220 Pa), a distinct clustering behavior was observed following 7 days culture (Figure 25, top 2 panels), with >90% of all cells present in clusters on 100 Pa and 210 Pa gels (Figure 27). These clusters were smaller in size (cell number, maximum dimension, and height) than clusters on BME gels (Table 1), but were still 3-dimensional (typically 2-3 cell layers high). Actin staining revealed a cortical arrangement with very few stress fibers or elongated cells. In contrast, NP cells on somewhat stiffer BME-functionalized gels (720 Pa) exhibited dramatically less clustering, with just 10% of cells present in clusters (Figure 27). Cells on this gel stiffness primarily formed a monolayer sheet (<25μm height), with elongated cell morphologies and numerous actin stress fibers (Figure 25). Similar behavior was observed on the stiffest gel substrates, with no cell clusters observed (0%, Figure 27).

Clustering behaviors of NP cells on collagen-functionalized acrylamide gels (Figure 26) were found to be notably different than on BME, with little cell clustering behavior observed at even the lowest substrate stiffnesses. As shown in Figure 27, just 5% of cells were present in clusters on the softest collagen substrates (100 Pa), and less than 1% of cells on stiffer collagen-functionalized substrates found in clusters (220-15200 Pa). On the softest substrates (100 and 220 Pa), cells assumed a spindle-shaped morphology, with long, thin projections extending from cell bodies (Figure 26). As substrate stiffness increased, cells were found to form a dense monolayer and contained numerous actin stress fibers.

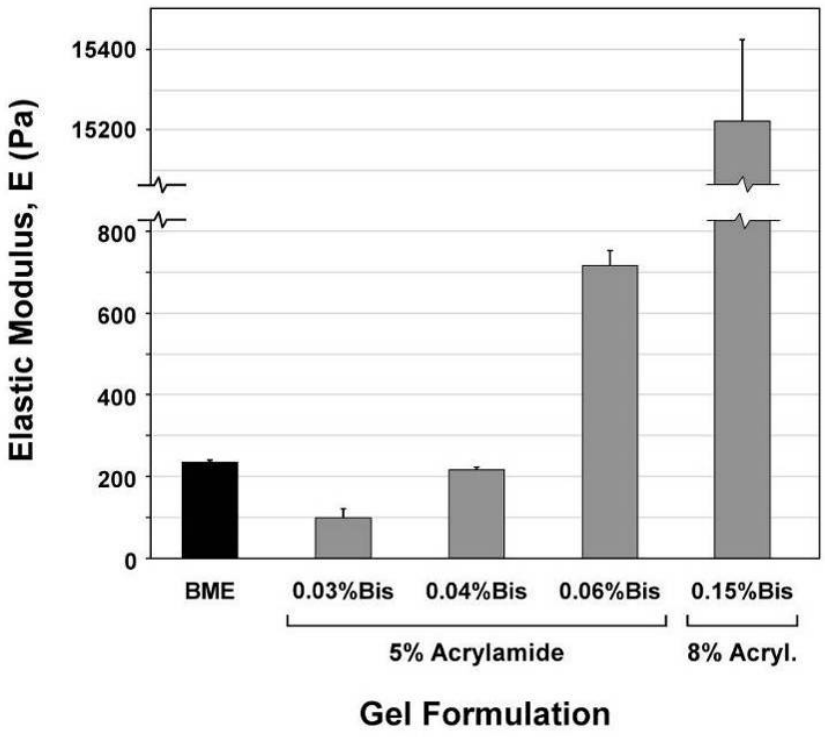

Figure 24: Elastic moduli of BME and polyacrylamide gel substrates used for NP cell-cell interaction studies.

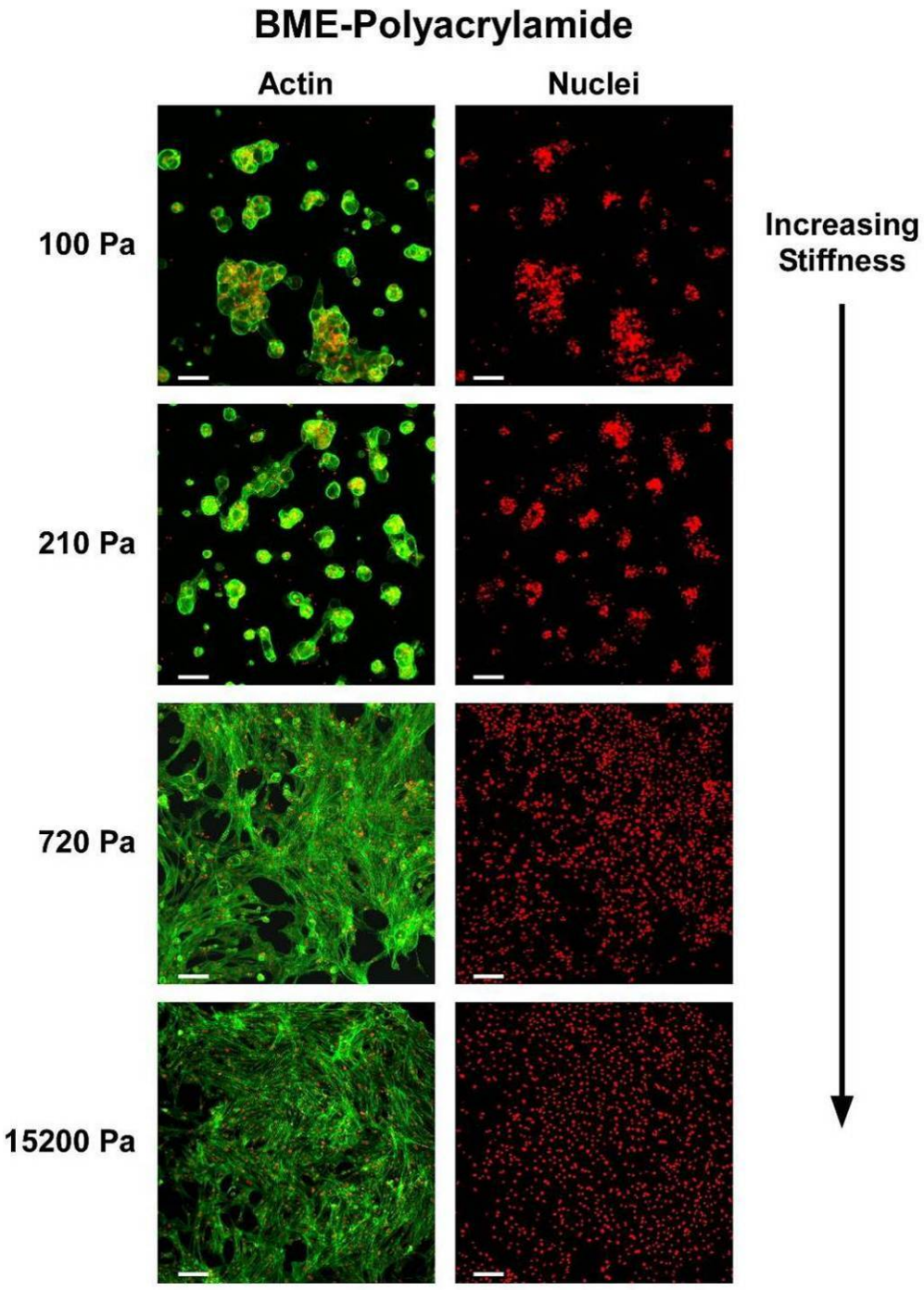

Figure 25: NP cell organization and morphology on BME-functionalized acrylamide gels of varying stiffness following 7 days of culture.

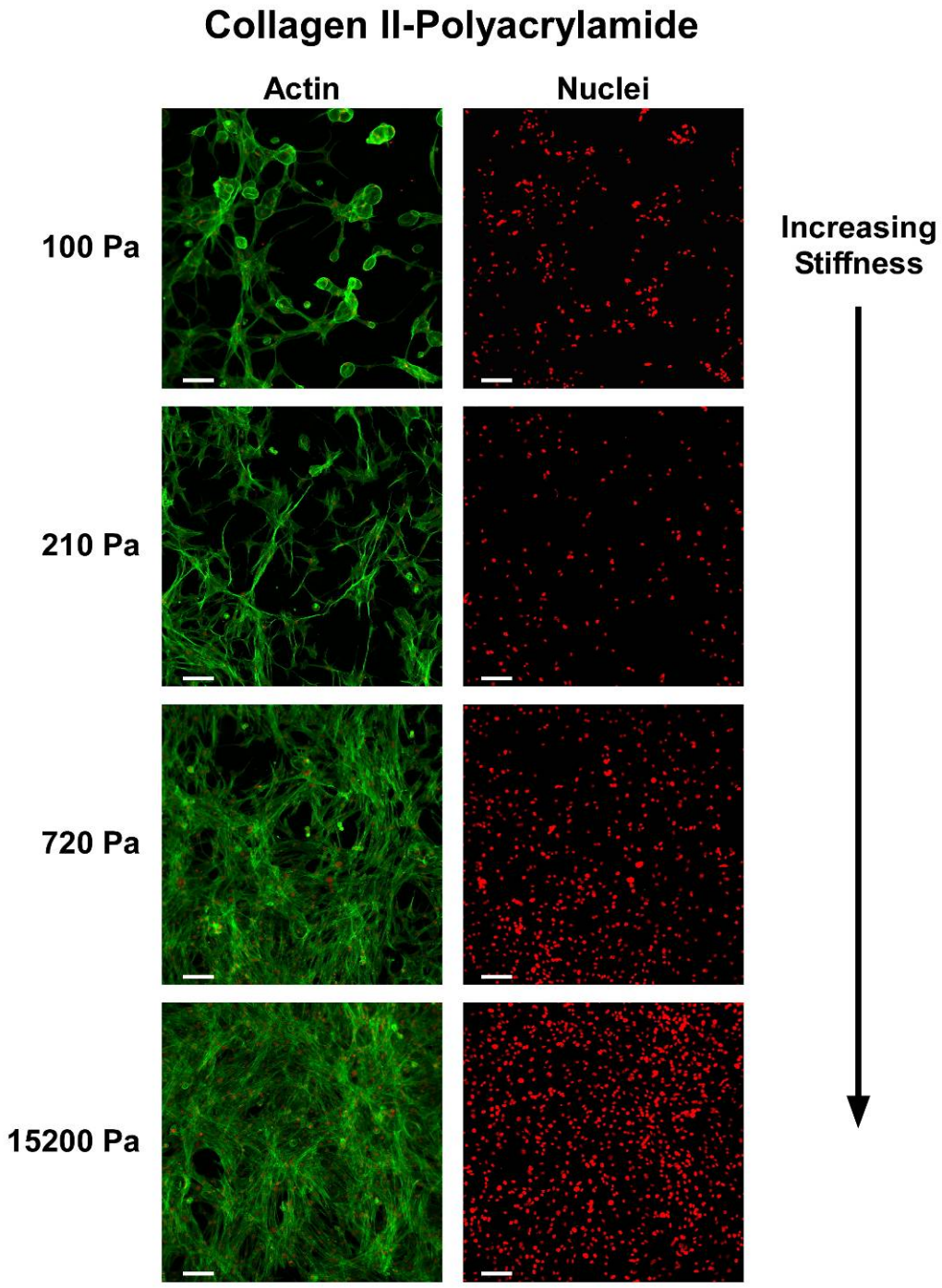

Figure 26: NP cell organization and morphology on type II collagen-functionalized acrylamide gels of varying stiffness following 7 days of culture.

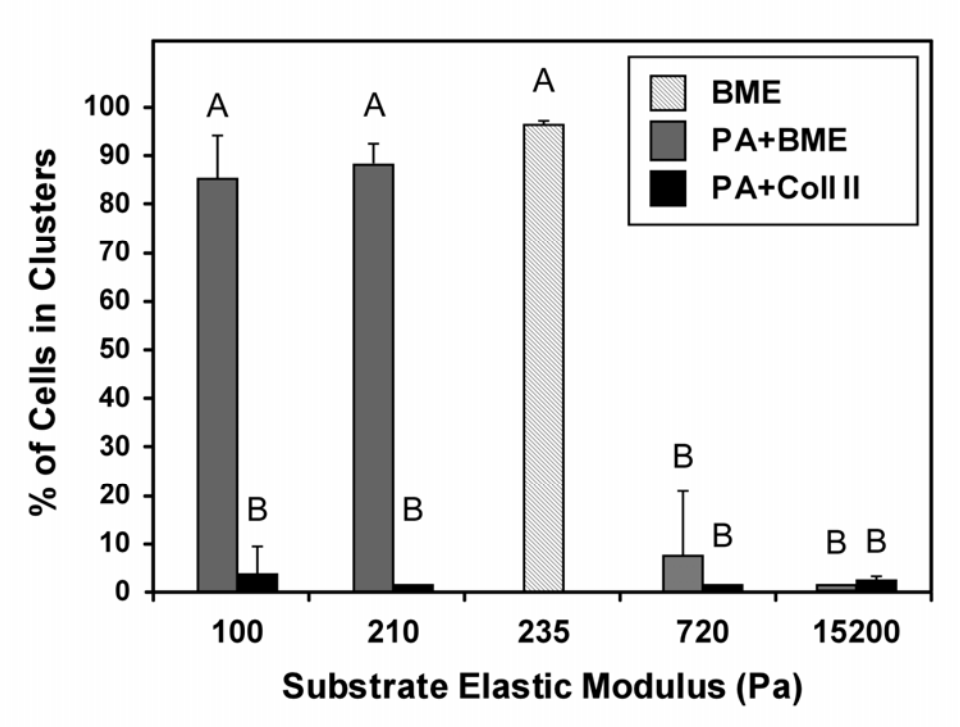

Figure 27: Percentage of NP cells present in multi-cell clusters (mean±SD) following 7 days of culture on BME gels and polyacrylamide (PA) gel substrates functionalized with either BME (PA+BME) or type II collagen (PA+Coll II). Percentage represents n=4-7 image fields per condition across multiple gels, >3000 cells per condition counted, NP cells from 2-3 separate cell isolations. Conditions with different letters were significantly different by Tukey's HSD, $p<0.0001$.

3.3.5 IVD Cell Mechanical Properties

In order to understand how the elastic modulus of individual NP cells compares to those of various culture substrates, we measured the moduli of freshly isolated NP cells using the same micro-mechanical testing method, AFM indentation. Additionally, we measured the moduli of cells from the adjacent AF region for a further point of reference. NP cells (n=30) were found to have an average elastic modulus of 345 ± 225

Pa (Fig. 18A), which was significantly lower than the modulus measured for AF cells (621 ± 337 Pa, n=28). Within NP cells, there was a fairly large range of moduli, varying from 49 Pa to 825 Pa. Cell height was also measured via AFM indentation, using the difference between indentation contact point on the cell and that of the adjacent substrate. As expected, NP cells were found to be significantly taller, with a mean cell height of 24.7 ± 5.8 μm (Figure 28B) compared to just 11.9 ± 1.5 μm for AF cells. There was a slight but statistically significant negative correlation between NP cell height and stiffness (Figure 28C, linear fit, $p=0.04$, $R^2=0.137$), with taller (i.e. larger) NP cells having lower elastic moduli. There was no correlation detected between AF cell height and stiffness ($p=0.70$).

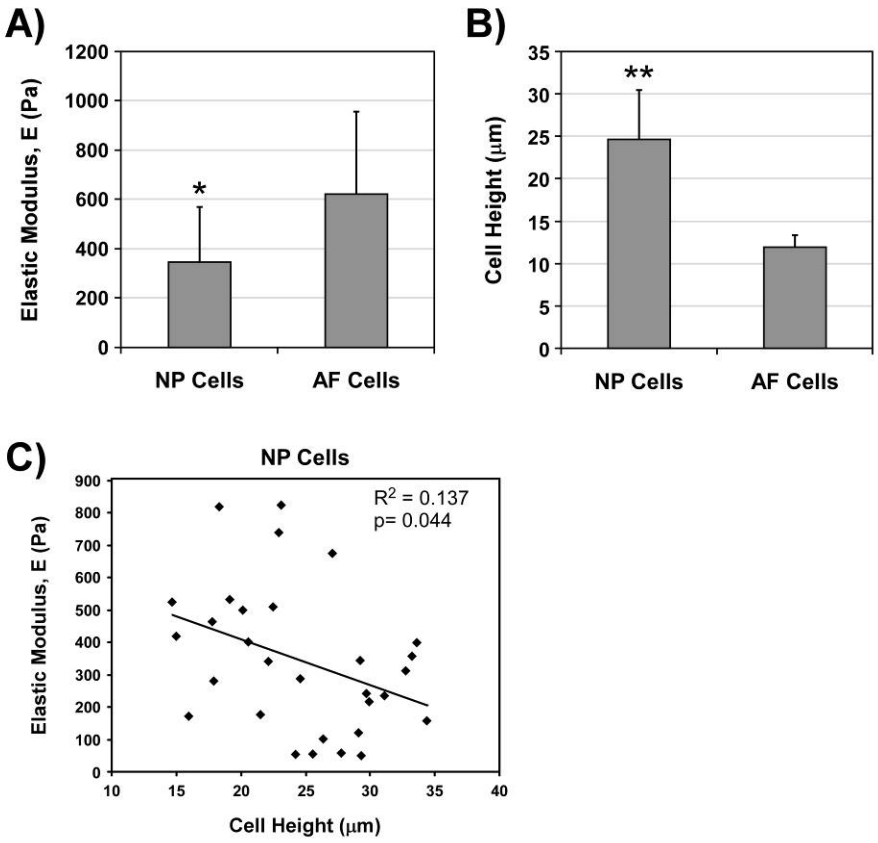

Figure 28: IVD cell elastic moduli and cell height measured via AFM. (A) Mean elastic moduli (±SD) for freshly isolated NP (n=30) and AF (n=28) cells. *NP cells stiffness was significantly less than AF cell stiffness (p<0.0001). (B) Mean cell heights for NP and AF cells, **NP significantly different from AF, p<0.001. (C) NP cell height versus elastic modulus, slope significantly different from zero (p=0.044).

3.4 Discussion

3.4.1 Mechanical Characterization of Polyacrylamide Gel Substrates

Atomic force microscopic measurements of polyacrylamide gels indicated substrates exhibited highly uniform surface properties. AFM indentation showed very consistent mechanical properties for gels of a given formulation, with standard

deviations of elastic moduli typically less than 5% of the mean. Force-indentation curves correlated highly with the Hertz spherical indentation model (R^2 values typically >0.99), consistent with previous studies [12,49] indicating that the instantaneous behaviors of polyacrylamide gels was elastic. Additionally, gels were found to have a uniform, smooth topography (surface heights typically varied <1μm over a 2500μm^2 testing area), suggesting that any voids or other features present on the gel surface were much smaller than the AFM's 5 μm diameter indenter tip.

The gel formulations examined resulted in a large range of stiffnesses, with elastic moduli varying from as low as 100 Pa for the softest 5% acrylamide gels to over 15 kPa for the stiffest 8% acrylamide gels. Moduli were found to increase approximately linearly with increasing crosslinker concentration up to 0.15% bis-acrylamide; beyond this concentration stiffness appeared to peak (0.25% bis-acrylamide) and then decrease (0.40%) for both 5% and 8% acrylamide gels. This behavior has been documented previously for polyacrylamide gels [12], and has been attributed to differential reactivity of the bis-acrylamide and acrylamide monomers, with the bis-acrylamide crosslinker being more reactive; at higher crosslinker concentrations a two-phase structure is formed, with crosslinker linking to itself to form highly crosslinked "islands" that do not contribute the elastic properties, which are linked together by a gel containing less crosslinker.

Elastic moduli measured for 5% acrylamide gels in this study were notably lower than those reported by Engler and co-workers for the same gel formulations (E values approximately half of 5% gels, Figure 19), measured using similar AFM micro-indentation methods. Contributing factors to this discrepancy may include actual differences in material properties resulting from different material sources or gelation procedures, as well as differences in measurement methods. Our testing of gels from a different material source (Source B, Figure 19) indicated gel properties could vary dramatically as a function of material source (with Source B having moduli approximately 4-fold higher than Source A), suggesting material variability was a major contributor to the differences observed. One difference in measurement method by Engler and co-workers was use of an unsharpened pyramidal-tip indenter; however, they commented that changing to a 5μm spherical indenter did not alter their modulus values. Thus it appears that acrylamide gel material properties are highly dependent upon material source, and gel mechanical properties should be verified each time stock solutions are replenished.

3.4.2 ECM Functionalization of Polyacrylamide Gel Substrates

Coupling of functional laminin (or BME) to polyacrylamide proved to be challenging, with covalently linked protein supporting very little cell adhesion. Fluorescent immuno-labeling of laminin suggested that a significant amount of protein

was coupled to the gel surface, with fluorescence levels comparable to those of protein adsorbed to glass (where NP cells were found to quickly attach and spread). Assuming that an adequate quantity of protein was coupled to the gel, there are several possibilities that may explain lack of cell attachment. First, random orientation or a lack of accessibility to laminin's cell binding region when coupled to a porous gel surface (where pores are likely smaller than cells, but larger than proteins) may have limited cell adhesion. As laminin is a large (~800 kDa) cross-shaped molecule with a primary integrin binding site (LG domain) located at the end of one arm, a critical concentration of properly oriented and accessible LG domains may not have been achieved, despite having adequate overall quantities of protein. Second, chemical crosslinking of laminin may have impaired the protein's functionality. Laminins have been reported to be sensitive to chemical modification [15], although reasons are not well understood. The LG domains do not contain a higher percentage of primary amines than the rest of the protein (LG domains comprise 17% of protein, contain 17% of lysine and arginine residues); however, the helical structure of the non-LG domain portions of the protein (see Figure 4 in Chapter 1) may make the LG domain most susceptible to chemical modification.

On soft gels, secondary coupling of laminin under self-polymerizing conditions was found to dramatically increase protein concentration (>3-fold, Figure 20A) and NP cell adhesion (>5-fold, Figure 20B). Increased protein concentration, orientation, and

accessibility may all have contributed to increased cell adhesion. NP cells still showed substrate stiffness-dependent spreading behaviors (Figure 20C) on gels with secondary polymerization, indicating that it did not grossly shield cells from sensing mechanical properties of the underlying substrate. AFM testing of gels with or without secondary coating of BME or LM-111 confirmed that observation, although a slightly lower modulus (5% less) was measured on LM-111-functionalized gels. Together, these results indicate a self-polymerizing secondary incubation with laminin ligands (BME or LM-111) is an effective method to improve NP cell adhesion on soft polyacrylamide substrates.

3.4.4 NP Cell-Cell Interactions on Basement Membrane Extract (BME) Gel Substrates

NP cells were found to rapidly attach to soft 2-dimensional BME (self-polymerizing) gels, with attached cells present as single, rounded cells following 5 hours of culture. Individual cells on BME gels showed minimal cell spreading at any time point, instead remaining spherical with a primarily cortical actin cytoskeleton (Figure 21A). Following 3-4 days culture, NP cells began to form multi-cell aggregates, and at 7 days practically all cells (98%) were found in large cell clusters. Clusters were 3-dimensional and typically greater than 5 cells layers high, with large areas of substrate surrounding a cluster devoid of cells (Figure 21A, Figure 21B, Figure 22). These observations suggest that NP cells favor cell-cell interactions over cell-substrate

interactions under these substrate culture conditions, possibly with the intent of maximizing cell-cell contact area.

The findings for increased cell-cell interactions and tissue-like cellular organization on (or within) soft BME substrates have been documented for a number of cell types, with a thoroughly explored culture model of particular interest being that of mammary epithelial cells (MECs) [112,153,177]. These epithelial cells form polarized, functional cell clusters in response to a 3-dimensional BME culture environment [108], and share several phenotypic and organizational characteristics with immature NP cells including strong cell-cell adhesions (e.g. desmosomes) and laminin cell-ECM adhesions (α6, β4 integrin expression, cell-associated LM-332 expression, as described in Chapter 1). Exploration of this model has determined that two signals provided by this culture environment are critical for phenotypic maintenance: (1) soft (<400 Pa) substrate elasticity [140], and (2) the presence of LM-111 ligand [73,161]. Together these factors drive organoid formation and mammary tissue-specific gene expression; in Chapter 4, we explore whether one key immature NP cell behavior (proteoglycan production) is promoted in response to similar culture conditions.

The spacing and size of NP cell clusters on BME gels was found to be remarkably uniform (Figure 22). Additionally, it was noted that the cell-free areas of the substrate surrounding a given cluster were typically proportional to the cluster size, which was particularly apparent in the (occasional) cases where larger clusters were observed

(Figure 22, arrow and dashed lines). These observations may indicate that NP cells migrate on the gel surface until coming into contact with a nearby group of cells, then proceed to join the group. This behavior would correspond with observations by Guo and co-workers [78], who noted that single cells (epithelial cells, fibroblasts) seeded onto soft polyacrylamide substrates (functionalized with fibronectin) migrate until contacting a cell aggregate, upon which they were "pulled into" the aggregate. They found that once cells joined an aggregate, none were observed to leave, and that this behavior occurred on "soft" (2.7 kPa) but not "stiff" (7.7 kPa) substrates.

How might the NP cell organization observed here develop? Assuming that NP cells remain within an aggregate following cell-cell contact, this cell clustering arrangement might indicate that small groups of cells continue to move together after contacting each other, but migration speed progressively slows or stops with the addition of more cells (i.e. if cell migration stopped after contacting an adjacent cell, many groups of just a few cells would be present; if groups of many cells continued to migrate rapidly, a single giant cluster would be eventually formed). Real-time observations using live-cell microscopy would be valuable to provide a better understanding this behavior.

In contrast to behavior on soft BME gels, NP cells cultured on tissue culture plastic coated with unpolymerized BME formed a monolayer of uniformly distributed cells (Figure 21C), with no evidence of cell clustering behavior. Cell morphology

appeared to be fibroblast-like, with numerous stress fibers and little evidence of intracellular vacuoles following 7 days of culture. This finding suggests ECM ligand alone is not a sufficient signal to promote NP cell-cell interactions, and that another feature of the BME gel such as ECM stiffness may be partially or solely responsible for the observed NP cell behaviors. However, ECM protein adsorbed to plastic is not an ideal control for long term culture, as non-specific adsorption of other ligands (cell-generated or from serum) is possible. Subsequent studies using polyacrylamide gel substrates (Section 3.3.5) allowed for more precise control of ECM ligand and stiffness variables in investigating these NP cell behaviors.

Higher resolution inspection of NP cell clusters via confocal microscopy (actin cytoskeleton, cell nuclei) revealed a network of interconnected cells, with the boundaries of individual cells being difficult to distinguish. Clusters were large multi-cell aggregates (115 ± 100 cells/cluster) with no obvious organization or polarity, and contained numerous large void spaces which were assumed to be intracellular vacuoles. This cluster organization and cell morphology was very similar to that documented *in situ* in immature NP tissues (porcine and rat tissues, e.g. Figure 3 in Chapter 1), where similar void spacing and an interconnected cell network was observed, and contrasted with morphology on rigid substrates were no vacuoles were observed and morphology was fibroblastic. Whether these morphological and organizational characteristics

observed on soft BME substrates translate into maintenance of an NP cellular phenotype was explored further in Chapter 4.

3.4.5 Role of ECM Ligand and Substrate Stiffness in Modulating NP Cell-Cell Interactions

NP cells cultured on BME-functionalized polyacrylamide substrates with elastic moduli less than (100 Pa) or similar to (220 Pa) that of E_{BME} showed significant clustering behavior following 7 days of culture (Figure 25), with over 90% of NP cells present in cell clusters. Clusters were again 3-dimensional (2-3 cell layers high), although generally smaller in size (cell number, dimensions) in comparison to clusters on BME gels (Table 2). Interestingly, there appeared to be a decrease in all cluster size measurements (cell number, maximum dimension, height) as gel stiffness increased from 100 Pa to 220 Pa. NP cells on these soft gels appeared to have a distinct cortical actin cytoskeleton, and maintained a large, vacuolated appearance. The differences in cluster size and cell morphology observed between BME gels and soft BME-functionalized acrylamide (E = 100, 220 Pa) may be due to differences in mechanical behavior of the two different types of gels; polyacrylamide gels are primarily elastic in nature [12,49], whereas BME gels may be more viscoelastic [158], particularly on the time scales relevant for cell adhesion probing and cell migration, and thus may "feel" softer to cells. Additionally, lower ligand densities on the PA gel surface could also contribute to observed morphological differences.

In contrast, on slightly stiffer BME-functionalized substrates (720 Pa) NP cell organization and morphology shifted dramatically to a uniform cell monolayer (primarily elongated morphologies, actin stress fibers), with very little clustering behavior observed (10% of cells in clusters, Figure 25 and Figure 27); on the stiffest substrates (15200 Pa), no cell clustering was observed. These findings point to a direct role of substrate elasticity in modulating NP cell-cell interactions, and suggest that there may be a fairly narrow range of mechanical stiffnesses over which this transition takes place (~200-700 Pa).

NP cell responses on the softest (100 Pa) collagen-functionalized acrylamide gels were found to be quite different than for BME-functionalized acrylamide, with little or no clustering behavior observed. NP cells instead exhibited a spindle-like morphology with long thin cell processes extending away from or between cells; in the few cases where rounded, vacuolated cells were observed, they appeared to be attached on top of other cells, where they were perhaps shielded from direct interactions with the substrate. Although few discrete cell clusters (isolated cell aggregates) were observed on 100 Pa collagen-functionalized gels, in many areas cells appeared to be connected or strung together end-to-end in a network, which is most evident when examining arrangement of cell nuclei (Figure 26, top right). This behavior appears similar to that reported by Califano and Reinhart-King [27], who found that endothelial cells formed end-to-end cell-cell networks of similar morphology when cultured on soft (200 Pa)

acrylamide gels functionalized with type I collagen. For NP cells in the present study, culture on just slightly stiffer collagen-functionalized gels (220 Pa) resulted in no signs of clustering or 'network' behavior, with cells exhibiting an elongated, stress-fiber rich morphology and practically no identifiable vacuoles. Similar NP cell morphology was noted on stiffer collagen substrates (720 Pa, 15200 Pa).

Together these results indicate that both substrate stiffness and ECM ligand are key factors controlling NP cell-cell interactions. This corresponds with the results of several studies examining the balance between cell-cell and cell-substrate adhesions on 2-dimensional surfaces (for epithelial [43] and endothelial [27] cells). In both studies cell-cell interactions were promoted by reducing substrate stiffness, and by reducing cell adhesivity to the ligand which was achieved by either: (1) reducing ligand density [27], or (2) using a less adhesive ligand (LM-111, which was measured to be less adhesive than collagen for the epithelial cells studied) [43]. The authors propose that cells' lack of ability to generate cell-substrate traction (on soft or less adhesive substrates) is compensated for by increasing traction on each other via cell-cell contacts, and that a "tug of war" may exist between cell-cell and cell-ECM adhesions. Similar evidence of this behavior exists for 3D cultures, where increasing the stiffness of BME/Type I collagen gels (by increasing collagen concentration) leads to disruption of cell-cell adhesions, perturbs polarity, and increases cell growth in an *in vitro* mammary epithelial cell model [140].

There are several possible implications for the findings of NP cell-cell interactions documented here. NP cell organization *in vitro* was shown to be sensitive to substrate stiffness, where an increase in substrate elastic modulus of ~500 Pa resulted in loss of cell clustering behavior. The stiffness of NP tissue has been documented to increase with increasing age and degeneration [91], and this change could be an contributing factor in dissociation, differentiation, or cell death of clustered immature (notochordal-like) NP cells. Likewise, clustering behaviors were only observed on BME-functionalized substrates, suggesting changes in ECM ligand environment (e.g. decreased presence of laminin ligands) may also play a role aging-related changes in NP cell phenotype. Additionally, the ECM ligand and substrate stiffness findings presented here may be useful for developing tissue engineering strategies for the NP, where soft, laminin-functionalized gels could potentially be used as cell-instructive biomaterials to promote an NP-like cell phenotype.

3.4.6 IVD Cell Mechanical Properties

AFM indentation testing of isolated porcine IVD cells found NP cells to be soft (E_{NP_Cells} = 345 ± 225 Pa), significantly lower than that measured for cells from the adjacent AF region (621 ± 337 Pa). This finding is in contrast to findings by Guilak and co-workers [75], where in micropipette aspiration experiments porcine NP cells were found have an instantaneous modulus, k1+k2 ≅ 800 Pa, which was found to be more than twice that of AF cells. Additionally, Guilak and co-workers found a positive correlation

between NP cell size and equilibrium elastic modulus; in the present study, a (weak) negative correlation was detected. These discrepancies may be a result of the different testing methods employed, with micropipette aspiration and cell indentation applying different types of loading (tensile and compressive, respectively) to the cell. In addition to testing method, differences in culture conditions prior to testing may also have been critical: for micropipette studies, cells were dissociated, suspended in alginate beads and cultured in serum-containing media (10% FBS) for 1-3 days prior to testing. In the present study, cells were tested within 3 hrs of dissociation. Further studies examining how NP cell properties change in culture may be necessary to better explain the observed differences. Despite different testing methods, the average NP cell moduli in both studies fell in a range between 350-800 Pa.

The magnitude of E_{NP_Cells} measured here is similar to the magnitude of (BME-functionalized) substrate stiffnesses where NP cells were found to transition from cell aggregates (exhibiting strong cell-cell interactions) to a monolayer sheet (where cells were observed to interact primarily with the underlying substrate). This finding may correspond with previous work by Guo and colleagues [78], who observed that cells from rat cardiac tissue would migrate out of soft tissue onto substrates which were stiffer than, but not softer than the native tissue. They (and others [43]) have proposed that cells may seek to maximize mechanical input (i.e. generate maximum traction) from their environment, via either cell-substrate or cell-cell interactions. However, the

findings that NP cell clustering was much more prevalent on BME-functionalized surfaces suggests that chemical cues (i.e. ligand signaling or adhesivity) are also critical in determining whether or where this transition occurs. It may be of interest to examine other cell types to see if they transition from cell-cell to cell-substrate interactions at a different "critical" stiffnesses, and whether this critical stiffness is dependent upon cell type, cell stiffness, cell contractility, or other factors.

3.5 Conclusions

Results presented in this chapter identify key roles for two environmental variables, ECM ligand and substrate elasticity, in modulating organization (i.e. cell-cell interactions) and morphology of isolated NP cells. Culture on soft, laminin-rich BME self-polymerizing 2D gel substrates promoted formation of large NP cell aggregates, and this behavior was determined to depend on both ECM ligand and substrate stiffness. The primary conclusions from the studies presented in this chapter include:

1. **NP cells self-assemble into 3-dimensional cell clusters on soft, laminin-rich BME gel substrates, confirming Hypothesis 3.A**. This behavior was found to be highly uniform, with practically all cells present in large aggregates after 7 days of culture. The vacuolated cell morphology and clustered organization observed on BME substrates was strikingly reminiscent of that documented in immature

NP tissues. NP cells appear to maximize cell-cell interactions in response to ECM cues presented by soft BME substrates. Whether this *in vitro* cell morphology and organization translates into NP cell phenotypic behaviors in culture will be explored in Chapter 4.

2. **The NP cell clustering behavior observed was found to be a function of both substrate stiffness and ECM ligand, which confirmed Hypothesis 3.B**. On BME-functionalized polyacrylamide gel substrates with tunable mechanical properties, NP cells transitioned from clustered to spread morphologies as substrate stiffness was increased, with most cells (>90%) in clusters on substrates with elastic moduli similar to or lower than that of self-polymerizing BME gel (100-220 Pa), and almost no cells found in clusters on slightly stiffer substrates (>720 Pa). In contrast, very minimal clustering behavior was observed on collagen-functionalized polyacrylamide substrates of any stiffness, indicating ECM ligand is also an important factor in modulating NP cell-cell interactions.

3. The elastic modulus of NP cells was measured to be 345 ± 225 Pa using the same AFM indentation method used to measure substrate properties. **This value fell within the range of substrate stiffnesses over which NP cells were found to transition from cell-cell to cell-substrate interactions (200-700 Pa), which**

supported Hypothesis 3.C. This finding may indicate that NP cells mechanically sense both their extracellular matrix and cellular environments, preferring to interact with the stiffest environment. NP cells were also found to be softer than cells from the adjacent AF tissue (621 ± 337 Pa), and a slight correlation was detected between increasing NP cell size (height) and decreasing modulus. Both of these findings were in contrast to a previous micropipette aspiration study of porcine IVD cell properties, although differences may be due to testing method or cell culture conditions. Both studies measured elastic (or instantaneous) moduli of immature porcine NP cells to be between 350-800 Pa.

4. Effects of Extracellular Matrix Environment on NP Cell Matrix Production

4.1 Introduction

The nucleus pulposus (NP) region of the intervertebral disc (IVD) is a highly hydrated, gelatinous tissue whose fluid-like behaviors serve to resist and redistribute compressive loads in the spine. Water in the NP is bound by a high concentration of negatively-charged proteoglycans, which make up approximately 65% of dry weight in NP tissues [70,162]. However, both proteoglycan and water content decrease in the NP with age and degeneration [25,70,143], and loss of (or failure to maintain) this proteoglycan-rich extracellular matrix is likely a key factor in progressive disc degeneration [154]. Thus, strategies to repair or replace IVD tissues (or inhibit degeneration) may involve stimulating proteoglycan production in remaining NP cells, or design of tissue engineered replacement strategies (combinations of cells and biomaterials) which maximize cells' proteoglycan production.

The notochordally-derived cells of the immature NP are thought to be key players in the generation and maintenance of this gelatinous, proteoglycan-rich NP tissue, and their loss with age in the human IVD coincides with decreased proteoglycan and water content [19,25]. *In vitro* studies indicate that these immature NP cells produce proteoglycans at high rates and also may stimulate other disc cells through release of soluble mediators [5,21,31,53,54]. However, factors which influence immature NP cell phenotype, including extracellular matrix production, are not well understood, with

almost all *in vitro* studies of immature NP cells performed by encapsulating cells in inert hydrogels (e.g. alginate) [5,21,31,53,54]. These culture systems maintain cells in a rounded state, but remove cells from physical interactions with their native extracellular matrix and neighboring cells.

The extracellular matrix environment may play a key role in controlling the phenotype of NP cells, including through cell receptor-ligand signaling (e.g. integrins), and modulating cell shape or cell-cell interactions, each of which has been shown to affect cell phenotype in cartilaginous tissues [2,16,44,116]. In this thesis, studies presented in Chapter 2 revealed that NP cells express laminin receptors (e.g. integrin α6) and preferentially interact with laminin ligands, as compared to other ECM ligands (e.g. collagens, fibronectin). Additionally, studies in Chapter 3 demonstrated that NP cell-cell interactions, which are prevalent in immature NP tissues, were promoted by soft, laminin-rich substrates *in vitro*, with cells assembling into large cell clusters following attachment to soft 2D gel substrates and exhibiting morphologies and cell-cell organization similar to those observed *in situ*. However, whether these morphological and organizational characteristics translate into functional phenotypic differences over time in culture is not yet known.

In this study, the role of extracellular matrix environment was examined on one key measure of immature NP cell function, proteoglycan synthesis. It was hypothesized that culturing immature NP cells on soft, laminin-rich 2D BME gel substrates would

promote proteoglycan production over the course of 12 days in culture (**Hypothesis 4.A**), as compared to cells cultured on rigid substrates functionalized with either the same ligand or type II collagen. Additionally, it was hypothesized that culture of NP cells on soft BME gels would promote cell growth over time in culture (**Hypothesis 4.B**), determined by measuring DNA content. Finally, it was hypothesized that culture on soft, BME gel substrates would maintain highly-vacuolated NP cell morphologies over 12 days in culture (**Hypothesis 4.C**), in contrast to culture on rigid substrates.

4.2 Methods

4.2.1 NP Cell Isolation and Culture

Lumbar spines were obtained from pigs (4-6 months old) within 24 hours of sacrifice. NP cells were isolated from IVD tissues (n=3 separate cell isolations) enzymatically in an overnight digestion. NP tissues were incubated overnight at 37°C in wash media (DMEM High Glucose (Invitrogen) containing 5% FBS (heat-inactivated, Hyclone), 1.65 mL of gentamycin (Gibco), 5 mL of kanamycin (Sigma), and 2 mL of amphotericyn B (Invitrogen) with 0.08% collagenase type 2 (Worthington Biochemicals) and 0.04% pronase (Roche Applied Science). The digested cell suspension was centrifuged (400g, 10 minutes) to pellet cells, and the remaining cells were washed twice with wash media. Cells were then suspended in 3 mL of cell dissociation buffer (5 minutes; Cell Stripper, Mediatech) and passed through a 70 μm cell strainer to break up

and remove any remaining cell clusters. Cells were pelleted (400g, 5 min.) and resuspended in culture media (Ham's F12 media (Gibco) with 5% FBS (Hyclone), 10 mM HEPES buffer (Gibco), 100 U/mL penicillin (Gibco) and 100 mg/mL streptomycin (Gibco). Cells were counted on a hemocytometer and seeded onto culture substrates at a density of 88,000 cells/cm^2.

Cells were cultured for 3, 6, 9, and 12 days under hypoxic conditions (5% O_2, 5% CO_2, 37°C), with media replaced (with fresh media pre-equilabrated at 5% O_2) every 3 days. Three wells per substrate condition were sacrificed for DNA measurements at each time point for n=3 independent experiments. NP cell morphology and organization were monitored over time in culture using phase contrast light microscopy. Live samples were imaged at various time points using an inverted light microscope (Zeiss S100, 10X objective) equipped with a Nikon Ds-QiMc digital camera, with images captured and processed using Nikon NIS-Elements BR software.

4.2.2 Substrates for NP Cell Culture

Thin two-dimensional substrates were formed by dispensing 90 μL of ice-cold, unpolymerized basement membrane extract (BME) solution (Trevigen, Inc.; growth factor-reduced, 14.2 mg/mL) into 12mm diameter wells (custom PDMS wells as shown in Figure 17) and allowed to gel for 30 minutes at 37°C in a humidified incubator. Resulting 2D gels were approximately 500 μm thick. As described in Section 3.3.2, BME is a self-polymerizing solubilized extract of tumor basement membrane containing high

concentrations of LM-111, as well as type IV collagen, entactin, and heparin sulfate [109]. For comparison with culture on soft BME gels, rigid substrates were created by adsorbing solutions of either unpolymerized BME ligand (200μg/mL, diluted in 50mM HEPES, pH 8.0, with 5mM EDTA to inhibit divalent cation-dependent self-polymerization) or type II collagen (50 μg/mL in PBS; Sigma) to wells of 24-well tissue culture plastic plates (BD Biosciences) overnight at 4°C. Wells were washed twice with cold HEPES (BME-coated wells) or PBS (collagen-coated wells) prior to cell seeding. Cell seeding densities were the same for all substrates.

4.2.3 NP Cell DNA Analysis

DNA content was measured for each sample well using the PicoGreen assay (Quant-iT PicoGreen dsDNA Kit, Invitrogen). DNA quantities for each substrate condition were measured following 3, 6, 9, and 12 days of culture. Cells and substrate proteins (including BME gel) remaining in sample wells after removal of media were digested in papain solution (300 μg/mL in PBS with 5mM EDTA and 5mM cysteine) at 65°C for 3 hours, vortexed, and stored at -20°C. Samples from control wells which contained no cells (but included substrates) were collected and processed similarly. Papain digests of NP cell/substrate samples were pipetted into black 96-well plates (20 μL sample digest per well, 2 replicate wells per sample; Corning Costar black opaque 96-well plates). DNA standards were created by diluting stock λ DNA (2 μg/mL,

Invitrogen) in papain solution, with diluted concentrations ranging from 50 to 1500 ng/mL. Stock 1X PicoGreen dye was diluted 1:200 in assay buffer (10 mM Tris-HCl, 1 mM EDTA, pH 7.5), and 100 μL of dye solution pipetted into each well. Wells were thoroughly mixed (multichannel pipette, followed by 30 sec on plate shaker), incubated for 5 minutes (covered from light), and fluorescent signal read on a plate reader (Excitation: 485 nm, Emission: 535 nm; Tecan Genios). Standards were fit to a linear curve, with resulting R^2 values always greater than 0.99. Signal from appropriate control wells was subtracted from sample values, and DNA concentrations from each sample were multiplied by sample volumes to yield total DNA per sample. Differences in DNA content amongst substrate conditions and over time in culture was analyzed via two-way ANOVA, with Tukey's HSD post hoc analysis.

4.2.4 Analysis of Sulfated Glycosaminoglycans

NP cell production of sulfated glycosaminoglycans (sGAGs) was analyzed using the dimethyl blue (DMMB) spectrophotometric method [57]. The assay utilizes the metachromatic shift in absorption maximum which occurs when a solution of 1,9-dimethylmethylene blue dye is complexed with sulfated glycosaminoglycans. Total sGAG produced by NP cells was assessed following 3, 6, 9, and 12 days of culture by measuring quantities of sGAG released into culture media and remaining on culture substrates (in papain digest, see Section 4.2.3). Total sGAG produced (media + substrate

digest) was then normalized to DNA content from each sample (measured in Section 4.2.3). Media from culture samples (3 wells per substrate condition for each of n=3 experiments) was collected following 3 day culture intervals and stored at -20°C until the assay. Samples from control wells which contained no cells (but included substrates) were collected and processed similarly. A 40 μL aliquot of sample (media or substrate digest) was combined with 125 μL of DMB dye (21 μg/mL stock solution) in a 96-well plate, mixed thoroughly, and absorbance (535 nm) measured on a plate reader (Tecan Genios, Mannendorf, Switzerland). Two replicate wells were measured for each sample. An sGAG standard was created (on each plate measured) by diluting a chondroitin-4 sulfate stock solution (10 mg/mL, diluted in culture media or papain solution; Sigma) to final concentrations ranging from 2.5 to 60 μg/mL (3 replicate wells/concentration). Standard known concentrations were plotted versus absorbance and fit linearly to create a standard curve, with resulting R^2 values always greater than 0.97. Sample concentrations (in media and digest) were calculated using the standard curve (corrected using readings from appropriate control samples), and sGAG concentration in each sample was multiplied by the sample volume to yield total sGAG. Differences in sGAG production amongst culture substrates over time in culture were detected via two-way ANOVA (substrate, time) and Tukey's HSD post hoc analysis.

4.3 Results

4.3.1. DNA Content

Analysis of NP cell numbers (as assessed by DNA content) over 12 days of culture revealed similar patterns of cell growth on both gel and rigid substrates, as shown in Figure 29. Analysis of variance detected significant effects of culture time ($p<0.001$) and culture substrate ($p=0.026$), with no significant interaction between these factors ($p=0.47$). Across all substrates cell numbers were found to increase from days 3 to 6, reach a plateau between days 6 and 9, and decrease between days 9 and 12. DNA levels on BME gels were found to be higher than those on type II collagen-coated rigid plastic substrates, but not higher than cells on plastic coated with unpolymerized BME (Figure 29). There was no difference between Day 0 and Day 12 DNA levels for any of the substrates examined.

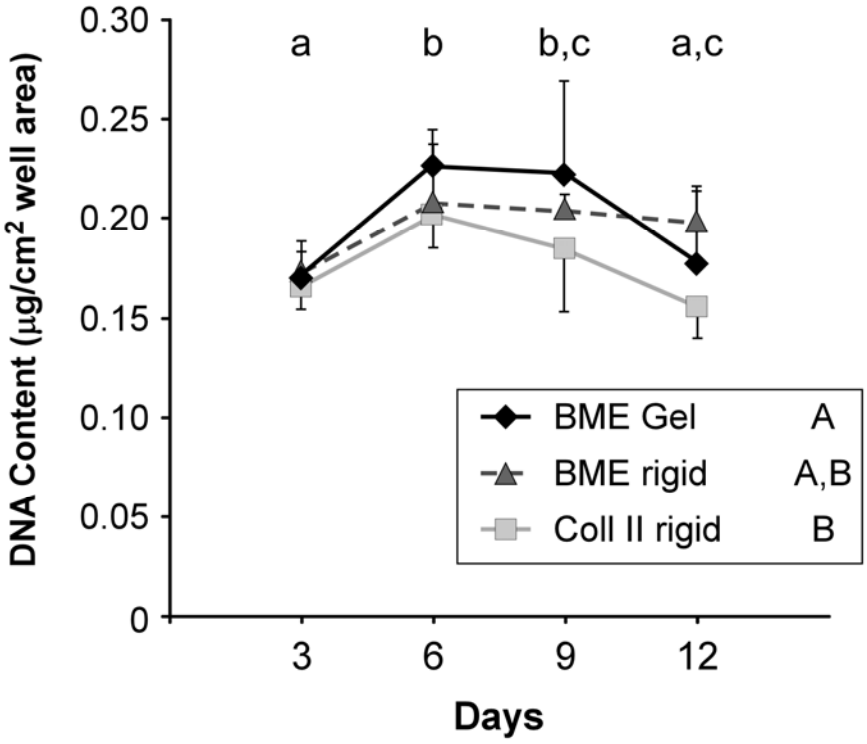

Figure 29: DNA content over time in culture. DNA levels for NP cells cultured on soft BME gels or rigid BME- or collagen II-coated tissue culture plastic were assessed via PicoGreen assay (n=3). DNA levels were normalized to well areas to account for different well sizes between gel and rigid substrates (cells were seeded at same densities). Significant effects of culture substrate ($p=0.026$) and day ($p<0.001$) were detected via ANOVA. Substrates and time points not labeled with the same letter (capital letters: substrate, lowercase: time point) were significantly different (Tukey's HSD, $p<0.05$) from each other.

4.3.2 sGAG Production

NP cells cultured on soft BME gel substrates were found to produce proteoglycan (sGAG/DNA) at significantly higher levels than NP cells cultured on rigid substrates ($p<0.0001$), as shown in Figure 30. This difference was apparent for each 3-

day culture period (Figure 30), and over 12 days of culture cells on BME gels produced sGAG at levels at least 1.7 times greater than cells cultured on rigid BME- or collagen-coated plastic (cumulative sGAG, Figure 31). No difference was detected between plastic substrates coated with different ECM ligands (unpolymerized BME, type II collagen), with cumulative totals on these two substrates appearing almost identical (Figure 31). Analysis of variance also detected a significant effect of culture period ($p < 0.0001$), with the highest quantities of sGAG produced in days 0-3, then progressively decreasing and leveling off (Figure 30; days 0-3 > days 3-6 > days 6-9, days 9-12).

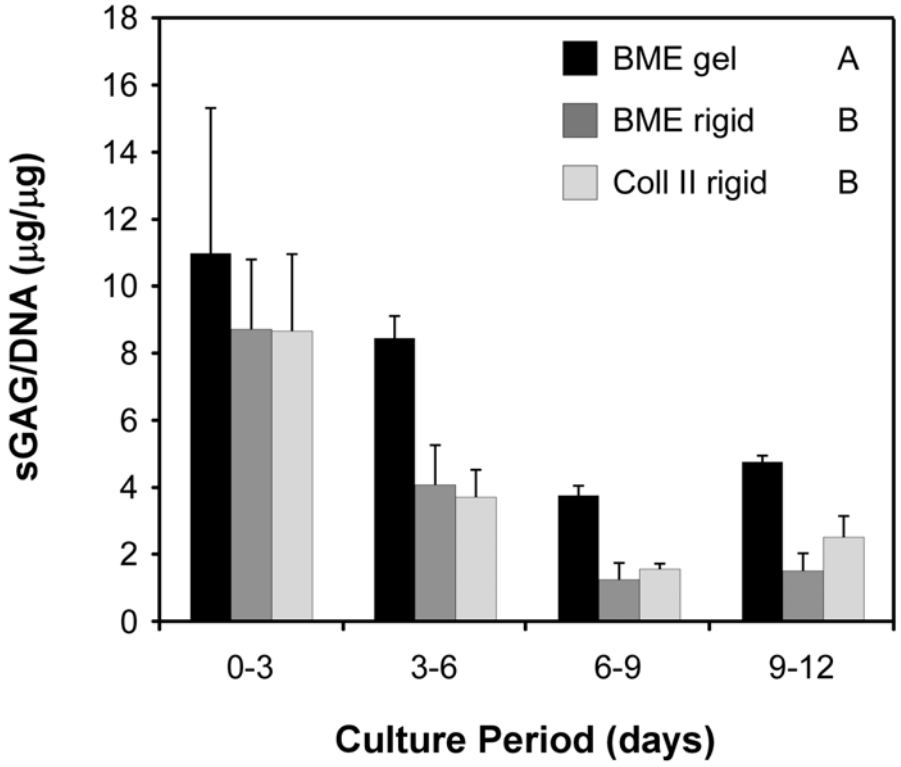

Figure 30: NP cell sGAG production (normalized to DNA content) over time in culture. Total sGAG (media plus substrate digest) analyzed for NP cells cultured on soft BME gels or ligand-coated tissue culture plastic (BME or type II collagen). NP cells cultured on BME gels produced significantly higher levels of sGAG as compared to rigid substrates (mean±SD, n=3, substrates with different letters were significantly different, $p<0.0001$). A significant effect of culture period was also detected, with Days 0-3 > Days 3-6 > Days 6-9 and 9-12 ($p<0.0001$).

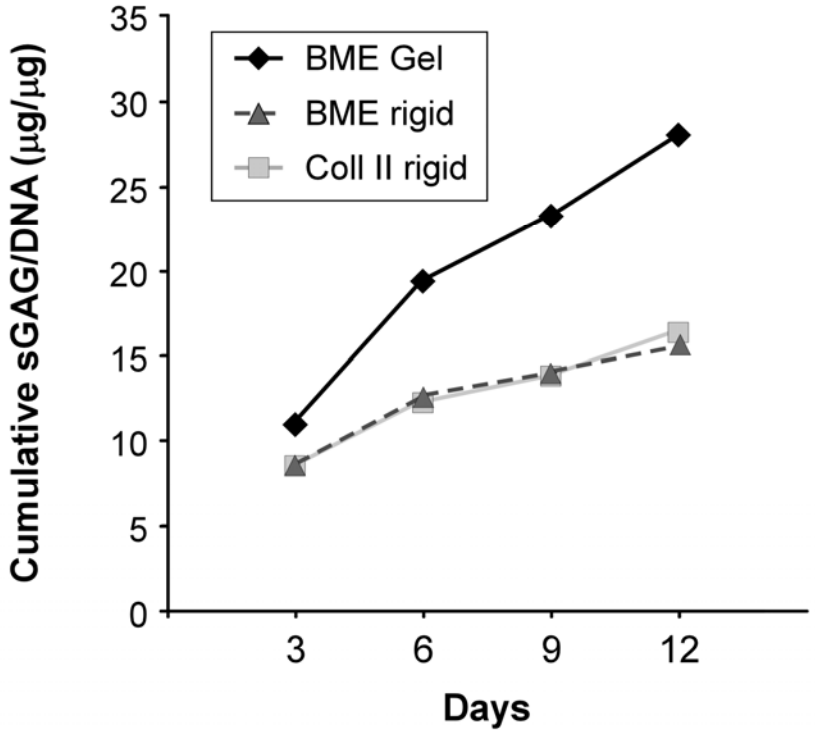

Figure 31: Cumulative sGAG production by NP cells over time in culture. NP cells cultured on soft BME gels produced 1.7 times greater than culture on rigid substrates over 12 days in culture. Error bars not shown for clarity.

4.3.3 NP Cell Morphology

NP cell morphology on BME gel substrates was similar to that found previously (see Chapter 3), with large, multi-cell clusters forming following 3 days of culture (Figure 32) and cells appearing to contain many large intracellular vacuoles. However, cell clusters appeared to compact with increasing time in culture, and following 12 days cell clusters resembled spheroids with vacuoles becoming less apparent. In contrast to gel substrates, on rigid substrates (e.g. unpolymerized BME-coated plastic, Figure 33)

cells formed a dense monolayer and initially (day 3) exhibited a highly-vacuolated morphology. Cells appeared to become elongated and form a dense monolayer over time (day 6), with very few vacuoles identifiable following 12 days of culture (Figure 33, bottom panel).

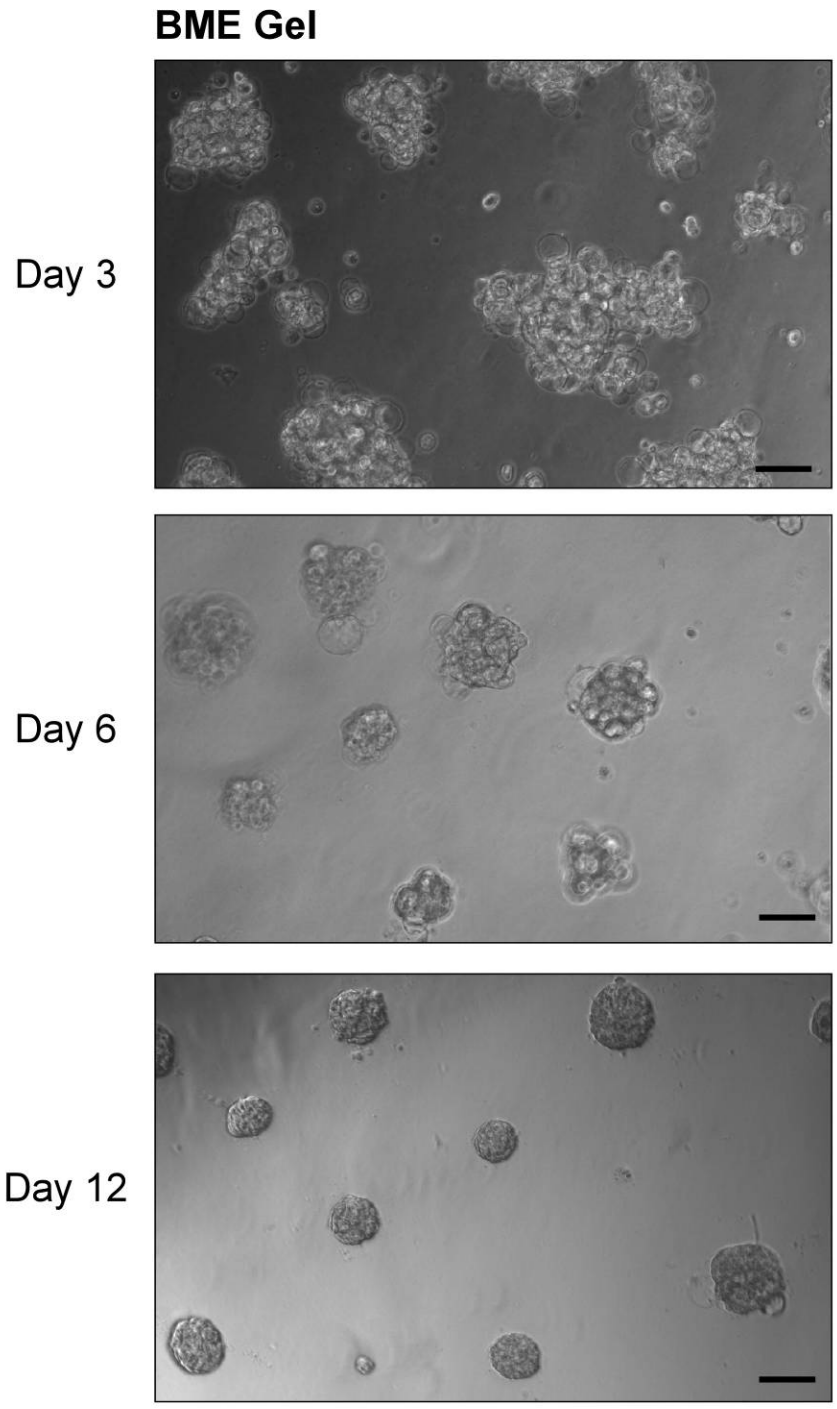

Figure 32: NP cell morphology changes on BME gels over time in culture. NP cells formed large multi-cell clusters following 3 days of culture (top). At 12 days (bottom), NP cells had compacted into spheroids.

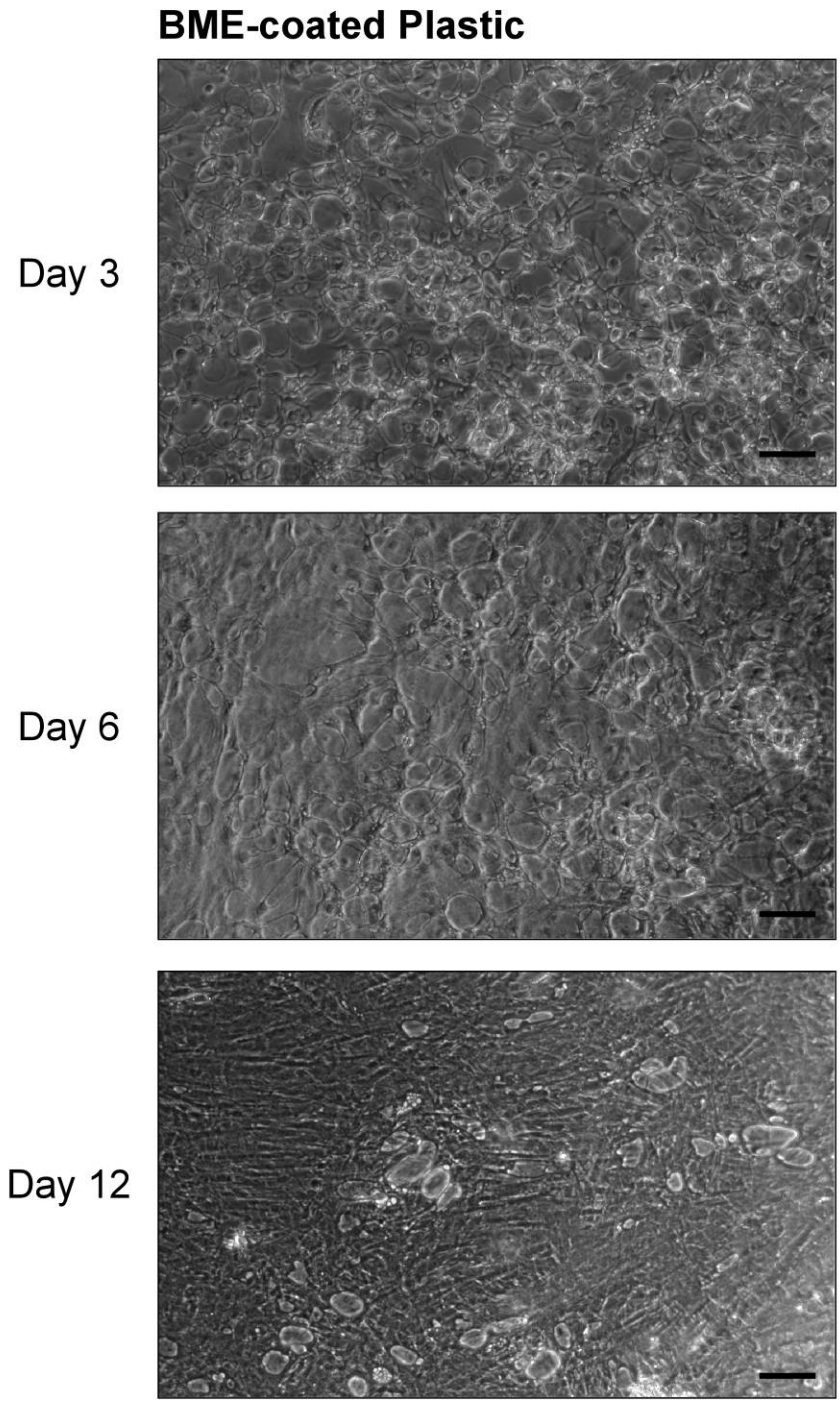

Figure 33: NP cell morphology on rigid substrates (unpolymerized BME-coated plastic) over time in culture. Day 3 cells (top) contain many intracellular vacuoles which are mostly lost by Day 12 in culture (bottom).

4.4 Discussion

4.4.1 NP Cell Proteoglycan Production

In this chapter, the effect of culture substrate on a key measure of immature NP cell bioactivity, proteoglycan production, was examined. Culture of NP cells on soft, laminin-rich BME gel substrates resulted in sGAG production levels which were significantly higher than culture on rigid substrates functionalized with BME or collagen ligands, confirming Hypothesis 4.A. Total sGAG production over 12 days of culture was found to be 70-80% greater than on rigid monolayer substrates (Figure 31), with BME gels showing higher levels during each 3-day culture interval (Figure 30). Although sGAG output was consistently higher on BME gels, the initial output rate for all substrates (gel or rigid) was not maintained over 12 days, with production shifting to a lower (but possibly steady) rate for days 6-12 (Figure 31).

The findings of enhanced NP cell sGAG production on BME gel substrates may be due to one or a combination of several extracellular matrix environmental factors which modulate NP cell phenotypic responses. First, ECM ligand may be translated directly into sGAG-producing intracellular cell signaling events via ECM ligand-receptor interactions (e.g. integrins, focal adhesions). Second, both ECM ligand and substrate stiffness may (individually or in combination) modulate cellular behaviors such as cell shape and cell-cell interactions (as demonstrated for immature NP cells in Chapter 3), which in turn translate into phenotypic responses.

Each of the factors described above has been shown to play key roles in proteoglycan expression in cartilaginous tissues. Cell shape has been demonstrated to be a critical factor modulating chondrocyte differentiation and phenotype, with cells maintained in a rounded shape by 3D culture (pellet culture, encapsulation in hydrogels [2,16]), or by culturing on 2D substrates with low adhesivity or at high cell densities [66]. Maintaining chondrocytes in a rounded shape has been shown to prevent dedifferentiation *in vitro* and promote production of cartilage matrix, including increased proteoglycan expression [2]. In the present study of immature NP cells, it is noted that largest differences in sGAG production between gel and rigid substrates occurred after Day 3 (production on BME gel was 25% greater than rigid substrates for Days 0-3, but 100-200% greater for Days 3-12, as shown in Figure 30). Morphologically, this corresponded with the time period when NP cells on rigid substrates had begun to spread out (Figure 33). NP cells cultured on BME gels did not appear to spread at any time point, although morphology after cell cluster formation was not easily assessed.

Additionally, cell-cell interactions are known to play key roles in cartilage development, and may have had an important effect on the NP cell matrix production differences documented in this study. In developing cartilage, homotypic cell-cell interactions which occur during mesenchymal condensation and chondrogenesis (mediated by n-cadherin and other cell-cell adhesion molecules) lead to chondrocyte differentiation and upregulate matrix production [44,45]. Similarly, in a recent study an

in vitro model of mesenchymal condensation was created using nano-fibrous mats of varying apparent stiffnesses, with human mesenchymal stem cells on the softest mats assembling into aggregates and producing sGAG at higher rates (~100% higher) than non-aggregated cells cultured on stiffer mats [63]. In the present study, it is noted that the NP cell-cell interactions (i.e. cell clusters) do not occur immediately following cell seeding, with cells instead attaching as individual cells and assembling into clusters over the course of 3-4 days. Thus, peak fold-differences in sGAG production between BME gel and rigid substrates (which occur after Day 3, Figure 30) also appear to coincide with time periods where cell-cell interactions have been maximized.

ECM ligand may also play a key role in modulating NP cell sGAG production, although the findings presented here (combined with those of Chapter 3) suggest that ligand may act in concert with substrate stiffness to modulate NP cell behaviors. NP cells cultured on BME-coated rigid plastic showed levels of sGAG production which were lower than those on soft BME gels and not different from cells on collagen II-coated plastic. Although not an ideal comparison due to the possibility of non-specific cell-ligand interactions on plastic substrates (see limitations discussed below), this finding suggests ligand alone is not sufficient to upregulate sGAG production. Additionally, it is noted that NP cells on BME gels form 3D aggregates, with a significant portion of cells not in contact with the gel surface following cluster formation (see Figure 23 in Chapter 3). It is noted that for *in vitro* culture models of mammary

epithelial cells which utilize BME gel substrates, cells initially interact with BME ligands while self-assembling into 3D clusters, but then secrete and interact with their own cell-associated matrix (which includes LM-332) to form differentiated clusters [176]. ECM ligand may still be critical to increased sGAG production, however, since the NP cell morphology and clustering behaviors observed on BME gel substrates in Chapter 3 were found to be a function of both substrate stiffness and BME ligand (Section 3.3.4). Thus, interactions with BME ligand (in combination with low substrate stiffnesses) may modulate NP cell-cell interactions and cell shape, which in turn may yield phenotypic outcomes such as increased sGAG production.

There are several limitations of studies presented here which should be considered when comparing findings between substrates. First, as mentioned above, isolating the effects of specific cell-ligand interactions over time in *in vitro* culture is challenging, particularly on plastic substrates where accumulating cell-deposited matrix or serum ECM proteins (e.g. fibronectin) may replace initial ligands. Additionally, BME ligand density and presentation may also have been different between gel and rigid substrates. Further experiments using the polyacrylamide gel system described in Chapter 3 (which resists non-specific protein adsorption) will be useful in more precisely defining the roles of ligand (including pure LM-111 ligand) and substrate stiffness on immature NP cell behaviors. Second, a possible difference between BME gels and rigid substrates independent of ligand and stiffness is that BME gels may bind chemical

factors (e.g. growth factors with heparin sulfate binding domains) present in culture medium or released by cells, acting as a depot which locally concentrates growth factor exposure at the cell surface and results in enhanced cellular responses. Additionally, the BME protein used in this study is known to contain trace amounts of several growth factors (e.g. TGF-β, IGF-1) [173]; however, concentrations in the gel are low and even complete release of these factors into the culture media would result in levels (approximately 1 ng/mL or less) which are likely much lower than those in the serum-supplemented media used for this study. Finally, it is noted that NP cells were seeded at high densities in this study, which likely limited cell spreading (resulted in a more rounded cell shape) on rigid substrates. Assuming that a rounded cell shape promotes sGAG production, it is possible that even greater differences between soft and rigid substrates may be observed at lower cell seeding densities which allow cells to fully spread.

4.4.2 NP Cell Growth

The hypothesis that NP cell culture on soft BME gels would promote cell growth (Hypothesis 4.B) did not prove true, as cells cultured on BME did not show increase in DNA content over 12 days of culture (Figure 29). Instead, NP cells on soft BME gels exhibited a similar growth pattern to cells on rigid substrates, with cell numbers increasing initially (Days 0-6), but then plateauing (Days 6-9) and decreasing during the

final 3 days of culture. No differences were detected in overall DNA levels between soft BME gels and rigid BME-coated substrates (Figure 29), with collagen-coated substrates slightly lower levels than soft BME gels. NP cell growth characteristics on rigid substrates could be explained by contact inhibition (i.e. cell crowding on substrate), as cell may have expanded until forming a high density monolayer with little room to expand after several days of culture. However, on BME gels contact inhibition on the gel surface was not a factor, as cells formed 3D clusters and left large areas of the substrate cell-free. The NP cell growth patterns shown here may be similar to those of chondrocytes, which expand on rigid substrates but cease growth when maintained in a spherical conformation [2]; however, in this study cell growth on BME substrates was detected over the first 6 days of culture, even though NP cells do not appear to spread on these substrates. It is also noted that other environmental factors, including chemical mediators such as growth factors, may be critical (possibly in combination with specific ECM environment) for optimal expansion of immature NP cells *in vitro.* Future studies using chemically defined media to examine the effects of specific growth factors, in combination with BME or other substrate combinations (e.g. soft substrates functionalized with other laminin isoforms), may yield an optimal culture environment for expansion of immature NP cells.

4.4.3 NP Cell Morphology

Finally, observations of NP cell morphology revealed that NP cells cultured on BME gel substrates formed cell clusters with obvious vacuolated morphologies that were remained apparent over the first 6 days of culture (as found in Chapter 3). However, with culture out to 12 days NP cell clusters were found to compact into dense spheroids and vacuolated cell morphologies were no longer apparent (Figure 32). Attempts to quantify changes in cell size over time in culture were unsuccessful, as cells in clusters (or dense monolayer) could not be dissociated with cell dissociation buffer or trypsin. These observations suggest that the cell morphologies and cell-cell interactions promoted by soft BME substrates are not by themselves (in combination with 5% FBS-supplemented media used here) sufficient to maintain a vacuolated NP cell morphology (and possibly immature NP cell phenotype) over time in culture, and that other mediators (e.g. growth factors, as discussed above) may play a role in the *in vitro* changes observed here.

4.5 Conclusions

In this study, the effect of extracellular matrix environment was studied on two important measures of immature NP cell behavior, proteoglycan production and cell growth. NP cells were cultured on 2D substrates of soft, laminin-rich BME or rigid plastic functionalized with (unpolymerized) BME or type II collagen ligands, with sGAG

production and total cell numbers (DNA content) monitored over the course of 12 days. This study produced several key findings:

1. NP cells cultured on 2D BME gel substrates were found to produce significantly higher levels of sGAG (70-80% greater) as compared to cells cultured on rigid substrates, confirming Hypothesis 4.A that a soft (~230 Pa), laminin-rich substrate would promote NP cell proteoglycan expression. The observed differences between substrates were maintained over each 3-day interval examined, although sGAG production was found to decrease over time in culture for cells on all substrates.
2. NP cells cultured on soft BME gels exhibited growth patterns similar to cells cultured on rigid substrates. Overall cell levels increased initially (Days 0-6) for all substrates, but decreased back to starting levels after 12 days of culture. Cell growth on rigid substrates may have been limited by cell contact (confluence), but this was not likely a factor on soft BME substrates where 3D cell clusters formed. These results indicate that soft BME substrates do not promote sustained NP cell growth under the culture conditions examined (i.e. standard culture medium with 5% FBS), which disproved Hypothesis 4.B.
3. NP cell morphology on soft BME gel substrates was found to be similar to that reported in Chapter 3, with NP cells assembling into large, highly-vacuolated cell clusters over the course of several days, with large vacuolated cells still apparent

after 6 days of culture. However, further time in culture led to compaction of cell clusters into spheroids with loss of vacuolated morphologies. These observations suggest that culture on soft BME substrates (when combined with standard serum-supplemented culture media) is not sufficient to maintain the unique vacuolated morphology of immature NP cells over an extended culture period. Future work examining unique immature NP cell phenotypic markers (which may include cell adhesion molecules, laminin cell-associated matrix, or cytokeratins) is necessary to more completely describe the phenotypic changes which may occur in this culture system.

5. Conclusions and Future Directions

The extracellular matrix environment is known to be a key regulator of cellular behaviors, modulating cell adhesion, migration, organization, differentiation, and phenotype. Cells of the intervertebral disc's nucleus pulposus (NP) region reside in a gelatinous, highly-hydrated ECM environment and exhibit *in situ* cell-matrix and cell-cell interactions which are quite distinct from cells in other regions of the disc or in other cartilaginous tissues. These include the expression of numerous laminin cell-matrix receptors, cell-associated laminin extracellular matrix proteins (isoforms LM-511, LM-332, as described in Chapter 1), and cell-cell adhesions (desmosomes, gap junctions). However, this cell population disappears in the maturing NP and the loss of this cell population may initiate degenerative changes in the IVD, with the possibility that alterations in NP cell-matrix interactions and environment play key roles in these changes. Additionally, the appropriate ECM environmental conditions necessary to phenotypically maintain or expand this immature NP cell population for *in vitro* studies or tissue engineering applications are currently unknown. The primary motivating hypothesis of this thesis is that immature NP cells will exhibit unique interactions with laminin ligands, and that laminin ligands, in combination with appropriate substrate stiffnesses, will promote immature NP cell adhesion, cell-cell interactions, and phenotype *in vitro.* Three studies described in this thesis addressed this hypothesis:

1. Studies undertaken in Chapter 2 examined integrin expression of IVD cells (immature NP cells, AF cells) via flow cytometry to determine whether laminin-binding integrins were uniquely expressed by immature NP cells, and whether expression patterns of key integrin subunits were maintained over time in culture. Additionally, IVD cell adhesion to laminin and other ECM proteins was investigated, with identification of the specific integrins responsible for mediating these interactions determined using function-blocking antibodies. Finally, NP cell interactions with specific laminin isoforms were investigated (and compared with other non-laminin ECM ligands), with cell attachment, cell spreading dynamics, and relative adhesion strength quantified on different substrates.

2. Studies in Chapter 3 examined the roles of ECM ligand and substrate elasticity in modulating NP cell-cell interactions. Immature NP cells were seeded on two-dimensional gel substrates with varying stiffnesses and ligands, and cell-cell interactions (cell clustering behaviors) were quantified. Additionally, the mechanical properties of IVD cells were measured via AFM indentation for comparison with the properties of culture substrates which promoted cell-cell interactions.

3. Finally, in Chapter 4 the effects of ECM substrate ligand and stiffness on one important measure of NP cell behavior, proteoglycan production, were examined. Isolated NP cells were cultured on soft (2D gel) and rigid laminin substrates, with sGAG production, cell numbers (DNA content), and cell morphologies assessed over 12 days in culture.

Studies performed in Chapter 2 produced several key findings relating to IVD cell integrin expression and cell adhesion. Immature NP cells isolated from IVD tissues were found to express high levels of the laminin-binding α6 integrin subunit as compared to AF cells, and these expression patterns were maintained over 7 days of monolayer culture. NP cells were found to readily adhere to the laminin isoform LM-111 (mediated by the α6 and β1 subunits, as identified in function-blocking studies), whereas AF cells did not attach to this laminin isoform. This finding can most likely be attributed to the lack of the α6β1 on AF cells, since this receptor is the primary integrin receptor known to bind the LM-111 isoform. These findings suggest that LM-111 ligands could be used to select NP cells from a mixed IVD cell population, a potentially useful tool for autologous IVD cell therapies. Additionally, studies of NP cell adhesion to various laminin isoforms showed that LM-511 and LM-332 are preferred ligands for immature NP cells, with NP cells attaching in high numbers, spreading rapidly, and resisting applied detachment forces on these ligands as compared to LM-111,

fibronectin, or collagen II substrates. The finding of rapid cell attachment and spreading on LM-511 and LM-332 is particularly noteworthy, as immature NP cells were not previously known to be highly adhesive to any culture substrate. These findings correspond with our knowledge of *in situ* cell-associated matrix in the immature NP (where LM-511 and LM-332 have been identified, but not LM-111), and with identified NP cell-matrix receptor expression (α6, β4, and β1 integrins, CD239). Together, studies in Chapter 2 confirmed our hypothesis that immature NP cell-matrix interactions and receptor expression observed in immature NP tissues would translate into *ex situ* cellular behaviors.

Studies undertaken in Chapter 3 produced new information on the role of the extracellular matrix environment in modulating NP cell-cell interactions. NP cells isolated from immature tissues and seeded onto soft, laminin-rich 2D gel substrates were found to self-assemble into large cell clusters, with cells appearing to maximize cell-cell interactions and exhibiting morphologies similar to those identified in tissues. Studies utilizing a mechanically-tunable polyacrylamide gel culture system determined this behavior to be a function of both substrate ligand and stiffness, with clustering behaviors not observed on stiffer substrates (>700 Pa) or collagen II-functionalized substrates of any stiffness. It was noted that the shift between cell-cell interactions (i.e. cell clustering) and cell-substrate interactions (cells spread in monolayer) was found to occur over a fairly narrow range of substrate stiffnesses, with an increase in substrate

stiffness of just 500 Pa (from 210 Pa to 720 Pa) leading to a dramatic decrease in clustering behavior (from > 90% clustered to < 10%). This finding suggests that NP cell organization may be very sensitive to alterations in ECM stiffness, and that an increase in NP stiffness (as documented with increasing age and degeneration [91]) could play a role in disrupting NP cell-cell interactions, with potential downstream effects on NP cell phenotype and survival. Additionally, the elastic moduli of NP cells was found to fall within this transition range, with clustering behaviors observed on BME-functionalized substrates which were softer, but not stiffer, than NP cells. Further investigation (as discussed below) is needed to identify how specific cell and ECM factors (e.g. ECM ligand, ECM stiffness, cell stiffness, cell contractility) may interact to determine cell-cell interactions. Together, studies presented in Chapter 3 supported the hypothesis that substrate elasticity and laminin ligands (BME ligands rich in LM-111) are important factors modulating NP cell-cell interactions.

Finally, studies presented in Chapter 4 examined the role of ECM environment on a key measure of NP cell function, proteoglycan production. NP cells cultured on soft, laminin-rich BME gel substrates produced proteoglycans at significantly higher levels (70-80% greater over 12 days of culture) than cells cultured on rigid substrates functionalized with either BME or collagen ligands. These findings may be a result of ECM-modulated cell shape, increased cell-cell interactions, direct signaling following cell binding to BME ligands, or some combination of these factors. Further work (as

discussed below) is necessary to identify which of these factors is critical to the observed increase in sGAG production, including whether pure laminin ligands are sufficient to promote this behavior. Examination of cell morphology over 12 days of culture revealed that although NP cells formed cell clusters and maintained a vacuolated morphologies initially (0-6 days), cells eventually compacted into dense spheroids and appeared to lose their distinct morphological appearance. These findings suggest that the ECM culture environment studied here is not by itself sufficient to maintain an morphologically distinct NP cell phenotype, and that use of a defined culture media with appropriate soluble factors (e.g. growth factors), in combination with this or other substrate conditions (e.g. other laminin isoforms), may be necessary to maintain an immature NP cell phenotype *in vitro*. In summary, the studies in Chapter 4 indicate that a soft, laminin-rich ECM environment promotes proteoglycan expression in immature NP cells.

The findings presented here also suggest a number of areas for future study:

1. Studies in Chapters 3 and 4 examined immature NP cell behaviors on substrates functionalized with basement membrane extract (BME), which contains a high concentration of LM-111 (~60%) but also includes other constituents with which cell may interact (e.g. collagen IV, heparin sulfate proteoglycans, growth factors). Whether similar behaviors (cell clustering, increased proteoglycan production)

will be observed on substrates functionalized with pure LM-111 ligand is not known. However, studies in other cell types have indicated that LM-111 is the key ECM factor driving cell-cell interactions in basement membrane culture models [73]. This knowledge may be used to develop biomaterials with defined compositions, such as soft gels functionalized with recombinant LM-111 or laminin-mimicking cell adhesive peptides.

2. Studies in Chapter 2 demonstrated that immature NP cells adhere to LM-111 ligands at much higher levels than AF cells. This finding may be relevant in the development of cell selection strategies for autologous IVD cell therapies. The mature human NP is thought to contain a mixed cell population which may include cells from the adjacent AF and cartilage endplates, as well as immature NP cells which are no longer morphologically identifiable. Selection of cells isolated from surgical tissues which adhere to LM-111 substrates may yield a more "NP-like" population of cells which could then be used for cell or tissue replacement therapies.

3. Studies presented in Chapter 3 and 4 focused on NP cell interactions with BME-functionalized substrates, which contain the LM-111 laminin isoform. However, studies in Chapter 2 indicated that two other laminin isoforms, LM-511 and LM-

332, are preferred ligands for NP cell attachment and spreading. NP cell behaviors, including phenotypic maintenance, on soft substrates functionalized with these laminin isoforms remain to be investigated. However, there are several challenges which must be overcome to facilitate studies with these ligands. First, availability of both ligands is very limited, as they are difficult to extract from tissues (where they are present in low concentrations and are highly crosslinked) or to purify from cell supernatant, and are not easily produced recombinantly. Second, coupling of these ligands (and all laminins) to gel substrates proved difficult, possibly due to the sensitivity of laminins to chemical modification, as well as difficulty in coupling ligands at sufficient densities and in the proper orientation. One possible approach would be to recombinantly express these isoforms (or a portion containing the LG cell-binding domain) with a biotin incorporated on the N-terminus of the laminin α-chain, allowing for high affinity binding to streptavidin-functionalized gel surfaces with the proper molecular orientation to facilitate cell adhesion. Developing new strategies to obtain and couple these ligands will be key to understanding their roles in modulating NP cell behaviors.

4. It was observed in Chapter 4 that NP cells cultured on BME gel substrates formed large cell clusters, but appeared to contract and lose their vacuolated

morphology over 12 days of culture. In addition to ECM environment, another key factor affecting NP cell phenotype are soluble mediators including growth factors. The studies presented here utilized culture media containing 5% FBS, which includes growth factors and other components (e.g. fibronectin) which may contribute to NP cell dedifferentiation. For example, serum may contain significant levels of TGF-β, a key factor contributing to epithelial cell dedifferentiation (i.e. epithelial-to-mesenchymal transition) [187]. Future work utilizing defined culture media may be critical in identifying the appropriate culture conditions to maintain or promote an NP cell phenotype *in vitro*.

5. Studies in Chapter 3 and 4 showed that NP cells self-assembled into large clusters with strong cell-cell interactions, and that this behavior promoted one key measure of NP cell behavior, proteoglycan production. Future work is necessary to determine the effects of this ECM environment (possibly in combination with appropriate defined culture media) on other measures of immature NP cell phenotype. Phenotypic markers for immature NP cells are not well-defined, but may include cytokeratin expression, laminin receptor expression (e.g. α6 integrin), or cell size. Additionally, in epithelial cell types, laminin ligands and resulting cell-cell interactions promote cell survival under environmental stress conditions (i.e. hypoxia, inflammation) [178]. This behavior

may be particularly relevant for NP cells, which must survive in the harsh environment of the NP. These studies will lend further insight into the effects of ECM environment on immature NP phenotype, as well as the function of immature NP cell-cell interactions observed *in situ*.

6. Finally, studies in Chapter 3 examined the roles of substrate stiffness and ligand on NP cell-cell interactions, with a sharp transition from cell-cell to cell-substrate interactions observed with increasing substrate stiffness on BME-functionalized (but not collagen-functionalized) substrates. Additionally, the stiffness of NP cells themselves appeared to fall within this substrate stiffness transition range, which could indicate that cells probe or sense the mechanical environment of adjacent cells as well as substrates. The mechanisms behind this observed transition behavior are not well understood, and may involve factors including ligand signaling, ligand adhesivity, cell stiffness, and cell contractility. Questions to be explored include: do other cells transition from cell-cell to cell-substrate interactions over the same range of substrate stiffnesses? How do laminin ligands (LM-111) modulate these behaviors? Understanding of these behaviors may lend insight into tissue development and patterning, and be applied to tissue engineering by designing biomaterials with spatially varying ligands and stiffnesses which locally direct cell organization and differentiation.

In summary, this dissertation demonstrated a role for the extracellular matrix environment in modulating the behaviors of immature NP cells of the intervertebral disc. Studies examined NP cells' unique interactions with laminin ligands and their sensitivity to ECM elasticity, demonstrating that these interactions play key roles in cell adhesion, cell-cell interactions, and matrix production. These findings indicate that the extracellular matrix environment of the NP may be a critical factor modulating the organization and phenotype of immature NP cells, and suggests that alterations in this ECM environment which occur in the IVD with aging and degeneration may play a key role in the loss of this unique cell population. Additionally, the information presented here may be useful in the design of NP tissue regeneration strategies, including the development biomaterials which present appropriate ECM ligands and elasticities to promote an NP cell phenotype and matrix regeneration.

References

[1] *The Burden of Musculoskeletal Diseases in the United States*: American Academy of Orthopaedic Surgeons. 2004.

[2] Abbott, J. and Holtzer, H., The loss of phenotypic traits by differentiated cells. 3. The reversible behavior of chondrocytes in primary cultures. *J Cell Biol* **28**: 473-487, 1966.

[3] Adams, J.C. and Watt, F.M., Regulation of development and differentiation by the extracellular matrix. *Development* **117**: 1183-1198, 1993.

[4] Adams, M.A., Freeman, B.J., Morrison, H.P., Nelson, I.W., and Dolan, P., Mechanical initiation of intervertebral disc degeneration. *Spine (Phila Pa 1976)* **25**: 1625-1636, 2000.

[5] Aguiar, D.J., Johnson, S.L., and Oegema, T.R., Notochordal cells interact with nucleus pulposus cells: regulation of proteoglycan synthesis. *Exp Cell Res* **246**: 129-137, 1999.

[6] Anderson, D.G., Li, X., and Balian, G., A fibronectin fragment alters the metabolism by rabbit intervertebral disc cells in vitro. *Spine* **30**: 1242-1246, 2005.

[7] Annunen, S., Paassilta, P., Lohiniva, J., Perala, M., Pihlajamaa, T., Karppinen, J., Tervonen, O., Kroger, H., Lahde, S., Vanharanta, H., Ryhanen, L., Goring, H.H., Ott, J., Prockop, D.J., and Ala-Kokko, L., An allele of COL9A2 associated with intervertebral disc disease. *Science* **285**: 409-412, 1999.

[8] Antoniou, J., Steffen, T., Nelson, F., Winterbottom, N., Hollander, A.P., Poole, R.A., Aebi, M., and Alini, M., The human lumbar intervertebral disc: evidence for changes in the biosynthesis and denaturation of the extracellular matrix with growth, maturation, ageing, and degeneration. *J Clin Invest* **98**: 996-1003, 1996.

[9] Aota, Y., An, H.S., Homandberg, G., Thonar, E.J., Andersson, G.B., Pichika, R., and Masuda, K., Differential effects of fibronectin fragment on proteoglycan metabolism by intervertebral disc cells: a comparison with articular chondrocytes. *Spine* **30**: 722-728, 2005.

[10] Aumailley, M., Bruckner-Tuderman, L., Carter, W.G., Deutzmann, R., Edgar, D., Ekblom, P., Engel, J., Engvall, E., Hohenester, E., Jones, J.C., Kleinman, H.K.,

Marinkovich, M.P., Martin, G.R., Mayer, U., Meneguzzi, G., Miner, J.H., Miyazaki, K., Patarroyo, M., Paulsson, M., Quaranta, V., Sanes, J.R., Sasaki, T., Sekiguchi, K., Sorokin, L.M., Talts, J.F., Tryggvason, K., Uitto, J., Virtanen, I., von der Mark, K., Wewer, U.M., Yamada, Y., and Yurchenco, P.D., A simplified laminin nomenclature. *Matrix Biol* **24**: 326-332, 2005.

[11] Baer, A.E., Laursen, T.A., Guilak, F., and Setton, L.A., The micromechanical environment of intervertebral disc cells determined by a finite deformation, anisotropic, and biphasic finite element model. *J Biomech Eng* **125**: 1-11, 2003.

[12] Baselga, J., Hernandez-Fuentes, I., Pierola, I.F., and Llorente, M.A., Elastic properties of highly crosslinked polyacrylamide gels. *Macromolecules* **20**: 3060-3065, 1987.

[13] Battie, M.C. and Videman, T., Lumbar disc degeneration: epidemiology and genetics. *J Bone Joint Surg Am* **88 Suppl 2**: 3-9, 2006.

[14] Bayliss, M.T., Johnstone, B., and O'Brien, J.P., 1988 Volvo award in basic science. Proteoglycan synthesis in the human intervertebral disc. Variation with age, region and pathology. *Spine* **13**: 972-981, 1988.

[15] Beningo, K.A., Lo, C.M., and Wang, Y.L., Flexible polyacrylamide substrata for the analysis of mechanical interactions at cell-substratum adhesions. *Methods Cell Biol* **69**: 325-339, 2002.

[16] Benya, P.D. and Shaffer, J.D., Dedifferentiated chondrocytes reexpress the differentiated collagen phenotype when cultured in agarose gels. *Cell* **30**: 215-224, 1982.

[17] Biyani, A. and Andersson, G.B., Low back pain: pathophysiology and management. *J Am Acad Orthop Surg* **12**: 106-115, 2004.

[18] Bogduk, N., *Clinical anatomy of the lumbar spine and sacrum /Nikolai Bogduk*: Elsevier/Churchill Livingstone. 2005.

[19] Boos, N., Weissbach, S., Rohrbach, H., Weiler, C., Spratt, K.F., and Nerlich, A.G., Classification of age-related changes in lumbar intervertebral discs: 2002 Volvo Award in basic science. *Spine* **27**: 2631-2644, 2002.

[20] Borradori, L. and Sonnenberg, A., Structure and function of hemidesmosomes: more than simple adhesion complexes. *J Invest Dermatol* **112**: 411-418, 1999.

[21] Boyd, L.M., Chen, J., Kraus, V.B., and Setton, L.A., Conditioned medium differentially regulates matrix protein gene expression in cells of the intervertebral disc. *Spine* **29**: 2217-2222, 2004.

[22] Boyd, L.M., Richardson, W.J., Allen, K.D., Flahiff, C., Jing, L., Li, Y., Chen, J., and Setton, L.A., Early-onset degeneration of the intervertebral disc and vertebral end plate in mice deficient in type IX collagen. *Arthritis Rheum* **58**: 164-171, 2008.

[23] Brault, M., Hootman, J., Helmick, C., Theis, K., and Armour, B., Prevalence and Most Common Causes of Disability Among Adults --- United States, 2005. *Morbidity and Mortality Weekly Report* **58**: 421-426, 2009.

[24] Bruehlmann, S.B., Rattner, J.B., Matyas, J.R., and Duncan, N.A., Regional variations in the cellular matrix of the annulus fibrosus of the intervertebral disc. *J Anat* **201**: 159-171, 2002.

[25] Buckwalter, J.A., Aging and degeneration of the human intervertebral disc. *Spine* **20**: 1307-1314, 1995.

[26] Butler, W.F., *Comparative Anatomy and Development of the Mammalian Disc*, in *The biology of the intervertebral disc*, P. Gosh, Editor. 1988, CRC Press: Boca Raton. p. 39-82.

[27] Califano, J. and Reinhart-King, C., A Balance of Substrate Mechanics and Matrix Chemistry Regulates Endothelial Cell Network Assembly. *Cellular and Molecular Bioengineering* **1**: 122-132, 2008.

[28] Camper, L., Hellman, U., and Lundgren-Akerlund, E., Isolation, cloning, and sequence analysis of the integrin subunit alpha10, a beta1-associated collagen binding integrin expressed on chondrocytes. *J Biol Chem* **273**: 20383-20389, 1998.

[29] Camper, L., Holmvall, K., Wangnerud, C., Aszodi, A., and Lundgren-Akerlund, E., Distribution of the collagen-binding integrin alpha10beta1 during mouse development. *Cell Tissue Res* **306**: 107-116, 2001.

[30] Cao, L., Guilak, F., and Setton, L.A., Three-dimensional morphology of the pericellular matrix of intervertebral disc cells in the rat. *J Anat* **211**: 444-452, 2007.

[31] Cappello, R., Bird, J.L., Pfeiffer, D., Bayliss, M.T., and Dudhia, J., Notochordal cell produce and assemble extracellular matrix in a distinct manner, which may be responsible for the maintenance of healthy nucleus pulposus. *Spine* **31**: 873-882; discussion 883, 2006.

[32] Chelberg, M.K., Banks, G.M., Geiger, D.F., and Oegema, T.R., Jr., Identification of heterogeneous cell populations in normal human intervertebral disc. *J Anat* **186 (Pt 1)**: 43-53, 1995.

[33] Chen, J., Jing, L., Gilchrist, C.L., Richardson, W.J., Fitch, R.D., and Setton, L.A., Expression of laminin isoforms, receptors and binding proteins unique to nucleus pulposus cells of immature intervertebral disc. *Connective Tissue Research* ***50***: 294–306, 2009.

[34] Chen, J., Yan, W., and Setton, L.A., Molecular phenotypes of notochordal cells purified from immature nucleus pulposus. *Eur Spine J* **15 Suppl 3**: S303-311, 2006.

[35] Chiba, K., Andersson, G.B., Masuda, K., Momohara, S., Williams, J.M., and Thonar, E.J., A new culture system to study the metabolism of the intervertebral disc in vitro. *Spine (Phila Pa 1976)* **23**: 1821-1827; discussion 1828, 1998.

[36] Chiba, K., Andersson, G.B., Masuda, K., and Thonar, E.J., Metabolism of the extracellular matrix formed by intervertebral disc cells cultured in alginate. *Spine (Phila Pa 1976)* **22**: 2885-2893, 1997.

[37] Choi, K.S., Cohn, M.J., and Harfe, B.D., Identification of nucleus pulposus precursor cells and notochordal remnants in the mouse: implications for disk degeneration and chordoma formation. *Dev Dyn* **237**: 3953-3958, 2008.

[38] Chung, J. and Mercurio, A.M., Contributions of the alpha6 integrins to breast carcinoma survival and progression. *Mol Cells* **17**: 203-209, 2004.

[39] Cloyd, J.M., Malhotra, N.R., Weng, L., Chen, W., Mauck, R.L., and Elliott, D.M., Material properties in unconfined compression of human nucleus pulposus, injectable hyaluronic acid-based hydrogels and tissue engineering scaffolds. *Eur Spine J*, 2007.

[40] Colognato, H. and Yurchenco, P.D., Form and function: the laminin family of heterotrimers. *Dev Dyn* **218**: 213-234, 2000.

[41] Cotten, A., Sakka, M., Drizenko, A., Clarisse, J., and Francke, J.P., Antenatal differentiation of the human intervertebral disc. *Surg Radiol Anat* **16**: 53-56, 1994.

[42] Darling, E.M., Topel, M., Zauscher, S., Vail, T.P., and Guilak, F., Viscoelastic properties of human mesenchymally-derived stem cells and primary osteoblasts, chondrocytes, and adipocytes. *J Biomech* **41**: 454-464, 2008.

[43] de Rooij, J., Kerstens, A., Danuser, G., Schwartz, M.A., and Waterman-Storer, C.M., Integrin-dependent actomyosin contraction regulates epithelial cell scattering. *J Cell Biol* **171**: 153-164, 2005.

[44] DeLise, A.M., Fischer, L., and Tuan, R.S., Cellular interactions and signaling in cartilage development. *Osteoarthritis Cartilage* **8**: 309-334, 2000.

[45] Delise, A.M. and Tuan, R.S., Analysis of N-cadherin function in limb mesenchymal chondrogenesis in vitro. *Dev Dyn* **225**: 195-204, 2002.

[46] Discher, D.E., Janmey, P., and Wang, Y.L., Tissue cells feel and respond to the stiffness of their substrate. *Science* **310**: 1139-1143, 2005.

[47] Discher, D.E., Mooney, D.J., and Zandstra, P.W., Growth factors, matrices, and forces combine and control stem cells. *Science* **324**: 1673-1677, 2009.

[48] Domogatskaya, A., Rodin, S., Boutaud, A., and Tryggvason, K., Laminin-511 but not -332, -111, or -411 enables mouse embryonic stem cell self-renewal in vitro. *Stem Cells* **26**: 2800-2809, 2008.

[49] Engler, A., Bacakova, L., Newman, C., Hategan, A., Griffin, M., and Discher, D., Substrate compliance versus ligand density in cell on gel responses. *Biophys J* **86**: 617-628, 2004.

[50] Engler, A.J., Carag-Krieger, C., Johnson, C.P., Raab, M., Tang, H.Y., Speicher, D.W., Sanger, J.W., Sanger, J.M., and Discher, D.E., Embryonic cardiomyocytes beat best on a matrix with heart-like elasticity: scar-like rigidity inhibits beating. *J Cell Sci* **121**: 3794-3802, 2008.

[51] Engler, A.J., Griffin, M.A., Sen, S., Bonnemann, C.G., Sweeney, H.L., and Discher, D.E., Myotubes differentiate optimally on substrates with tissue-like stiffness:

pathological implications for soft or stiff microenvironments. *J Cell Biol* **166**: 877-887, 2004.

[52] Engler, A.J., Sen, S., Sweeney, H.L., and Discher, D.E., Matrix elasticity directs stem cell lineage specification. *Cell* **126**: 677-689, 2006.

[53] Erwin, W.M., Ashman, K., O'Donnel, P., and Inman, R.D., Nucleus pulposus notochord cells secrete connective tissue growth factor and up-regulate proteoglycan expression by intervertebral disc chondrocytes. *Arthritis Rheum* **54**: 3859-3867, 2006.

[54] Erwin, W.M. and Inman, R.D., Notochord cells regulate intervertebral disc chondrocyte proteoglycan production and cell proliferation. *Spine* **31**: 1094-1099, 2006.

[55] Evans, N.D., Minelli, C., Gentleman, E., LaPointe, V., Patankar, S.N., Kallivretaki, M., Chen, X., Roberts, C.J., and Stevens, M.M., Substrate stiffness affects early differentiation events in embryonic stem cells. *Eur Cell Mater* **18**: 1-13; discussion 13-14, 2009.

[56] Eyre, D.R. and Muir, H., Quantitative analysis of types I and II collagens in human intervertebral discs at various ages. *Biochim Biophys Acta* **492**: 29-42, 1977.

[57] Farndale, R.W., Sayers, C.A., and Barrett, A.J., A direct spectrophotometric microassay for sulfated glycosaminoglycans in cartilage cultures. *Connect Tissue Res* **9**: 247-248, 1982.

[58] Folkman, J. and Moscona, A., Role of cell shape in growth control. *Nature* **273**: 345-349, 1978.

[59] Forsyth, C.B., Pulai, J., and Loeser, R.F., Fibronectin fragments and blocking antibodies to alpha2beta1 and alpha5beta1 integrins stimulate mitogen-activated protein kinase signaling and increase collagenase 3 (matrix metalloproteinase 13) production by human articular chondrocytes. *Arthritis Rheum* **46**: 2368-2376, 2002.

[60] Galou, M., Gao, J., Humbert, J., Mericskay, M., Li, Z., Paulin, D., and Vicart, P., The importance of intermediate filaments in the adaptation of tissues to mechanical stress: evidence from gene knockout studies. *Biol Cell* **89**: 85-97, 1997.

[61] Geiger, B., Bershadsky, A., Pankov, R., and Yamada, K.M., Transmembrane crosstalk between the extracellular matrix--cytoskeleton crosstalk. *Nat Rev Mol Cell Biol* **2**: 793-805, 2001.

[62] Georgatos, S.D. and Blobel, G., Lamin B constitutes an intermediate filament attachment site at the nuclear envelope. *J Cell Biol* **105**: 117-125, 1987.

[63] Ghosh, S., Laha, M., Mondal, S., Sengupta, S., and Kaplan, D.L., In vitro model of mesenchymal condensation during chondrogenic development. *Biomaterials* **30**: 6530-6540, 2009.

[64] Giannone, G. and Sheetz, M.P., Substrate rigidity and force define form through tyrosine phosphatase and kinase pathways. *Trends Cell Biol* **16**: 213-223, 2006.

[65] Gilchrist, C.L., Chen, J., Richardson, W.J., Loeser, R.F., and Setton, L.A., Functional integrin subunits regulating cell-matrix interactions in the intervertebral disc. *J Orthop Res* **25**: 829-840, 2007.

[66] Glowacki, J., Trepman, E., and Folkman, J., Cell shape and phenotypic expression in chondrocytes. *Proc Soc Exp Biol Med* **172**: 93-98, 1983.

[67] Goto, S. and Uhthoff, H.K., Notochord action on spinal development. A histologic and morphometric investigation. *Acta Orthop Scand* **57**: 85-90, 1986.

[68] Gotwals, P.J., Chi-Rosso, G., Lindner, V., Yang, J., Ling, L., Fawell, S.E., and Koteliansky, V.E., The alpha1beta1 integrin is expressed during neointima formation in rat arteries and mediates collagen matrix reorganization. *J Clin Invest* **97**: 2469-2477, 1996.

[69] Gotz, W., Kasper, M., Fischer, G., and Herken, R., Intermediate filament typing of the human embryonic and fetal notochord. *Cell Tissue Res* **280**: 455-462, 1995.

[70] Gower, W.E. and Pedrini, V., Age-related variations in proteinpolysaccharides from human nucleus pulposus, annulus fibrosus, and costal cartilage. *J Bone Joint Surg Am* **51**: 1154-1162, 1969.

[71] Grunhagen, T., Wilde, G., Soukane, D.M., Shirazi-Adl, S.A., and Urban, J.P., Nutrient supply and intervertebral disc metabolism. *J Bone Joint Surg Am* **88 Suppl 2**: 30-35, 2006.

[72] Gu, J., Fujibayashi, A., Yamada, K.M., and Sekiguchi, K., Laminin-10/11 and fibronectin differentially prevent apoptosis induced by serum removal via phosphatidylinositol 3-kinase/Akt- and MEK1/ERK-dependent pathways. *J Biol Chem* **277**: 19922-19928, 2002.

[73] Gudjonsson, T., Ronnov-Jessen, L., Villadsen, R., Rank, F., Bissell, M.J., and Petersen, O.W., Normal and tumor-derived myoepithelial cells differ in their ability to interact with luminal breast epithelial cells for polarity and basement membrane deposition. *J Cell Sci* **115**: 39-50, 2002.

[74] Guilak, F., Cohen, D.M., Estes, B.T., Gimble, J.M., Liedtke, W., and Chen, C.S., Control of stem cell fate by physical interactions with the extracellular matrix. *Cell Stem Cell* **5**: 17-26, 2009.

[75] Guilak, F., Ting-Beall, H.P., Baer, A.E., Trickey, W.R., Erickson, G.R., and Setton, L.A., Viscoelastic properties of intervertebral disc cells. Identification of two biomechanically distinct cell populations. *Spine* **24**: 2475-2483, 1999.

[76] Gullberg, D., Tingstrom, A., Thuresson, A.C., Olsson, L., Terracio, L., Borg, T.K., and Rubin, K., Beta 1 integrin-mediated collagen gel contraction is stimulated by PDGF. *Exp Cell Res* **186**: 264-272, 1990.

[77] Guo, S. and Akhremitchev, B.B., Packing density and structural heterogeneity of insulin amyloid fibrils measured by AFM nanoindentation. *Biomacromolecules* **7**: 1630-1636, 2006.

[78] Guo, W.H., Frey, M.T., Burnham, N.A., and Wang, Y.L., Substrate rigidity regulates the formation and maintenance of tissues. *Biophys J* **90**: 2213-2220, 2006.

[79] Halliday, N.L. and Tomasek, J.J., Mechanical properties of the extracellular matrix influence fibronectin fibril assembly in vitro. *Exp Cell Res* **217**: 109-117, 1995.

[80] Hayes, A.J., Benjamin, M., and Ralphs, J.R., Role of actin stress fibres in the development of the intervertebral disc: cytoskeletal control of extracellular matrix assembly. *Dev Dyn* **215**: 179-189, 1999.

[81] Hayes, A.J., Benjamin, M., and Ralphs, J.R., Extracellular matrix in development of the intervertebral disc. *Matrix Biol* **20**: 107-121, 2001.

[82] Herard, A.L., Pierrot, D., Hinnrasky, J., Kaplan, H., Sheppard, D., Puchelle, E., and Zahm, J.M., Fibronectin and its alpha 5 beta 1-integrin receptor are involved in the wound-repair process of airway epithelium. *Am J Physiol* **271**: L726-733, 1996.

[83] Herrmann, H., Bar, H., Kreplak, L., Strelkov, S.V., and Aebi, U., Intermediate filaments: from cell architecture to nanomechanics. *Nat Rev Mol Cell Biol* **8**: 562-573, 2007.

[84] Hertz, H.J., On contact between elastic bodies. *Reine Angew. Math.* **92**: 156-171, 1881.

[85] Homandberg, G.A., Potential regulation of cartilage metabolism in osteoarthritis by fibronectin fragments. *Front Biosci* **4**: D713-730, 1999.

[86] Hunter, C.J., Matyas, J.R., and Duncan, N.A., The three-dimensional architecture of the notochordal nucleus pulposus: novel observations on cell structures in the canine intervertebral disc. *J Anat* **202**: 279-291, 2003.

[87] Hunter, C.J., Matyas, J.R., and Duncan, N.A., Cytomorphology of notochordal and chondrocytic cells from the nucleus pulposus: a species comparison. *J Anat* **205**: 357-362, 2004.

[88] Hunter, C.J., Matyas, J.R., and Duncan, N.A., The functional significance of cell clusters in the notochordal nucleus pulposus: survival and signaling in the canine intervertebral disc. *Spine* **29**: 1099-1104, 2004.

[89] Hurri, H. and Karppinen, J., Discogenic pain. *Pain* **112**: 225-228, 2004.

[90] Hynes, R.O., Integrins: versatility, modulation, and signaling in cell adhesion. *Cell* **69**: 11-25, 1992.

[91] Iatridis, J.C., Setton, L.A., Weidenbaum, M., and Mow, V.C., Alterations in the mechanical behavior of the human lumbar nucleus pulposus with degeneration and aging. *J Orthop Res* **15**: 318-322, 1997.

[92] Iatridis, J.C., Setton, L.A., Weidenbaum, M., and Mow, V.C., The viscoelastic behavior of the non-degenerate human lumbar nucleus pulposus in shear. *J Biomech* **30**: 1005-1013, 1997.

[93] Iatridis, J.C., Weidenbaum, M., Setton, L.A., and Mow, V.C., Is the nucleus pulposus a solid or a fluid? Mechanical behaviors of the nucleus pulposus of the human intervertebral disc. *Spine* **21**: 1174-1184, 1996.

[94] Ido, H., Harada, K., Futaki, S., Hayashi, Y., Nishiuchi, R., Natsuka, Y., Li, S., Wada, Y., Combs, A.C., Ervasti, J.M., and Sekiguchi, K., Molecular dissection of the alpha-dystroglycan- and integrin-binding sites within the globular domain of human laminin-10. *J Biol Chem* **279**: 10946-10954, 2004.

[95] Jahnke, M.R. and McDevitt, C.A., Proteoglycans of the human intervertebral disc. Electrophoretic heterogeneity of the aggregating proteoglycans of the nucleus pulposus. *Biochem J* **251**: 347-356, 1988.

[96] Johnstone, B. and Bayliss, M.T., The large proteoglycans of the human intervertebral disc. Changes in their biosynthesis and structure with age, topography, and pathology. *Spine (Phila Pa 1976)* **20**: 674-684, 1995.

[97] Jokinen, J., Dadu, E., Nykvist, P., Kapyla, J., White, D.J., Ivaska, J., Vehvilainen, P., Reunanen, H., Larjava, H., Hakkinen, L., and Heino, J., Integrin-mediated cell adhesion to type I collagen fibrils. *J Biol Chem* **279**: 31956-31963, 2004.

[98] Kalson, N.S., Richardson, S., and Hoyland, J.A., Strategies for regeneration of the intervertebral disc. *Regen Med* **3**: 717-729, 2008.

[99] Kandel, R., Roberts, S., and Urban, J.P., Tissue engineering and the intervertebral disc: the challenges. *Eur Spine J* **17 Suppl 4**: 480-491, 2008.

[100] Kasper, M., Cytokeratins in intracranial and intraspinal tissues. *Adv Anat Embryol Cell Biol* **126**: 1-82, 1992.

[101] Katz, J.N., Lumbar disc disorders and low-back pain: socioeconomic factors and consequences. *J Bone Joint Surg Am* **88 Suppl 2**: 21-24, 2006.

[102] Kikkawa, Y., Sanzen, N., Fujiwara, H., Sonnenberg, A., and Sekiguchi, K., Integrin binding specificity of laminin-10/11: laminin-10/11 are recognized by alpha 3 beta 1, alpha 6 beta 1 and alpha 6 beta 4 integrins. *J Cell Sci* **113 (Pt 5)**: 869-876, 2000.

[103] Kim, K.W., Ha, K.Y., Park, J.B., Woo, Y.K., Chung, H.N., and An, H.S., Expressions of membrane-type I matrix metalloproteinase, Ki-67 protein, and

type II collagen by chondrocytes migrating from cartilage endplate into nucleus pulposus in rat intervertebral discs: a cartilage endplate-fracture model using an intervertebral disc organ culture. *Spine* **30**: 1373-1378, 2005.

[104] Kim, K.W., Lim, T.H., Kim, J.G., Jeong, S.T., Masuda, K., and An, H.S., The origin of chondrocytes in the nucleus pulposus and histologic findings associated with the transition of a notochordal nucleus pulposus to a fibrocartilaginous nucleus pulposus in intact rabbit intervertebral discs. *Spine* **28**: 982-990, 2003.

[105] Klaffky, E.J., Gonzales, I.M., and Sutherland, A.E., Trophoblast cells exhibit differential responses to laminin isoforms. *Dev Biol* **292**: 277-289, 2006.

[106] Klees, R.F., Salasznyk, R.M., Kingsley, K., Williams, W.A., Boskey, A., and Plopper, G.E., Laminin-5 induces osteogenic gene expression in human mesenchymal stem cells through an ERK-dependent pathway. *Mol Biol Cell* **16**: 881-890, 2005.

[107] Klees, R.F., Salasznyk, R.M., Vandenberg, S., Bennett, K., and Plopper, G.E., Laminin-5 activates extracellular matrix production and osteogenic gene focusing in human mesenchymal stem cells. *Matrix Biol* **26**: 106-114, 2007.

[108] Kleinman, H.K., McGarvey, M.L., Hassell, J.R., Star, V.L., Cannon, F.B., Laurie, G.W., and Martin, G.R., Basement membrane complexes with biological activity. *Biochemistry* **25**: 312-318, 1986.

[109] Kleinman, H.K., McGarvey, M.L., Liotta, L.A., Robey, P.G., Tryggvason, K., and Martin, G.R., Isolation and characterization of type IV procollagen, laminin, and heparan sulfate proteoglycan from the EHS sarcoma. *Biochemistry* **21**: 6188-6193, 1982.

[110] Lammerding, J., Kazarov, A.R., Huang, H., Lee, R.T., and Hemler, M.E., Tetraspanin CD151 regulates alpha6beta1 integrin adhesion strengthening. *Proc Natl Acad Sci U S A* **100**: 7616-7621, 2003.

[111] Lehtonen, E., Stefanovic, V., and Saraga-Babic, M., Changes in the expression of intermediate filaments and desmoplakins during development of human notochord. *Differentiation* **59**: 43-49, 1995.

[112] Li, M.L., Aggeler, J., Farson, D.A., Hatier, C., Hassell, J., and Bissell, M.J., Influence of a reconstituted basement membrane and its components on casein

gene expression and secretion in mouse mammary epithelial cells. *Proc Natl Acad Sci U S A* **84**: 136-140, 1987.

[113] Li, S., Edgar, D., Fassler, R., Wadsworth, W., and Yurchenco, P.D., The role of laminin in embryonic cell polarization and tissue organization. *Dev Cell* **4**: 613-624, 2003.

[114] Litjens, S.H., de Pereda, J.M., and Sonnenberg, A., Current insights into the formation and breakdown of hemidesmosomes. *Trends Cell Biol* **16**: 376-383, 2006.

[115] Lo, C.M., Wang, H.B., Dembo, M., and Wang, Y.L., Cell movement is guided by the rigidity of the substrate. *Biophys J* **79**: 144-152, 2000.

[116] Loeser, R.F., Integrins and cell signaling in chondrocytes. *Biorheology* **39**: 119-124, 2002.

[117] Loeser, R.F., Carlson, C.S., and McGee, M.P., Expression of beta 1 integrins by cultured articular chondrocytes and in osteoarthritic cartilage. *Exp Cell Res* **217**: 248-257, 1995.

[118] Lotz, M.M., Burdsal, C.A., Erickson, H.P., and McClay, D.R., Cell adhesion to fibronectin and tenascin: quantitative measurements of initial binding and subsequent strengthening response. *J Cell Biol* **109**: 1795-1805, 1989.

[119] Maldonado, B.A. and Oegema, T.R., Jr., Initial characterization of the metabolism of intervertebral disc cells encapsulated in microspheres. *J Orthop Res* **10**: 677-690, 1992.

[120] Maniotis, A.J., Chen, C.S., and Ingber, D.E., Demonstration of mechanical connections between integrins cytoskeletal filaments, and nucleoplasm that stabilize nuclear structure. *Proc. Natl. Acad. Sci. USA* **94**: 849-854, 1997.

[121] Marchand, F. and Ahmed, A.M., Investigation of the laminate structure of lumbar disc anulus fibrosus. *Spine (Phila Pa 1976)* **15**: 402-410, 1990.

[122] Masuda, K., Biological repair of the degenerated intervertebral disc by the injection of growth factors. *Eur Spine J* **17 Suppl 4**: 441-451, 2008.

[123] Masuda, K. and An, H.S., Prevention of disc degeneration with growth factors. *Eur Spine J* **15 Suppl 3**: S422-432, 2006.

[124] Matsui, Y., Mirza, S.K., Wu, J.J., Carter, B., Bellabarba, C., Shaffrey, C.I., Chapman, J.R., and Eyre, D.R., The association of lumbar spondylolisthesis with collagen IX tryptophan alleles. *J Bone Joint Surg Br* **86**: 1021-1026, 2004.

[125] McGuire, L.J., Ng, J.P., and Lee, J.C., Coexpression of cytokeratin and vimentin. *Appl Pathol* **7**: 73-84, 1989.

[126] Melrose, J., Ghosh, P., and Taylor, T.K., A comparative analysis of the differential spatial and temporal distributions of the large (aggrecan, versican) and small (decorin, biglycan, fibromodulin) proteoglycans of the intervertebral disc. *J Anat* **198**: 3-15, 2001.

[127] Mercurio, A.M., Bachelder, R.E., Chung, J., O'Connor, K.L., Rabinovitz, I., Shaw, L.M., and Tani, T., Integrin laminin receptors and breast carcinoma progression. *J Mammary Gland Biol Neoplasia* **6**: 299-309, 2001.

[128] Miner, J.H. and Yurchenco, P.D., Laminin functions in tissue morphogenesis. *Annu Rev Cell Dev Biol* **20**: 255-284, 2004.

[129] Miyamoto, S., Akiyama, S.K., and Yamada, K.M., Synergistic roles for receptor occupancy and aggregation in integrin transmembrane function. *Science* **267**: 883-885, 1995.

[130] Miyamoto, S., Teramoto, H., Coso, O.A., Gutkind, J.S., Burbelo, P.D., Akiyama, S.K., and Yamada, K.M., Integrin function: molecular hierarchies of cytoskeletal and signaling molecules. *J Cell Biol* **131**: 791-805, 1995.

[131] Nettles, D.L., Richardson, W.J., and Setton, L.A., Integrin expression in cells of the intervertebral disc. *J Anat* **204**: 515-520, 2004.

[132] Nguyen, N.M. and Senior, R.M., Laminin isoforms and lung development: all isoforms are not equal. *Dev Biol* **294**: 271-279, 2006.

[133] Nievers, M.G., Schaapveld, R.Q., and Sonnenberg, A., Biology and function of hemidesmosomes. *Matrix Biol* **18**: 5-17, 1999.

[134] Nishiuchi, R., Takagi, J., Hayashi, M., Ido, H., Yagi, Y., Sanzen, N., Tsuji, T., Yamada, M., and Sekiguchi, K., Ligand-binding specificities of laminin-binding integrins: a comprehensive survey of laminin-integrin interactions using

recombinant alpha3beta1, alpha6beta1, alpha7beta1 and alpha6beta4 integrins. *Matrix Biol* **25**: 189-197, 2006.

[135] Nomura, T., Mochida, J., Okuma, M., Nishimura, K., and Sakabe, K., Nucleus pulposus allograft retards intervertebral disc degeneration. *Clin Orthop Relat Res*: 94-101, 2001.

[136] Noponen-Hietala, N., Kyllonen, E., Mannikko, M., Ilkko, E., Karppinen, J., Ott, J., and Ala-Kokko, L., Sequence variations in the collagen IX and XI genes are associated with degenerative lumbar spinal stenosis. *Ann Rheum Dis* **62**: 1208-1214, 2003.

[137] Oegema, T.R., Jr., The role of disc cell heterogeneity in determining disc biochemistry: a speculation. *Biochem Soc Trans* **30**: 839-844, 2002.

[138] Oegema, T.R., Jr., Johnson, S.L., Aguiar, D.J., and Ogilvie, J.W., Fibronectin and its fragments increase with degeneration in the human intervertebral disc. *Spine* **25**: 2742-2747, 2000.

[139] Okuma, M., Mochida, J., Nishimura, K., Sakabe, K., and Seiki, K., Reinsertion of stimulated nucleus pulposus cells retards intervertebral disc degeneration: an in vitro and in vivo experimental study. *J Orthop Res* **18**: 988-997, 2000.

[140] Paszek, M.J., Zahir, N., Johnson, K.R., Lakins, J.N., Rozenberg, G.I., Gefen, A., Reinhart-King, C.A., Margulies, S.S., Dembo, M., Boettiger, D., Hammer, D.A., and Weaver, V.M., Tensional homeostasis and the malignant phenotype. *Cancer Cell* **8**: 241-254, 2005.

[141] Pazzaglia, U.E., Salisbury, J.R., and Byers, P.D., Development and involution of the notochord in the human spine. *J R Soc Med* **82**: 413-415, 1989.

[142] Peacock, A., Observations on the prenatal development of the intervertebral disc in man. *J Anat* **85**: 260-274, 1951.

[143] Pearce, R.H., Grimmer, B.J., and Adams, M.E., Degeneration and the chemical composition of the human lumbar intervertebral disc. *J Orthop Res* **5**: 198-205, 1987.

[144] Pelham, R.J., Jr. and Wang, Y., Cell locomotion and focal adhesions are regulated by substrate flexibility. *Proc Natl Acad Sci U S A* **94**: 13661-13665, 1997.

[145] Pelham, R.J., Jr. and Wang, Y.L., Cell locomotion and focal adhesions are regulated by the mechanical properties of the substrate. *Biol Bull* **194**: 348-349; discussion 349-350, 1998.

[146] Plopper, G., Falk-Marzillier, J., Glaser, S., Fitchmun, M., Giannelli, G., Romano, T., Jones, J.C., and Quaranta, V., Changes in expression of monoclonal antibody epitopes on laminin-5r induced by cell contact. *J Cell Sci* **109 (Pt 7)**: 1965-1973, 1996.

[147] Plopper, G.E., Domanico, S.Z., Cirulli, V., Kiosses, W.B., and Quaranta, V., Migration of breast epithelial cells on Laminin-5: differential role of integrins in normal and transformed cell types. *Breast Cancer Res Treat* **51**: 57-69, 1998.

[148] Praemer, A., Furner, S., Rice, D.P., and American Academy of Orthopaedic, S., *Musculoskeletal conditions in the United States / Allan Praemer, Sylvia Furner, Dorothy P. Rice*: American Academy of Orthopaedic Surgeons. 1999.

[149] Racine-Samson, L., Rockey, D.C., and Bissell, D.M., The role of alpha1beta1 integrin in wound contraction. A quantitative analysis of liver myofibroblasts in vivo and in primary culture. *J Biol Chem* **272**: 30911-30917, 1997.

[150] Reyes, C.D. and Garcia, A.J., A centrifugation cell adhesion assay for high-throughput screening of biomaterial surfaces. *J Biomed Mater Res A* **67**: 328-333, 2003.

[151] Roberts, S., Evans, H., Trivedi, J., and Menage, J., Histology and pathology of the human intervertebral disc. *J Bone Joint Surg Am* **88 Suppl 2**: 10-14, 2006.

[152] Roberts, S., Menage, J., Duance, V., Wotton, S., and Ayad, S., 1991 Volvo Award in basic sciences. Collagen types around the cells of the intervertebral disc and cartilage end plate: an immunolocalization study. *Spine* **16**: 1030-1038, 1991.

[153] Roskelley, C.D., Desprez, P.Y., and Bissell, M.J., Extracellular matrix-dependent tissue-specific gene expression in mammary epithelial cells requires both physical and biochemical signal transduction. *Proc Natl Acad Sci U S A* **91**: 12378-12382, 1994.

[154] Roughley, P.J., Biology of intervertebral disc aging and degeneration: involvement of the extracellular matrix. *Spine* **29**: 2691-2699, 2004.

[155] Rowley, J.A. and Mooney, D.J., Alginate type and RGD density control myoblast phenotype. *J Biomed Mater Res* **60**: 217-223, 2002.

[156] Rufai, A., Benjamin, M., and Ralphs, J.R., The development of fibrocartilage in the rat intervertebral disc. *Anat Embryol (Berl)* **192**: 53-62, 1995.

[157] Sambrook, P.N., MacGregor, A.J., and Spector, T.D., Genetic influences on cervical and lumbar disc degeneration: a magnetic resonance imaging study in twins. *Arthritis Rheum* **42**: 366-372, 1999.

[158] Semler, E.J., Ranucci, C.S., and Moghe, P.V., Mechanochemical manipulation of hepatocyte aggregation can selectively induce or repress liver-specific function. *Biotechnol Bioeng* **69**: 359-369, 2000.

[159] Stabenfeldt, S.E., Garcia, A.J., and LaPlaca, M.C., Thermoreversible laminin-functionalized hydrogel for neural tissue engineering. *J Biomed Mater Res A* **77**: 718-725, 2006.

[160] Stosiek, P., Kasper, M., and Karsten, U., Expression of cytokeratin and vimentin in nucleus pulposus cells. *Differentiation* **39**: 78-81, 1988.

[161] Streuli, C.H., Schmidhauser, C., Bailey, N., Yurchenco, P., Skubitz, A.P., Roskelley, C., and Bissell, M.J., Laminin mediates tissue-specific gene expression in mammary epithelia. *J Cell Biol* **129**: 591-603, 1995.

[162] Taylor, J.R. and Twomey, L.T., *The development of the human intervertebral disc*, in *The biology of the intervertebral disc*, P. Gosh, Editor. 1988, CRC Press: Boca Raton. p. 39-82.

[163] Theodore, P.R., Simon, A.R., Warrens, A.N., Sackstein, R., and Sykes, M., Porcine mononuclear cells adhere to human fibronectin independently of very late antigen-5: implications for donor-specific tolerance induction in xenotransplantation. *Xenotransplantation* **9**: 277-289, 2002.

[164] Tiger, C.F., Fougerousse, F., Grundstrom, G., Velling, T., and Gullberg, D., alpha11beta1 integrin is a receptor for interstitial collagens involved in cell migration and collagen reorganization on mesenchymal nonmuscle cells. *Dev Biol* **237**: 116-129, 2001.

[165] Trout, J.J., Buckwalter, J.A., Moore, K.C., and Landas, S.K., Ultrastructure of the human intervertebral disc. I. Changes in notochordal cells with age. *Tissue Cell* **14**: 359-369, 1982.

[166] Tulla, M., Pentikainen, O.T., Viitasalo, T., Kapyla, J., Impola, U., Nykvist, P., Nissinen, L., Johnson, M.S., and Heino, J., Selective binding of collagen subtypes by integrin alpha 1I, alpha 2I, and alpha 10I domains. *J Biol Chem* **276**: 48206-48212, 2001.

[167] Urban, J.P., The role of the physicochemical environment in determining disc cell behaviour. *Biochem Soc Trans* **30**: 858-864, 2002.

[168] Urban, J.P. and Roberts, S., Degeneration of the intervertebral disc. *Arthritis Res Ther* **5**: 120-130, 2003.

[169] Urban, J.P., Smith, S., and Fairbank, J.C., Nutrition of the intervertebral disc. *Spine (Phila Pa 1976)* **29**: 2700-2709, 2004.

[170] Velling, T., Kusche-Gullberg, M., Sejersen, T., and Gullberg, D., cDNA cloning and chromosomal localization of human alpha(11) integrin. A collagen-binding, I domain-containing, beta(1)-associated integrin alpha-chain present in muscle tissues. *J Biol Chem* **274**: 25735-25742, 1999.

[171] Videman, T., Nurminen, M., and Troup, J.D., 1990 Volvo Award in clinical sciences. Lumbar spinal pathology in cadaveric material in relation to history of back pain, occupation, and physical loading. *Spine (Phila Pa 1976)* **15**: 728-740, 1990.

[172] Videman, T., Saarela, J., Kaprio, J., Nakki, A., Levalahti, E., Gill, K., Peltonen, L., and Battie, M.C., Associations of 25 structural, degradative, and inflammatory candidate genes with lumbar disc desiccation, bulging, and height narrowing. *Arthritis Rheum* **60**: 470-481, 2009.

[173] Vukicevic, S., Kleinman, H.K., Luyten, F.P., Roberts, A.B., Roche, N.S., and Reddi, A.H., Identification of multiple active growth factors in basement membrane Matrigel suggests caution in interpretation of cellular activity related to extracellular matrix components. *Exp Cell Res* **202**: 1-8, 1992.

[174] Wang, J.Y., Baer, A.E., Kraus, V.B., and Setton, L.A., Intervertebral disc cells exhibit differences in gene expression in alginate and monolayer culture. *Spine* **26**: 1747-1751; discussion 1752, 2001.

[175] Wang, Y.K., Wang, Y.H., Wang, C.Z., Sung, J.M., Chiu, W.T., Lin, S.H., Chang, Y.H., and Tang, M.J., Rigidity of collagen fibrils controls collagen gel-induced down-regulation of focal adhesion complex proteins mediated by alpha2beta1 integrin. *J Biol Chem* **278**: 21886-21892, 2003.

[176] Weaver, V.M. and Bissell, M.J., Functional culture models to study mechanisms governing apoptosis in normal and malignant mammary epithelial cells. *J Mammary Gland Biol Neoplasia* **4**: 193-201, 1999.

[177] Weaver, V.M., Howlett, A.R., Langton-Webster, B., Petersen, O.W., and Bissell, M.J., The development of a functionally relevant cell culture model of progressive human breast cancer. *Semin Cancer Biol* **6**: 175-184, 1995.

[178] Weaver, V.M., Lelievre, S., Lakins, J.N., Chrenek, M.A., Jones, J.C., Giancotti, F., Werb, Z., and Bissell, M.J., beta4 integrin-dependent formation of polarized three-dimensional architecture confers resistance to apoptosis in normal and malignant mammary epithelium. *Cancer Cell* **2**: 205-216, 2002.

[179] Wolfe, H.J., Putschar, W.G.J., and Vickery, A.L., Role of the notochord in human intervertebral discs. I. Fetus and infant. *Clinical Orthopaedics & Related Research* **39**: 205-212, 1965.

[180] Wondimu, Z., Gorfu, G., Kawataki, T., Smirnov, S., Yurchenco, P., Tryggvason, K., Patarroyo, M., Herard, A.L., Pierrot, D., Hinnrasky, J., Kaplan, H., Sheppard, D., Puchelle, E., and Zahm, J.M., Characterization of commercial laminin preparations from human placenta in comparison to recombinant laminins 2 (alpha2beta1gamma1), 8 (alpha4beta1gamma1), 10 (alpha5beta1gamma1). *Matrix Biol* **25**: 89-93, 2006.

[181] Woolf, A.D. and Pfleger, B., Burden of major musculoskeletal conditions. *Bull World Health Organ* **81**: 646-656, 2003.

[182] Yu, J., Elastic tissues of the intervertebral disc. *Biochem Soc Trans* **30**: 848-852, 2002.

[183] Yu, S.W., Haughton, V.M., Lynch, K.L., Ho, K.C., and Sether, L.A., Fibrous structure in the intervertebral disk: correlation of MR appearance with anatomic sections. *AJNR Am J Neuroradiol* **10**: 1105-1110, 1989.

[184] Yurchenco, P.D., Amenta, P.S., and Patton, B.L., Basement membrane assembly, stability and activities observed through a developmental lens. *Matrix Biol* **22**: 521-538, 2004.

[185] Yurchenco, P.D., Tsilibary, E.C., Charonis, A.S., and Furthmayr, H., Laminin polymerization in vitro. Evidence for a two-step assembly with domain specificity. *J Biol Chem* **260**: 7636-7644, 1985.

[186] Yurchenco, P.D. and Wadsworth, W.G., Assembly and tissue functions of early embryonic laminins and netrins. *Curr Opin Cell Biol* **16**: 572-579, 2004.

[187] Zavadil, J. and Bottinger, E.P., TGF-beta and epithelial-to-mesenchymal transitions. *Oncogene* **24**: 5764-5774, 2005.

Biography

Christopher Lee Gilchrist was born on March 12, 1972 in Monticello, Iowa to Dr. David Gilchrist and Susan Gilchrist. He attended Purdue University and earned a Bachelor of Science degree in Civil Engineering with highest honors in 1995. During this time he was inducted into the Tau Beta Pi Engineering Honorary, Chi Epsilon Civil Engineering Honorary, and was the recipient of the Martin Gutzwiller Award for outstanding structural engineering student. He then earned a Master's of Science degree in Civil Engineering from The University of Texas at Austin in 1997, where he studied buckling behavior of steel box girders. He worked as a structural design engineer for 4 years in Texas and Iowa before returning to study biomedical engineering at Duke University in 2001. While at Duke, he was named a James B. Duke fellow, an NIH Center for Biological and Tissue Engineering (CBTE) fellow, and was awarded the CBTE Student Achievement Award.

His publications include:

Gilchrist, CL, Xia, Q, Setton, LA, and Hsu, E, "High-resolution determination of soft tissue deformations using MRI and first-order texture correlation" *IEEE Transactions on Medical Imaging* 23 (5): 546-553, 2004.

Gilchrist, CL, Witvoet-Braam, SB, Guilak, F, and Setton, L, "Measurement of intracellular strain on deformable substrates with texture correlation", *Journal of Biomechanics,* 40(4):786-794, 2007.

Gilchrist, CL, Chen, J, Richardson, WJ, Loeser, RF, and Setton, LA, "Functional Integrin Subunits Regulating Cell-Matrix Interactions in the Intervertebral Disc", *Journal of Orthopaedic Research,* 25(6):829-40, 2007.

Choi, JB, Youn, I, Cao, L, Leddy, HA, **Gilchrist, CL**, Setton,LA, Guilak, F, "Zonal changes in the three-dimensional morphology of the chondron in articular cartilage under compression: The relationship between cellular, pericellular, and extracellular deformation.", *Journal of Biomechanics*, 40(12):2596-603, 2007.

Gilchrist, CL, Guilak, F, and Setton, LA. "Intracellular Measurements of Strain Transfer using Texture Correlation", in *Biomechanics at Micro- and Nanoscale Levels, Volume III*, Ed: H.Wada (*invited chapter*), 2007.

Upton, ML, **Gilchrist, CL**, Guilak, F, and Setton, LA. "Extracellular matrix strain is coupled to strain in the microenvironment of meniscus cells", *Biophysical Journal*, 95(4):2116-24, 2008.

Chen J, Jing L, **Gilchrist CL**, Richardson WJ, Fitch RD and Setton, LA. "Expression of Laminin Isoforms, Receptors and Binding Proteins Unique to Nucleus Pulposus Cells of Immature Intervertebral Disc", *Connective Tissue Research*, 50:294–306, 2009.